MONITORING FIRE EFFECTS IN THE NEW JERSEY PINE BARRENS WITH BURN SEVERITY INDICES

By

MICHAEL RICHARD GALLAGHER

A dissertation submitted to the

Graduate School-New Brunswick

Rutgers, The State University of New Jersey

In partial fulfillment of the requirements

For the degree of

Doctor of Philosophy

Graduate Program in Ecology and Evolution

Written under the direction of

Jason Grabosky

And approved by

_____

_____

_____

_____

_____

_____

New Brunswick, New Jersey

OCTOBER 2017

ABSTRACT OF THE DISSERTATION

MONITORING FIRE EFFECTS IN THE NEW JERSEY PINE BARRENS WITH BURN SEVERITY INDICES

By Michael R. Gallagher

Dissertation Director:

Jason Grabosky

Fire effects refer to the range of direct and indirect impacts wildland fire has on the biotic and abiotic components of the environment. Monitoring fire effects is important for quantifying the results of management activities and identifying patterns of success that can help hone management strategy for the future. Unfortunately, fire effects are usually poorly monitored, if at all, because of the large technical expenditure required to accomplish monitoring activities across broad enough spatial scales to accurately capture variability in effects. However, relatively new approaches for deriving burn severity indices from field and multispectral data can accurately detect change in vegetation and soils reduction. Further, a limited number of studies have recently found these data to also be correlated with changes in carbon pools, fuel loads, stand structure, and regeneration patterns, which are relevant for both risk and ecological management. Of the studies presently available, all have been focused in western pyrogenic forests, which provide limited insight to effects in eastern pyrogenic forests, but do suggest the potential for research with an eastern forest focus. I therefore conducted a series of studies using these approaches to quantify burn severity and identify correlations between burn severity and rates of fuel reduction and tree mortality in eastern pitch pine-oak forests of the New Jersey Pinelands National Reserve, which have the highest fire frequency and

most active fire management agency in the North Atlantic region. I also investigated patterns of burn severity within fire types and timing using burn severity indices. The results presented provide a directly applicable and rapidly deployable method to monitor general fire effects, in a way that can be easily archived for future reference. These results can be incorporated into current burn strategy to maximize the effectiveness of activities intended to reduce fuels and thinning pitch pine stands, and provide a foundation for additional work in determining correlations between burn severity index data and other effects of interest to forest managers. Further, the results of this work suggests that burn severity can be used to predict these rates more accurately than simply knowing if a region burned or not, and identify key differences of fire of differing type and timing.

ACKNOWLEDGEMENTS

As with any dissertation, the work presented here represents the efforts of more than one person; it is the product of wisdom, patience, opportunities, and encouragement of numerous people. These people have been with me throughout the process of completing this dissertation, and have imparted upon me an invaluable education in wildland fire, forest ecology, and life in general. I sincerely thank Nicholas Skowronski for his kindness and patience while helping me over the years. He has been my biggest advocate throughout this process, and through sharing with me a rich network of scientists and managers, enabled me to fill gaps in my education where coursework left off. I thank my colleagues at the US Forest Service, Warren Heilman, Dave Hollinger, and especially Ken Clark, for their support of my graduate work and opportunities to grow as a researcher. I thank Jason Grabosky for that cup of coffee back in 2007, and for still offering me my first opportunity to conduct independent research despite my poor grades. Your confidence in me and consistent encouragement to continue on my path, especially when times seemed impossibly tough, has been invaluable and has made me a better person. I thank Rick Lathrop and Ed Green for giving me the analytical tools to conduct my research and accepting nothing less than excellence. I thank Mark Vodak for teaching me dendrology and for always being available to bounce an idea off of. I thank Peter Smouse and John Hom for getting me that first job with the US Forest Service at the Silas Little Experimental Forest, which I thought was only going to last for two weeks (that was 9 years ago). I also thank Peter for his tremendous help editing my chapters. I thank John Earlin for asking me to join his crew on what would become the first of many experiences prescribed burning and managing wildfire in the Pines, and eventually in other parts of the country. I thank Tom Gerber and the crew of Section B1 for sharing many of those fire experiences with me, sharing their observations, and educating me in fire ecology and management. I also thank the staff of New

Jersey Forest Fire Service, particularly Michael Achey, Jim Dusha, Shawn Judy, Sam Moore, Scott Knaurer, Brian Corvinis, and Ashley House, for providing the opportunities to conduct my research. I thank Marsha Morin for guiding me through the administrative aspects of the graduate program and promptly answering my questions with kindness and understanding. I thank Jim Pope for encouraging me to go to college in first place and for helping me to appreciate criticism and laugh off misfortune. I thank Shern Kier and Alec Slater for inspiring me to take chances and pursue excellence. I thank Dennis Gallagher, Carolyn Gallagher, and Jeffrey Hoerst, and Bethany Hall for their love, support, patience, and encouragement.

DEDICATION

I dedicate this dissertation to my parents, who taught me to appreciate the beauty of nature and the allure of its mysteries, as well the values of hard work, dedication, and independent thought.

TABLE OF CONTENTS

LIST OF TABLES

CHAPTER 1

CHAPTER 2

LIST OF FIGURES

CHAPTER 2

CHAPTER 3

CHAPTER 4

CHAPTER 5

CHAPTER 1: An introduction to field and remote sensing burn severity indices for monitoring fire effects in forest ecosystems

Abstract

Metrics that quantify the effects of wildland and prescribed fire are needed by managers and policy makers to support decisions that will impact public health, property, and natural resources. New remote sensing techniques for mapping burn severity, have enabled rapid quantification of wildland fire effects over broad spatial scales, opening the door to new research and monitoring opportunities for both scientists and managers. Using these new techniques, effects relating to fuel loads, carbon sequestration, and population dynamics of flora and fauna have been better characterized, yielding better understanding from a management perspective. Specialized remote sensing technology that is uncommon between these groups, however, and a review of the literature to synthesize the scope of work and considerations necessary to conduct burn severity studies, has limited the use of these methods as a whole. The aim of this chapter, is to provide managers and researchers with an understanding of the (1) needs and challenges of monitoring fire effects, (3) advantages of using burn severity approaches to monitoring fire effects, and (3) a synthesis of the current knowledge and limitations for estimating fire effects with burn severity.

Introduction: Why monitor fire effects?

Resource managers and policy makers need consistent, reproducible metrics of fire effects to support planning, evaluate management efforts, and refine management policy (Mercer and Prestemon 2005). Such information is useful for evaluating prior management activities, refining existing methods, justifying objectives, and characterizing wildfire and prescribed fire impacts across space and time (Key and Benson 2006). The need to quantify management outcomes is especially important for prescribed fire activities, where the efficacy

of fuel treatments is poorly evaluated (Harden 2016, Penman et al. 2011). Further, if fire effects were monitored over long periods of time and across landscapes, they could be compared to other long term datasets to assess how factors other than fire management, such as climate and social factors, influence wildland fires and their effects. Overall, fire effects data provide the details needed describe the interactions between humans and their environment that are linked by fire.

Fire effects refer, broadly, to the set of biotic and abiotic outcomes that result from fire, which are observable in minutes to years following a fire (Reinhardt, Keane and Brown 2001). The range of fire effects and their relative importance can be complex, and vary with time since fire. Hence they are broadly grouped as first order fire effects and second order fire effects, which reflect the time frame in which they occur and their mechanistic origin. First order fire effects are direct results of combustion, heat transfer, and associated chemical processes that occur during a fire event and are observable as an immediate consequence of fire (Reinhardt and Dickinson 2010, Reinhardt 2003). Such effects include the injury and mortality of plants and animals, the alteration or consumption of forest organic material (e.g. woody debris, forest floor litter, standing dead material, and soil organic material), and changes in soil chemistry. Second order fire effects happen in the hours to years following fire events, and are considered are indirect consequences of fire because additional processes are required to cause them. These effects can include erosion, tree mortality or injury caused by infection or insect damage that arises after fire, falling trees, vegetation recovery, shifts in species diversity, particulate dispersal, and altered watershed function.

Traditional recording of fire activity has often been limited to the delineation of fire perimeter and size, but may fall short of identifying the actual extent of burned area and degree of fire effects. For example, Kolden et al. (2012) found that over a 25 year period,

approximately 19% of the area within reported fire perimeters in three national parks did not actually burn. Furthermore, fire effects are not uniformly distributed across burn units, and typically reflect variation in topography, vegetation types, and weather, all of which can vary substantially across burn units; such effects are not directly proportional to fire size (Duffy et al. 2007, Turner et al. 1994). Specialized field methods can be employed to estimate specific fire effects, but those also have their limitations. Using field methods to estimate fire effects, requires expertise in ecological measurement techniques and provides only estimates of change at points, as opposed to full wall-to-wall coverage. Complex topography, access issues, and uncertainty of pre-burn conditions can also make post-fire surveys tedious and limit the interpretability of results (Escuin, Navarro and Fernandez 2008). Further, the timing of post-fire surveys makes them inherently more dangerous due to multiple hazardous conditions. Falling trees and tree material, for instance, are more common after fires when fire effects surveys would take place, and have accounted for over 50 serious injuries or deaths among wildland fire workers in the past ten years (NIFC 2016). Additional exposure to high levels of airborne particulate matter during or shortly after fire are also linked to short term acute respiratory asthma (Dennekamp and Abramson 2011), diminished pulmonary function (Liu et al. 1992, Rothman et al. 1991), and systemic inflammatory responses, which can be life threatening and should not be encountered regularly (Swiston et al. 2008, van Eeden et al. 2005). In summary, broad limitations on the abilities of management and research efforts to collect and adequately interpolate fire effects data across the scales required has hinders fire effects monitoring as a whole and the knowledge that it could provide.

Burn severity as a surrogate for of fire effects

Burn severity reflects many first order fire effects that are difficult to measure using traditional methods, making it a useful alternative for many research and monitoring

applications (De Santis and Chuvieco 2009, Perry et al. 2011). *Burn severity* indices describe the magnitude of environmental change resulting from fire and is increasingly used to evaluate fire effects in a more general sense in the days to years following a fire event (Keeley 2009, Kolden, Smith and Abatzoglou 2015). This differs from *fire intensity*, or the energetic properties of fire observed while it is burning (Byram 1959, Rothermel 1972). *Burn severity* can also be differentiated from *fire severity*, which typically relates specifically to the effects of fire on the observed biomass (post-fire), although the latter is used inconsistently in the literature (Keeley 2009). Although it is easy to draw natural connections between burn severity, fire intensity, and fire severity, via the functions of combustion and heat transfer on biomass (Ryan and Noste 1985, Cram, et al. 2006), the characteristics of fire that they describe, the way they are measured, and the time frame for which they are relevant are distinct (Lentile et al. 2006, Keeley 2009), and therefore draw a key distinction between the aim of this chapter and other work focused on fire behavior, energetics, and specific effects on biomass.

Burn severity reflects overall environmental change and can also be useful for estimating a wide range of specific fire effects, such as: fuel consumption (Boby et al. 2010, Meigs et al. 2009), carbon emissions (Allen and Sorbel 2008, Rogers et al. 2014), changes in soil properties (Parson et al. 2010, Robichaud et al. 2007), stand composition change and regeneration patterns (Johnstone and Kasischke 2005, Johnstone and Chapin III 2006), changes in leaf area index (De Santis and Chuvieco 2009), altered productivity (Meigs et al. 2009, Rocha and Shaver 2011), and forest community dynamics (Bailey and Whitham 2002, Koivula and Schmiegelow 2007, Kotliar, Kennedy and Ferree 2007). Burn severity has also proven useful for evaluating the role fuel treatments and previous wildfire events play in reducing impacts of subsequent fires (Prichard, Peterson and Jacobson 2010, Prichard and Kennedy 2014, Strom and Fulé 2007). *Post hoc* multi-decadal burn severity monitoring can now be used to extrapolate as

far back as 1984 with archival remote sensing data, and has been used to evaluate long term patterns in fire activity for some regions of the United States (Dennison et al. 2014, Holden, Morgan and Hudak 2010a, Miller and Safford 2012, Picotte et al. 2016).

The appropriateness of using burn severity to estimate fire effects varies greatly by region and vegetation type. For instance, burn severity is highly correlated with fire effects in boreal forests (French et al. 2008, Kasischke et al. 2008), tundra (Allen and Sorbel 2008) and western temperate coniferous forests (Chen et al. 2011, Key and Benson 1999, Miller and Thode 2007), but has been less correlated with fire effects in some sparse woodlands where trees are a less dominant than other types of vegetation (Allen and Sorbel 2008, Stambaugh, Hammer and Godfrey 2015). Further, fire effect correlations with burn severity are often different between different forest cover types, and models used to estimate fire effects from burn severity in one environment may not directly transfer to another environment (Key and Benson 2006). While substantial work has defined the use of burn severity in boreal forests, tundra, and temperate coniferous and deciduous forest types of the western United States and Canada, relatively little has been done with burn severity in forest types of the eastern United States.

Initial vs. Extended Burn Severity Assessments

Initial and extended assessments reflect the timing of burn severity studies, which is important for interpreting results. Characteristics of burned areas are not static, and as time passes since fire, second order fire effects and recovery processes make differentiating first order fire effects more difficult. Where initial assessments typically take place within days to months following fire, extended assessments take place in the following years (Key and Benson 2006). Whether to conduct an initial assessment or extended assessment depends on the goals of the assessment, the time frame over which it must be completed in, and the forest type being assessed. Changes in reflectance, detected in satellite data used to estimate remotely sensed

burn indices, continue to change, following fire, as second-order effects and vegetation recovery begin to occur. For instance, Burned Area Emergency Response (BAER) teams use initial assessments as a rough guide to areas within a fire perimeter that may need immediate restoration efforts aimed at managing post-fire erosion and water quality. Ecological studies, however, tend to deploy long term assessments, because it is often difficult to conduct the required field work within days of a fire. Correlations between field and remotely sensed burn indices have been found to be relatively similar within the first two years since fire for black spruce forests (Allen and Sorbel 2008), ponderosa pine (Chen et al. 2011), and eastern oak woodlands (Stambaugh et al. 2015). In tundra, field and *dNBR* data are significantly more correlated in the second year than in the first ($r_2^2 = 0.81 > r_1^2 = 0.43$). However, after the second year following a fire correlations between field and remotely sensed burn indices tend to weaken. To summarize, correlations are consistently found in vegetated areas but can vary greatly with time since fire and vegetation type.

Field Methods for Quantifying Burn Severity

Burn severity is often quantified as a continuous index that is unitless and can be estimated using both field and remote sensing methods. This index is often classified, based on thresholds, into four discrete severity classes: no effect, low severity, moderate severity, and high severity. Field – derived measures of burn severity are useful for providing statistical estimates, and are also used to calibrate and validate remotely sensed indices to provide continuous estimates of burn severity across a landscape. Field methods for measuring burn severity require technicians to work among post-fire hazards to obtain data, but can be conducted more rapidly than typical ecological survey methods, thereby reducing exposure.

The primary field methods for gathering burn severity data are used to calculate Composite Burn Index (CBI) (Key and Benson 2006), and it's variant, the Geometrically

Structured Composite Burn Index (GeoCBI) (De Santis and Chuvieco 2009). CBI is calculated as the composite of 24 severity indicator scores (e.g., % crown scorch, amount of litter consumption, etc.). These indicators are divided among 5 forest strata (substrates, low shrubs and herbs, tall shrubs and small trees, intermediate trees, and dominant trees), and observations of change within each of these strata are scored on a [0 – 3] scale (Key and Benson 2006). Scoring is conducted according to guidelines outlined on the CBI field sheet, such that indicators with the highest degrees of change are ranked as 3, while indicators with are ranked as 0 when they have not been effected by fire. These criteria, are then summarized into a stratum-specific Burn Indices (BI) by adding values together, and are finally combined into Understory CBI, overstory CBI, and an overall Total CBI by averaging BI in lower strata, upper strata, and all strata (see Key and Benson (2006) for full description of methods). Resultant CBI estimates have a continuous range of [0 – 3], but are oftentimes reclassified as "No Effect", "Low Severity", "Moderate Severity", and "High Severity", according to thresholds defined in the CBI methodology, to simplify descriptions of fire effects. Weighting CBI estimates, based on density of cover, can improve estimates of change, and has been suggested to be more correlated with remote sensing data than raw CBI (De Santis and Chuvieco 2009, Cansler and McKenzie 2012, Soverel, Perrakis and Coops 2010). One weighted variant of CBI is GeoCBI which weights BI estimates by leaf area index (See De Santis and Chuvieco (2009)). More recently, weighted composite burn index WCBI has been presented as a similar alternative, which uses ocular estimates of percent cover to weight BI for each strata (Soverel et al. 2010, Cansler and McKenzie 2012). Although both estimates have been shown to produce results that are more correlated with remote sensing data than CBI, CBI still remains the most commonly used method in current field work (Veraverbeke et al. 2010).

Other variants to CBI and its weighted variants may also be useful for providing coarse descriptions of burn severity. In southern Appalachian pine and oak dominated forest, a simplified version of CBI that included only crown scorch and shrub damage was found to be well correlated with remotely sensed burn severity (Wimberly and Reilly 2007). Similarly, Koivula et al. (2006) evaluated severity solely on scorch class for one study, which provided useful context for beetle population data they had observed. Brewer et al. (2005) developed a mortality- based severity index for the Northern Rockies, calibrated on remotely sensed burn severity, to classify post-fire vegetative cover classes as Unburned Shrub, Unburned Tree, Unburned Grass, Lethal Tree, Burned Shrub, Burned Grass, and Mixed Lethal Tree, although substantial research suggests that relationships between vegetative mortality and remotely sensed indices varies among vegetation types. In the Pacific Northwest, a scheme has been proposed to estimate burn severity from post-fire forest census plot data, such as that collected by FIA, which plots are classified into seven severity classes ranging from Unburned to Severe, based on tree mortality (Whittier and Gray 2016).

When a field method for assessing burn severity has been chosen, a final step should be the selection of field plot locations. This can be done in a few ways. The most common method used in recent studies is a stratified random sampling scheme, in which a calibrated or uncalibrated remote sensing burn severity index is used to map of the burn unit to estimate regions of “No Effect”, “Low Severity”, “Moderate Severity”, and “High Severity”. Plots are then typically centered within clusters of pixels that are believed to have similar burn severities, which minimizes the potential for edge effects that could occur due to spatial incongruence between field and remote sensing datasets (Chen et al. 2011, Cocke, Fulé and Crouse 2005, Holden et al. 2010b). This type of method may be appropriate in topographically complex landscapes, where obtaining spatially precise estimates is difficult (Congalton and Green 2008).

However, complete random sampling, which does not involve stratifying samples, has also been used in a flat landscape to produce equally strong correlations between field and satellite data (Warner, Skowronski and Gallagher 2017).

Remote Sensing Methods for Quantifying Burn Severity

Fire also alters the spectral reflectance patterns of forest vegetation and soils (see Figure 2 in Pereira and Govaerts (2001)). By identifying patterns of change at particular spectral wavelengths, it is possible to represent burn severity across broad spatial extents with the remote sensing data collected by specialized sensors on satellites or aircraft. Remotely sensed burn severity indices represent deviations of post-fire reflectance from pre-fire reflectance. Calculations typically use near infrared (NIR; 750nm – 1400nm) and short wave infrared (SWIR; 1400nm – 3000nm) wavelength data, which are highly sensitive to changes in chlorophyll content, leaf area, moisture conditions, and char (Warner et al. 2017). Indices based on these bandwidths include the Normalized Burn Ratio *(NBR)*, Differenced Normalized Burn Ratio *(dNBR*), Relative Differenced Normalized Burn Ratio *(RdNBR)*, and the Relative Burn Ratio *(RBR)* (Parks, Dillon and Miller 2014). Indices computed from other spectral bands have also been tested, and typically yield less reliable estimates, although they can be useful in cases where NIR and SWIR data are not available or perform poorly for a particular environment.

Correlations between remotely sensed burn severity indices and field data have been found to vary greatly among forest types and cover densities, and therefore must be calibrated for novel environments, typically using some form of CBI. Calibration is typically accomplished by fitting non-linear models to field data, which often produce a better fit than linear regressions (Chen et al. 2011, Miller and Thode 2007, Miller et al. 2009b). Non-linear regression is considered to be sensible, because SWIR reflectance saturates and NIR reflectance approaches zero as burn severity increases (Chuvieco et al. 2006). When thresholds are is used

to reclassify burn severity pixel values pixels into the four severity classes (No Effect, Low Effect, Moderate Effect, High Effect), a confusion matrix is often used to evaluate classification accuracies (Miller and Thode 2007). Both regression and confusion matrix results can be used to compare calibrations and justify calibration selection, but either method may be more useful, depending on the goal of the calibration. For instance, if classifying burned and unburned area is the primary goal of the study, then a calibration that accurately classifies "No Effect" pixels may have greater value than a calibration with a high linear regression coefficient or one that accurately distinguishes "Moderate Effect" and "High Effect" pixels.

Normalized Burn Ratio (NBR)

The normalized burn ratio (*NBR*) is perhaps the simplest burn severity index, and is an important pre-cursor in calculations of other more complex burn severity indices. *NBR* is computed as follows, where NIR is the value of reflectance observed for a spectral band within the 750nm – 1400nm range and SWIR is the value of reflectance observed for a spectral band within the 1400nm – 3000nm:

$$NBR = \frac{NIR - SWIR}{NIR + SWIR}$$ (Key and Benson 1999)

This is the simplest remote sensing strategy available, and does not require the same amount of normalization to remove atmospheric and phenological effects as other strategies (Veraverbeke et al. 2010, Verbyla, Kasischke and Hoy 2008). Of course, single date observations have the obvious drawback of not being amenable to differentiation of pre- and post-burn conditions that would allow us to assess impacts of previous fires, drought, or insect damage, which are common in forest environments and some cases are correlated with fire activity. *NBR*, used alone, is therefore most useful for quickly quantifying burn severity across individual burn units that do not need to be compared with other fires.

Differenced Normalized Burn Ratio (dNBR)

The differenced normalized burn ratio (*dNBR*) has emerged as a robust tool for evaluating burn severity across heterogeneous terrain and vegetation conditions, and has become the most widely used burn severity metric (Lutz et al. 2011, Sunderman and Weisberg 2011, Miller et al. 2016). This calculation uses pre- and post-fire *NBR* to account for the influence of pre-burn vegetation conditions, using the following equation:

$$dNBR = (NBR_{pre} - NBR_{post}) * 1000 \qquad \text{(Key and Benson 2006)}$$

By using bi-temporal data, this method accounts for pre-fire vegetation characteristics, and provides results that are less likely to be influenced by disturbance effects that were present before the fire. An optional offset in the equation for *dNBR*, calculated as an average value of unchanged forest in imagery, can be used to account for variation in phenology of imagery between fires (Key and Benson 2006, Miller and Thode 2007). As an absolute measure of ecological change, however, the degree of severity reflected by *dNBR* is correlated to the amount of pre-burn vegetation present, and can result in misclassification of change (Miller and Thode 2007). For instance, when two plots are burned with a similarly high severity, but one plot has approximately half of the pre-fire vegetation as the other, *dNBR* of the denser plot will be approximately double that of the other plot. For this reason, *dNBR* may not be an effective calculation for comparing burn severity between areas with differing dominant vegetation types or vegetation density, however, this remains debated in the literature.

Relative Differenced Normalized Burn Ratio (RdNBR)

The Relative Differenced Normalized Burn Ratio (*RdNBR)* is a relative measure of burn severity, developed to allow for the comparison of burn severity of numerous fires across heterogeneous landscapes and through time. As a relative measure of burn severity, *RdNBR* is normalized based on pre-burn *NBR*, and therefore, provides results that are not correlated with pre-burn vegetation conditions, unlike *dNBR*. In calculating *RdNBR*, a square root

transformation is applied to the absolute value NBR_{pre} in the denominator to better match the distributional form of field data. The absolute value of NBR_{pre} is used in the denominator, rather than its raw form, to avoid the problem of calculating a square root of negative NBR_{pre} values (Miller and Thode 2007):

$$RdNBR = dNBR/\text{sqrt}\left|\frac{NBR_{pre}}{1000}\right| \qquad \text{(Miller and Thode 2007)}$$

Although *RdNBR* may avoid bias associated with heterogeneity in pre-burn vegetation density that other indices do not avoid, the operations in the denominator of this equation also introduce other bias to results, albeit small, and allow for equation failure under certain circumstances. For instance, bias is introduced when taking the absolute value of negative NBR_{pre} values because the full variability of pre-burn vegetation conditions is obscured (Miller and Thode 2007, Parks et al. 2014). Further, *RdNBR* calculations fail when NBR_{pre} is equal to zero, resulting in a zero in the denominator. This calculation can occasionally produce outlier results when NBR_{pre} is very close to zero (Parks et al. 2014).

While *RdNBR* theoretically solves some of the problems associated with *dNBR*, the literature suggests that advantages of one method over another are regionally specific. For instance, in a comparison of the two indices in mixed conifer forests of the Sierra Nevada, non-linear regression found *RdNBR* to significantly outperform *dNBR*, however differences were less apparent among classified data (Miller and Thode 2007). Soverel et al. (2010) found the opposite, in a comparison in Canadian boreal forest, in which regression correlation coefficients were not appreciably different, but *dNBR* had a substantially higher accuracy at thresholding. Minor inconsistencies in the methodologies of these studies exist, including different usage of bandwidths and timing of field data collection, making an objective comparison of results difficult.

Relativized Burn Ratio (RBR)

RBR is a relativized form of *dNBR*, described by Parks (2014), and may offer slight gains in results, when compared to *dNBR* and *RdNBR*, and is mathematically more robust. In a study comparing *dNBR*, *RdNBR*, and *RBR*, Parks et al. found *RBR* performed slightly better on average, but that *dNBR* and *RdNBR* performed better for certain individual fires (Parks et al. 2014). *RBR* is also attractive, when compared to *dNBR*, because it is less correlated with the variation of pre-burn vegetation cover than *dNBR* and *RdNBR*, and is therefore provides more robust results across different levels of vegetation cover. *RBR* also has mathematical advantages to *dNBR* and *RdNBR* in that the equation does not fail when NBR_{pre} is zero.

$$RBR = \left(\frac{dNBR}{NBR_{pre}+1.001}\right) \quad \text{(Parks et al. 2014)}$$

Less common remote sensing indices used in burn severity studies

Remote sensing indices of terrestrial conditions or change have also been tested. Generally, these indices have not performed as well as the indices described above but they may have merits in certain geographic areas, in cases where NIR or SWIR data are not available, or when effects cause reflectance changes in other bandwidths. Indices that have traditionally been used for the monitoring of vegetation, such as the normalized difference vegetation index (NDVI) and the enhanced vegetation index (EVI), for instance, have also been used to estimate forest productivity following perturbation by wildfires (Chen et al. 2011, Rocha and Shaver 2009). Despite relatively little use in burn severity studies, and work suggesting that other bandwidths of reflectance are theoretically more correlated with forest change (Garcia and Caselles 1991), work suggests that indices based on reflectance in the NIR and visible spectrum (namely, normalized differenced burn index (NDVI) or the enhanced vegetation index (EVI)) can provide similarly useful results as NIR and SWIR based indices (Chen et al. 2011, Escuin et al. 2008).

Burn Severity Index Selection

Published correlations of linear regressions between field data and remotely sensed indices vary greatly among and within vegetation types. For instance, correlations between field and *dNBR* values for various boreal forest vegetation types have ranged dramatically [$r^2 = 0.00 – 0.91$], but generally have stronger correlations where trees, particularly conifers, dominate (See Appendix C). While results of Epting et al. (2005) suggest that single-date NBR outperforms bi-temporal *dNBR*, in terms of predicting field observations of burn severity, most other studies in boreal vegetation types indicate otherwise (See Appendix C). *dNBR* is the most widely used remotely sensed burn severity index, however, *RdNBR* is clearly the second most popular of this type of index. The mathematical operations involved in computing *RdNBR* are in some ways stronger and in other ways weaker than *dNBR*, and while individual studies tend provide evidence for choosing one method over the other, a review of the published correlation coefficients (T) and classification accuracies (Table 1) fail to provide clear evidence for one method being superior.

Data and Processing Considerations for Remote Sensing of Burn Severity

Data Sources for Remote Sensing Burn Severity Indices

Numerous satellites collect imagery that is useful for estimating burn severity. Landsat 4/5, Landsat 7, and Landsat 8, ASTER, MODIS, VIIRS, AVIRIS, and Worldview 3 all collect data in the VIS, NIR, and SWIR ranges needed to compute common burn severity indices. Data from each of these sensors, with the exception of Worldview 3 and Quickbird, are in the public domain, and, therefore, can be retrieved online at no cost. Each sensor produces data with different spatial and spectral resolutions (Table 2), however, which can yield in notably different indices produced within the similar vegetation types (Chen et al. 2011, Holden et al. 2010b). This suggests that unique correlations between field and remote sensing data for unique

vegetation types, however, many correlations have been provided for a variety of environments in existing publications (Table 1). Availability of data also varies substantially among sensors. Most current satellites collect data with a flyover time of about 2 weeks, while other satellites only collect data when they are tasked to a capture a specific scene. Similarly, some sensors have only become available in the past decade, while others that have provided useful historic data, as far back as the 1980s and 90s have been decommissioned (Table 2). Since no single sensor is optimal for all environments or burn severity applications, selection of data source should be determined based on project goals, availability of data, and required spatial resolution of data.

Landsat sensors are the most appropriate sensors currently available for the majority of burn severity monitoring and research applications. Medium resolution, appropriateness of bandwidths, and data availability have made data from the Landsat sensors a popular choice for burn severity monitoring and research. The Landsat program is the longest running satellite program to collect NIR and SWIR data, beginning in 1984 and continuing today, making Landsat a popular choice for historic, current, and multi-decadal studies of burn severity. Thematic Mapper (TM) sensors of Landsat 4, 5, and 7 collect NIR and SWIR data as bands 4 and 7, and have nearly identical bandwidth specifications making them interchangeable (Table 1). Landsat's 30m pixel resolution is considered to be relatively high, compared to other publicly available satellites, and therefore is useful for capturing burn severity across fires of most sizes and where environmental heterogeneity occurs on a relatively small spatial scale. In addition, these spectral bands are the most sensitive bands to changes in reflectance, due to fire, while having low correlations with each other (see Figure 2 in Garcia and Caselles (1991)). Despite the 16 day revisit time of Landsat 4, 5, and 7 sensors, data availability can create challenges. Landsat 4 and 5 sensors have reached the ends of their service lives and were decommissioned

in 1987 and 2012, respectively, and irreparable damage to Landsat 7's Thematic Mapper has resulted in large, regular swaths of missing data in all imagery since 2003 (Markham et al. 2004), which require addition processing for gap-filling (Howard and Lacasse 2004).

Landsat 8's Operational Land Manager Sensor (OLI) is the newest sensor of this program, and calibrations of its NIR and SWIR bands differs somewhat from those of previous Landsat sensors (Table 2). *NBR* estimates have been found to be relatively similar, with less than 5% variation, in one study in Thailand, suggesting that *NBR* between the sensors is relatively comparable; however it is unclear 1) how well burn severity actually correlates with field observations in this environment and 2) if burn severity estimates were for isolated fire events, or were for the entire region, which contained substantial unburned area and may not accurately reflect the performance of these indices in burned vegetation (Li, Jiang and Feng 2013). Few other studies have compared burn severity estimates from differences in burn severity derived from data of Landsat 8 and previous Landsat satellites, however, bandwidth differences may confound the use of Landsat 8 data use with that of other Landsat satellites, and for this reason Landsat 7 remains the most common source for current remote sensing of burn severity.

MODIS band 2 (NIR) and 7 (SWIR) data have been used to predict *dNBR* and *rdNBR* in areas with expansive fires, due to the relatively large pixel size of MODIS data (Table 2), such as in boreal forests of Central Siberia and sagebrush steppe of the Great Basin region of the US (Loboda, O'Neal and Csiszar 2007). Boelman et al. found that the mismatch between pixel scale and scale of affected areas on the ground ($100m^2$ and $1m^2$) was too great to yield adequate severity estimates, despite the fact that the overall fire size was over $1000km^2$ (Boelman, Rocha and Shaver 2011). Likewise, MODIS under-predicted the total low severity area burned and the maximum burn severity Landsat, however it was able to provide adequate severity mapping.

Worldview3 is a commercial sensor that produces multiple different bands of NIR and SWIR data at a 7m spatial resolution. With the exception of AVIRIS, Worldview3 has higher spectral resolution bandwidths than other available sensors that collect NIR and SWIR range data (Table 2). Since the sensor was launched in 2014, very little fire data has been collected with Worldview3, in part due to the fact that it does not automatically collect regular data, and must be tasked to collect specific imagery. However, Warner et al. tasked this satellite to capture pre- and post- fire imagery over prescribed fires and, incidentally, a wildfire, and compared *dNBR* results with field data in a pine-oak forest (Warner et al. 2017). Strong correlations were found between *dNBR* computed with nearly all combinations of Worldview3 NIR and SWIR bands and field data, although, bands 7 and 14 produced the best results for Total CBI ($R^2 = 0.84$). Interestingly, different band combinations produced higher $R^2 =$ values for Overstory and Understory CBI. Since Worldview3 is not in the public domain and thus imagery is not free, nor does it collect with a predictable frequency necessary to opportunistic to capture wildfires as they occur, it may not be a practical sensor for assessing impacts of large scale wildfires; however, given that resultant *dNBR* is highly correlated with field data, this sensor may be an optimal choice for high value controlled burn projects.

The hyperspectral Airborne Visible and Infrared Imaging Spectrometer (AVIRIS) has been used in a limited number of burn severity studies, but may also be a useful source of remotely sensed burn severity data. AVIRIS data is collected by a high altitude aircraft and its data is attractive because it is available in numerous bandwidths at relatively high spatial resolution of 2.4m (Table 2). In a steep slope environment of mixed grass, shrubs, and trees in California, visible shortwave infrared bands of AVIRIS were used to produce a unique remote sensing burn severity index that was highly correlated with GeoCBI data [$r^2 = .86$] (Veraverbeke, Stavros and Hook 2014). Researchers also found that burn severity estimated using AVIRIS provided more

spatially accurate estimates of post fire tree damage, soil change, and ash cover than that estimated from Landsat TM data in a ponderosa pine dominated landscape of New Mexico (Kokaly et al. 2007). Conversely, in the Sierra Nevada *dNBR* calculated from Landsat TM and AVIRIS had correlation coefficients of [$r^2 = 0.89$] and [$r^2 = 0.85$], respectively, suggesting that burn severity derived from Landsat TM may be as useful in that environment, despite the higher spatial resolution of burn severity derived from AVIRIS (Van Wagtendonk, Root and Key 2004). One explanation for this may be an asynchrony between in the spatial scale of variability of fire effects between these two landscapes and the spatial resolution of the best sensor available. While the relatively small pixel size of AVIRIS data is attractive, there are be many challenges to using this data for burn severity purposes. Despite collecting high resolution narrow band reflectance data, AVIRIS does not collect continuous data, and must be tasked to collect for specific projects. This limits the use of AVIRIS for burn severity, especially for wildfire; however, since AVIRIS, has the ability to collect much higher spectral resolution imagery, it has been useful for identifying specific wavelengths of maximum change following fire and validating the use of Landsat mid-IR and near-IR bands for estimating burn severity in the Sierra Nevada (Van Wagtendonk et al. 2004). Likewise, combining actual AVIRIS data with simulated data from other sensors has yielded improved burned area estimates, with mapping results that were highly correlated with field observations at a large wildfire in California (Veraverbeke et al. 2014).

Quickbird2 also produced high resolution (2.4m) imagery between 2001 and 2014, but is no longer collecting new data. Because this sensor collected NIR and VIS, but not SWIR data, this burn severity applications with this satellite were primarily based on *EVI* or *NDVI*, rather than *NBR* or *NBR*-like indices. This satellite also required tasking (*i.e.* did not collect regular imagery) and therefore received limited attention for producing burn severity indices. Still,

Holden et al. found that Quickbird2 based EVI maps were highly correlated with field observed burn severity (r^2 = 0.84) (2010b). More commonly, however, this imagery is has been used in conjunction with NIR and SWIR based estimates to improve accuracy of burn severity predictions (Huang et al. 2007, Mitchell and Yuan 2010).

Data and Processing Considerations

The spatial scale of imagery use to produce maps is of key importance. Presently four scales of imagery are available (Table 1). In areas where fires burn thousands of hectares, larger sized pixels may be sufficient to classify change, however, in areas where fires are frequent but relatively small, smaller pixels are more appropriate. Spatial scale and bandwidth differences between sensors can drastically affect results in comparisons of field and remotely sensed data. Holden et al. (2010b), demonstrates this well in a study of burned areas in the Gila National Forest showing that three different remotely sensed burn severity indices had vastly different relationships with field data when computed at different scales using Quickbird, ASTER, Landsat, and MODIS data. In this study, correlations between field data and remotely sensed data differed considerably for when these sensors were used to calculate *dNBR* (r^2 = 0.78 - 0.84), *dNDVI* (r^2 = 0.38 - 0.79), and *dEVI* (r^2 = 0.03 – 0.82). Timing of imagery, in relation to fires and seasonality is also a key consideration. While many studies have used pre-and post-fire imagery from within a two week window of the fire, phenological differences associated with dormant, growing season, and transitional periods in temperate deciduous ecosystems may confound the meaning of results if this approach is used in those systems. This effect has received little attention in the literature with respect to burn severity indices. Raw satellite imagery will require processing to convert digitally stored numbers to top of atmosphere reflectance values, rectify atmospheric distortion, and normalize spectral inconsistencies related to phenology and atmospheric interference, although methods have been well established. Cloud cover and

interannual variability of challenge the use of remotely sensed burn severity metrics (Key and Benson 2006, Verbyla et al. 2008). Clouds obscure surface reflectance of NIR and SWIR bandwidths, and must be removed from imagery. Mosaicking multi-temporal imagery, within a short time span, can be used to fill in areas in imagery where cloud covered areas have been omitted (Veraverbeke et al. 2011).

Incorporation of burn severity indices in ecological research

Carbon dynamics

Field indicators of burn severity, such as vegetation and foliage, are highly correlated with changes in forest carbon pools and CO_2 exchange processes in many forested landscapes, providing a means of estimating the impacts of fire on carbon dynamics. Soil and terrestrial fuel consumption, for instance, is well correlated with field observed burn severity in boreal forest and tundra, which can be used with fuel-specific emissions factors and pre-burn fuel loading estimates to estimate total carbon emissions, in response to fires (Allen and Sorbel 2008, Boby et al. 2010). In one study, field observed burn severity accounted for 61% of the variation in relative depth and percent change in mass of aboveground and belowground biomass pools in a boreal forest fire (Boby et al. 2010). Rogers et al. (2014) demonstrated substantial improvement in emissions estimates when remotely sensed burn severity was calibrated with field observed burn severity. Further, Campbell et al. (2007) and Meigs et al. (2009) have provided carbon emissions factors that can be used to estimate total wildfire emissions from burn severity maps (Appendix A), however it should also be noted that emissions factors are subject to error (Wiedinmyer and Neff 2007). Burn severity can also be used to estimate variability in forest productivity and recovery rates following fire. Meigs et al. (2009) used burn severity to scale changes observed in post-fire net ecosystem productivity (NEP) and net primary production (NPP) in ponderosa pine and mixed conifer forests over two years following fire, to estimate an

overall fire-wide loss in carbon and productivity. Similarly, carbon and nutrient flux rates measured at flux towers in burned tundra have been scaled across a fire scar using remotely sensed burn severity, enabling the evaluation of the recovery of ecosystem productivity over a five year post-fire period (Jiang et al. 2015, Rocha and Shaver 2011). Burn severity may also be useful in improving regional and national scale carbon inventory estimates (e.g., those produced by the Forest Inventory and Analysis (FIA) program) by improving estimates of emissions and altered productivity in plots that are often missed in fire events (Williams et al. 2014).

Wildfires and Fuel Treatments Moderate Subsequent Fires

Wildland fire dynamics can be modified by preceding wildland fires and fuel treatments, an effect that can be evaluated using field and remote sensing burn severity indices (Parks et al. 2015, Prichard et al. 2010, Prichard and Kennedy 2014). Fuel reduction treatments include thinning, prescribed burning, mastication, and combinations of these techniques, and are used across the country, with varying degrees of effectiveness (Cochrane et al. 2013). Stand density, for instance, has been linked to burn severity patterns in ponderosa pine dominated forests in New Mexico (Amato et al. 2013). In mixed conifer forests, fuel reduction treatments have been found to substantially reduce burn severity of subsequent fires (Prichard et al. 2010) and can reduce emissions by more than 50% when removed biomass is converted to product that postpones its decomposition (North and Hurteau 2011). Field surveys of burn severity have also been useful in northern Arizona, for linking transition zones of fire behavior (Kennedy and Johnson 2014) and reductions in tree mortality (Strom and Fulé 2007) with fuel treatments in mixed conifer forest. Again, in a mixed conifer forest in Washington, field observations of burn severity were used to evaluate the efficacy of thin and burn treatments versus thin only treatments, and revealed that reductions in burn severity and mortality were greater in thin and burn treatments (Prichard et al. 2010, Prichard and Kennedy 2012). However, thinning

treatments that leave substantial fuel on the forest floor, however may actually *increase* burn severity (Schoennagel, Veblen and Romme 2004). Similar reductions in burn severity have been observed in fire scars (e.g. areas that have been burned recently enough to exhibit visible differences from surrounding areas) that reencounter wildfire, with severity of reburns increasing with time since fire (Parks et al. 2013, Parks et al. 2015). Parks et al. (2013) found in reburned conifer forest types of Idaho and New Mexico that reductions in burn severity were most evident shortly after fires, but could be seen for at least 22 years since fire. Parks et al. (2013) and Holden et al. (2010a) suggest, however, that scars with burn severities above a certain threshold may exhibit similar or increased burn severity in subsequent fires in the Gila National Forest of New Mexico. Conversely, high severity fire drastically limited subsequent fire severity in the Sierra Nevada (Collins et al. 2009). Collins et al. found that in this environment, successive adjacent fires that occurred within 9 years of each other were limited to the first fire's edge, except under extreme weather conditions. The recurrence of high burn severity in some environments but not others is poorly understood, but is believed to be linked to static, highly flammable vegetation types, conversion of vegetation types between fires, weather that favors high intensity fire, or factors that predispose some sites reflectance patterns to suggest high severity fire.

Forest Stand Dynamics

Burn severity can be useful for estimating vegetation mortality rates and regeneration patterns following fire. Burn severity, for instance, was positively correlated with mortality rates of aspen, ponderosa pine, limber pine, and Douglas fir within the first year after the fire (Cocke et al. 2005). Numerous secondary stressors can make disentangling mortality rates difficult after the first post fire year, but fractions of dead stems were still positively related to burn severity for ponderosa pine, three years after fire (Lentile, Smith and Shepperd 2005). Gamble

oak (*Quercus kelloggii* Newb.) mortality patterns were similarly linked to burn severity 12 years post-fire (Crotteau et al. 2015). Moreover, burn severity is correlated with patterns of regeneration among woody forest species (See Appendix B) 2). Johnstone (2005) found different patterns of seedling establishment of black spruce (*Picea mariana* (Mill.) BSP) and trembling aspen (*Populus tremuloides* Michx.), related to burn severity, in plots near fire edges in Alaskan boreal forest. Distance from the edge of unburned or lesser burned areas into burned areas, however, is often also an important predictor of conifer regeneration. For instance, multiple studies have found little to no regeneration of ponderosa pine more than 30m into areas classified with high severity from edges of areas with lower severities (Chambers et al. 2016, Lentile et al. 2005). Conversely, gamble oak has been found to sprout most prolifically in areas of high severity fire (Crotteau et al. 2015).

Burn Severity and Wildlife

Wildfire can positively or negatively impact wildlife habitat, depending on species and the burn severity characteristics of the fire. Following the Rodeo-Chedeski Fire, forage production in low severity areas was threefold of that in high severity areas (Schoennagel et al. 2004). In contrast, aspen ramet production is positively correlated with burn severity which elk have been observed to preferentially browse over ramets in lower and moderate severity areas (Bailey and Whitham 2002).

Changes in post-fire insect and arthropod populations have also been linked to burn severity. For instance, abundances of the pyrophillus caribad beetles, *Sericoda quadripuntata* and S. *bembidioides*, for instance, have been found to be positively correlated with burn severity in forests in Finland (Koivula et al. 2006), as have saproxylic insect populations in Canadian boreal forest (Nappi et al. 2010). In a mixed conifer forest, arthropod population diversity and abundance were strongest in moderate intensity fires, likely due to positive changes to their

habitats that were linked to aspen regeneration and elk activity that were also modulated by fire (Bailey and Whitham 2002). In boreal forests however, strong negative correlations have been found between burn severity, abundances, and population recovery rates of soil arthropods (Colembola) (Malmström 2006).

Wildfire, particularly for a variety of bird species (Kotliar et al. 2002), is also an important contributor to habitat modification, and numerous studies have identified relationships between burn severity and bird usage of forested areas. In a study in southeastern Arizona, burn severity was shown to be positively or negatively correlated with the abundances of most of the 97 bird species observed, with 73% having positive correlations with burn severity (Kirkpatrick, Conway and Jones 2006). Similarly, a study in New Mexico found that the abundances of 71% of species observed were either positively or not related to burn severity, while abundances of other species were negatively related to burn severity (Kotliar et al. 2007). In boreal forests, burn severity has been positively correlated with increased population abundances of black-backed woodpeckers (Koivula and Schmiegelow 2007), while three toed woodpeckers and brown creeper abundance increases are linked to low severity fire (Nappi et al. 2010). Shifts in bat assemblages are have also been linked to burn severity, and are thought to be proportional to changes in vegetation density and insect prey, although a limited studies are available to verify this (Buchalski et al. 2013, Malison and Baxter 2010). Post-fire bird and bat species occurrences are also related to severity (Rose et al. 2016, Malison and Baxter 2010). Spatial redistributions to avifaunal populations within burned areas may be linked to population shifts of insect prey and forest structure, also impacted differentially by burn severity.

Publicly available burn severity products

Currently, the USDA Forest Service's Monitoring Trends in Burn Severity (MTBS) program is the only outlet for off the shelf burn severity products, serving initial assessment and

extended assessment burn severity map products for fires across the continental United States (www.mtbs.gov). MTBS's automatic system independently records burn severity of fires in the western US that are greater than 400 ha in extent and in the eastern US greater than 200ha in extent. Burn severity products offered by this program include 30m resolution pdf and raster maps of *NBR, dNBR, rdNBR*, and *BAER* severity classes. These data are frequently used by *BAER* teams to identify areas in urgent need of erosion mitigation and watershed protection after wildfires (Parson et al. 2010), and by researchers to deduce regional patterns in fire activity that have occurred since 1984 (Dennison et al. 2014, Picotte et al. 2016).

Spectral and temporal inconsistencies in calculations complicate the use burn severity indices for some research and monitoring applications (Kolden et al. 2015). Likewise, the meanings of *BAER* classifications can be difficult to interpret between vegetation types because of inconsistent ranges of error between vegetation types, resulting in unclear classification accuracies (Kolden et al. 2012). This is rooted in the fact that relationships, and their significance, between field and remote sensing burn severity data are variable and often unavailable across vegetation types (Eidenshink et al. 2007).

Another challenge with using the MTBS products is the omission small fires, which despite seeming inconsequential, may make up a large proportion of fire activity and area burned in some regions. In New Jersey, for instance, 1244 ± 493 (mean ± 1SD) wildfires and numerous prescribed fires have annually impacted forested land and have collectively burned approximately 76000 ha between 2005 and 2014, (New Jersey Department of the Treasury 2006, 2008, 2010, 2012, 2014, 2016), however burn severity was only captured in less than 14000 ha of the burned area (www.mtbs.gov). Similarly, the Pennsylvania Forestry Commission reports a total of over 14000 ha have burned during the same timeframe, however MTBS recorded only recorded burn severity across fewer than 3300 ha (www.mtbs.gov,

http://www.dcnr.state.pa.us/forestry/wildlandfire/firestatistics/index.htm). A comprehensive discussion of the current limitations of MTBS data, and possible solutions, has been presented by Kolden et al. (2015). MTBS products can be useful for a limited range of management purposes in certain regions, and have facilitated improvements to the national scale monitoring effort of wildland fire. Users should be aware that MTBS products may not be suitable for research purposes, may have limited or inconsistent utility for predicting fire effects, and may represent only a limited selection of the actual fire activity in certain regions.

Summary

As challenges of managing wildland fire gain increased awareness from the perspectives of public health, spending, firefighter safety, wildlife, and forest health, predicting the outcomes of various management options remains challenging. Lack of quantification of fire effects hinders the ability to objectively synthesize outcomes of many fires through time to adapt management and explain external factors affecting fire activity. Over the past decade, remote sensing change detection methods have been used to estimate burn severity across broad spatial extents. Remotely sensed burn severity indices allow for accurate estimation of burned area and also continuous estimates of fire severity that cannot be obtained by using field methods, and can be conducted more safely. For instance, burn severity indices have been used to successfully estimate carbon emissions and recovery patterns, tree mortality and regeneration patterns, impacts of fuel treatments, and trends in wildlife population dynamics. Further, archival remote sensing data can be used to study fires days, months, or years, after they have happened, without prior planning.

The selection of approaches should be based on study objectives. Field based methods are available and useful for providing simple, course resolution estimates, that can be used to calibrate and evaluate remote sensing calibrations in specific vegetation types. Both weighted

and unweighted field methods provide useful results, but should be interpreted as having slightly different meanings. Few studies have evaluated weighted methods, and further research is required to objectively determine whether one weighted or unweighted methods are more appropriate. Numerous options for remote sensing of burn severity are available and defendable as monitoring techniques, but methodological selection for monitoring purposes will determined by availability of field calibration data and the availability of suitable remote sensing data. In most cases, indices derived from Landsat NIR and SWIR imagery (*e.g. NBR, dNBR, RdNBR*, or *+*) will be the most pragmatic approach, because of the multitude of existing calibrations, availability of archival data in the public domain, and suitability of the data's medium spatial resolution for most applications. However, special collections of higher resolution imagery can be scheduled with commercial satellelite operators if required. Off the shelf MTBS products may be useful in monitoring efforts are only concerned with large fires, but will be limited where small fires make up a large proportion of the area burned and lack validation.

While substantial literature is available to guide the implementation of monitoring and research in North American boreal, tundra, and western temperate coniferous and mixed forest types, there is an ongong need for more calibrations in coniferous, deciduous, and mixed forest types of the central and eastern United States. One vegetation type where substantial success could be made are the widespread pitch pine, chestnut oak, and mixed pine-oak forests of the eastern us, such as those in Pennsylvania and New Jersey that burn frequently each year and are highly valued for public safety and habitat management. Linking fuel consumption, silvicultural effects, and the influence of weather and seasonality on effects are key focuses that would aid management and be useful for informing ecological research with additional focuses. Expanding applications of burn severity to additional forest types where fire once was, but has been has

been suppressed would also be helpful in developing management strategies to reverse mesophication, restore habitat for threatened and endangered species, and promote ecological resilience in northeastern forests.

Finally, more research that examines the relationship between burn severity and fire behavior is needed. While many indicators of burn severity demonstrate a link between burn severity and fire behavior, such as scorch height relating to flame height and intensity for specific environments (Alexander and Cruz 2012, Wagner 1973), correlations between burn severity and fire intensity have not been sufficiently evaluated (Heward et al. 2013). Benefits of such correlations would allow managers to compare how fire behavior differed between treated and untreated areas, in different fuel types, and under different burning conditions. Further, this link would help scientists developing physics-based fire behavior prediction models better understand the nature of fire behavior and intensity in large heterogeneous burn units.

Conclusions

Burn severity indices are useful and increasingly popular for monitoring fire effects for management and research applications. Multiple field and remote sensing methods are available, however, not all methods will provide equivalent results or will be feasible for every monitoring goal, and, therefore, careful consideration of methods and monitoring goals is crucial to ensure a feasible and appropriate method is selected. Ongoing research is continuously advancing the utility of burn severity indices, however, the focus of burn severity research has been variable between regions. Additional research that produces more calibrations, especially in under-represented regions, and links burn severity to fuel consumption and fire intensity would be useful to management and research communities, interested in predicting fire behavior and outcomes of fuel treatments and wildland fire.

References

Alexander, M. E. & M. G. Cruz (2012) Interdependencies between flame length and fireline intensity in predicting crown fire initiation and crown scorch height. *International Journal of Wildland Fire,* 21**,** 95-113.

Allen, J. L. & B. Sorbel (2008) Assessing the differenced Normalized Burn Ratio's ability to map burn severity in the boreal forest and tundra ecosystems of Alaska's national parks. *International Journal of Wildland Fire,* 17**,** 463-475.

Amato, V. J. W., D. Lightfoot, C. Stropki & M. Pease (2013) Relationships between tree stand density and burn severity as measured by the Composite Burn Index following a ponderosa pine forest wildfire in the American Southwest. *Forest Ecology and Management,* 302**,** 71-84.

Bailey, J. K. & T. G. Whitham (2002) Interactions among fire, aspen, and elk affect insect diversity: reversal of a community response. *Ecology,* 83**,** 1701-1712.

Boby, L. A., E. A. Schuur, M. C. Mack, D. Verbyla & J. F. Johnstone (2010) Quantifying fire severity, carbon, and nitrogen emissions in Alaska's boreal forest. *Ecological Applications,* 20**,** 1633-1647.

Boelman, N. T., A. V. Rocha & G. R. Shaver (2011) Understanding burn severity sensing in Arctic tundra: exploring vegetation indices, suboptimal assessment timing and the impact of increasing pixel size. *International journal of remote sensing,* 32**,** 7033-7056.

Brewer, C. K., J. C. Winne, R. L. Redmond, D. W. Opitz & M. V. Mangrich (2005) Classifying and mapping wildfire severity. *Photogrammetric Engineering & Remote Sensing,* 71**,** 1311-1320.

Buchalski, M. R., J. B. Fontaine, P. A. Heady III, J. P. Hayes & W. F. Frick (2013) Bat response to differing fire severity in mixed-conifer forest California, USA. *PloS one,* 8**,** e57884.

Byram, G. M. (1959) Combustion of forest fuels. *Forest fire: control and use,* 1**,** 61-89.

Campbell, J., D. Donato, D. Azuma & B. Law (2007) Pyrogenic carbon emission from a large wildfire in Oregon, United States. *Journal of Geophysical Research: Biogeosciences,* 112.

Cansler, C. A. & D. McKenzie (2012) How robust are burn severity indices when applied in a new region? Evaluation of alternate field-based and remote-sensing methods. *Remote sensing,* 4**,** 456-483.

Chambers, M. E., P. J. Fornwalt, S. L. Malone & M. A. Battaglia (2016) Patterns of conifer regeneration following high severity wildfire in ponderosa pine–dominated forests of the Colorado Front Range. *Forest Ecology and Management,* 378**,** 57-67.

Chen, X., J. E. Vogelmann, M. Rollins, D. Ohlen, C. H. Key, L. Yang, C. Huang & H. Shi (2011) Detecting post-fire burn severity and vegetation recovery using multitemporal remote sensing spectral indices and field-collected composite burn index data in a ponderosa pine forest. *International Journal of Remote Sensing,* 32**,** 7905-7927.

Chuvieco, E., D. Riaño, F. Danson & P. Martin (2006) Use of a radiative transfer model to simulate the postfire spectral response to burn severity. *Journal of Geophysical Research: Biogeosciences,* 111.

Cochrane, M. A., M. C. Wimberly, J. C. Eidenshink, Z.-L. Zhu, D. Ohlen, M. Finney & M. Reeves (2013) Fuel treatment effectiveness in the United States. *Joint Fire Science Program 06-3-3-11Final Project Report***,** 1-44.

Cocke, A. E., P. Z. Fulé & J. E. Crouse (2005) Comparison of burn severity assessments using Differenced Normalized Burn Ratio and ground data. *International Journal of Wildland Fire,* 14**,** 189-198.

Collins, B. M., J. D. Miller, A. E. Thode, M. Kelly, J. W. Van Wagtendonk & S. L. Stephens (2009) Interactions among wildland fires in a long-established Sierra Nevada natural fire area. *Ecosystems,* 12**,** 114-128.

Congalton, R. G. & K. Green. 2008. *Assessing the accuracy of remotely sensed data: principles and practices*. CRC press.

Crotteau, J. S., M. W. Ritchie, J. M. Varner & J.-P. Berrill (2015) Quercus kelloggii (Newb.) sprout response to fire severity in northern California.

De Santis, A. & E. Chuvieco (2009) GeoCBI: A modified version of the Composite Burn Index for the initial assessment of the short-term burn severity from remotely sensed data. *Remote Sensing of Environment,* 113**,** 554-562.

Dennekamp, M. & M. J. Abramson (2011) The effects of bushfire smoke on respiratory health. *Respirology,* 16**,** 198-209.

Dennison, P. E., S. C. Brewer, J. D. Arnold & M. A. Moritz (2014) Large wildfire trends in the western United States, 1984–2011. *Geophysical Research Letters,* 41**,** 2928-2933.

Duffy, P. A., J. Epting, J. M. Graham, T. S. Rupp & A. D. McGuire (2007) Analysis of Alaskan burn severity patterns using remotely sensed data. *International Journal of Wildland Fire,* 16**,** 277-284.

Eidenshink, J. C., B. Schwind, K. Brewer, Z.-L. Zhu, B. Quayle & S. M. Howard (2007) A project for monitoring trends in burn severity. *Fire ecology,* 3**,** 3-21.

Epting, J., D. Verbyla & B. Sorbel (2005) Evaluation of remotely sensed indices for assessing burn severity in interior Alaska using Landsat TM and ETM+. *Remote Sensing of Environment,* 96**,** 328-339.

Escuin, S., R. Navarro & P. Fernandez (2008) Fire severity assessment by using NBR (Normalized Burn Ratio) and NDVI (Normalized Difference Vegetation Index) derived from LANDSAT TM/ETM images. *International Journal of Remote Sensing,* 29**,** 1053-1073.

French, N. H., E. S. Kasischke, R. J. Hall, K. A. Murphy, D. L. Verbyla, E. E. Hoy & J. L. Allen (2008) Using Landsat data to assess fire and burn severity in the North American boreal forest region: an overview and summary of results. *International Journal of Wildland Fire,* 17**,** 443-462.

Garcia, M. L. & V. Caselles (1991) Mapping burns and natural reforestation using Thematic Mapper data. *Geocarto International,* 6**,** 31-37.

Harden, G. 2016. Audit Report: Forest Service Wildland Fire Activities – Hazardous Fuels Reduction. 42. US Department of Agriculture.

Heward, H., A. M. S. Smith, D. P. Roy, W. T. Tinkham, C. M. Hoffman, P. Morgan & K. O. Lannom (2013) Is burn severity related to fire intensity? Observations from landscape scale remote sensing. *International Journal of Wildland Fire,* 22**,** 910.

Holden, Z. A., P. Morgan & J. S. Evans (2009) A predictive model of burn severity based on 20-year satellite-inferred burn severity data in a large southwestern US wilderness area. *Forest Ecology and Management,* 258**,** 2399-2406.

Holden, Z. A., P. Morgan & A. T. Hudak (2010a) Burn severity of areas reburned by wildfires in the Gila National Forest, New Mexico, USA.

Holden, Z. A., P. Morgan, A. M. Smith & L. Vierling (2010b) Beyond Landsat: a comparison of four satellite sensors for detecting burn severity in ponderosa pine forests of the Gila Wilderness, NM, USA. *International Journal of Wildland Fire,* 19**,** 449-458.

Howard, S. M. & J. M. Lacasse (2004) An evaluation of gap-filled Landsat SLC-off imagery for wildland fire burn severity mapping. *Photogrammetric Engineering and Remote Sensing,* 70**,** 877-880.

Hoy, E. E., N. H. French, M. R. Turetsky, S. N. Trigg & E. S. Kasischke (2008) Evaluating the potential of Landsat TM/ETM+ imagery for assessing fire severity in Alaskan black spruce forests. *International Journal of Wildland Fire,* 17**,** 500-514.

Huang, C.-y., S. E. Marsh, M. P. McClaran & S. R. Archer (2007) Postfire stand structure in a semiarid savanna: Cross-scale challenges estimating biomass. *Ecological Applications,* 17**,** 1899-1910.

Jiang, Y., E. B. Rastetter, A. V. Rocha, A. R. Pearce, B. L. Kwiatkowski & G. Shaver (2015) Modeling carbon–nutrient interactions during the early recovery of tundra after fire. *Ecological Applications,* 25**,** 1640-1652.

Johnstone, J. F. & F. S. Chapin III (2006) Effects of soil burn severity on post-fire tree recruitment in boreal forest. *Ecosystems,* 9**,** 14-31.

Johnstone, J. F. & E. S. Kasischke (2005) Stand-level effects of soil burn severity on postfire regeneration in a recently burned black spruce forest. *Canadian Journal of Forest Research,* 35**,** 2151-2163.

Karau, E. C., P. G. Sikkink, R. E. Keane & G. K. Dillon (2014) Integrating satellite imagery with simulation modeling to improve burn severity mapping. *Environ Manage,* 54**,** 98-111.

Kasischke, E. S., M. R. Turetsky, R. D. Ottmar, N. H. French, E. E. Hoy & E. S. Kane (2008) Evaluation of the composite burn index for assessing fire severity in Alaskan black spruce forests. *International Journal of Wildland Fire,* 17**,** 515-526.

Keeley, J. E. (2009) Fire intensity, fire severity and burn severity: a brief review and suggested usage. *International Journal of Wildland Fire,* 18**,** 116-126.

Kennedy, M. C. & M. C. Johnson (2014) Fuel treatment prescriptions alter spatial patterns of fire severity around the wildland–urban interface during the Wallow Fire, Arizona, USA. *Forest Ecology and Management,* 318**,** 122-132.

Key, C. H. & N. C. Benson (1999) The Normalized Burn Ratio (NBR): A Landsat TM radiometric measure of burn severity. *United States Geological Survey*.

Key, C. H. & N. C. Benson (2006) Landscape assessment (LA). *FIREMON: Fire effects monitoring and inventory system. Gen. Tech. Rep. RMRS-GTR-164-CD, Fort Collins, CO: US Department of Agriculture, Forest Service, Rocky Mountain Research Station*.

Kirkpatrick, C., C. J. Conway & P. B. Jones (2006) Distribution and relative abundance of forest birds in relation to burn severity in southeastern Arizona. *Journal of Wildlife Management,* 70**,** 1005-1012.

Koivula, M., T. Cobb, A. D. Dechene, J. Jacobs & J. R. Spence (2006) Responses of two Sericoda Kirby, 1837 (Coleoptera: Carabidae) species to forest harvesting, wildfire, and burn severity. *Entomologica Fennica,* 17**,** 315.

Koivula, M. J. & F. K. Schmiegelow (2007) Boreal woodpecker assemblages in recently burned forested landscapes in Alberta, Canada: effects of post-fire harvesting and burn severity. *Forest Ecology and Management,* 242**,** 606-618.

Kokaly, R. F., B. W. Rockwell, S. L. Haire & T. V. King (2007) Characterization of post-fire surface cover, soils, and burn severity at the Cerro Grande Fire, New Mexico, using hyperspectral and multispectral remote sensing. *Remote Sensing of Environment,* 106**,** 305-325.

Kolden, C. A., J. A. Lutz, C. H. Key, J. T. Kane & J. W. van Wagtendonk (2012) Mapped versus actual burned area within wildfire perimeters: characterizing the unburned. *Forest Ecology and Management,* 286**,** 38-47.

Kolden, C. A., A. M. Smith & J. T. Abatzoglou (2015) Limitations and utilisation of Monitoring Trends in Burn Severity products for assessing wildfire severity in the USA. *International Journal of Wildland Fire,* 24**,** 1023-1028.

Kotliar, N. B., S. J. Hejl, R. L. Hutto, V. A. Saab, C. P. Melcher & M. E. McFadzen (2002) Effects of fire and post-fire salvage logging on avian communities in conifer-dominated forests of the western United States.

Kotliar, N. B., P. L. Kennedy & K. Ferree (2007) Avifaunal responses to fire in southwestern montane forests along a burn severity gradient. *Ecological Applications,* 17**,** 491-507.

Lentile, L. B., Z. A. Holden, A. M. Smith, M. J. Falkowski, A. T. Hudak, P. Morgan, S. A. Lewis, P. E. Gessler & N. C. Benson (2006) Remote sensing techniques to assess active fire characteristics and post-fire effects. *International Journal of Wildland Fire,* 15**,** 319-345.

Lentile, L. B., F. W. Smith & W. D. Shepperd (2005) Patch structure, fire-scar formation, and tree regeneration in a large mixed-severity fire in the South Dakota Black Hills, USA. *Canadian Journal of Forest Research,* 35**,** 2875-2885.

Li, P., L. Jiang & Z. Feng (2013) Cross-comparison of vegetation indices derived from landsat-7 enhanced thematic mapper plus (ETM+) and landsat-8 operational land imager (OLI) sensors. *Remote Sensing,* 6**,** 310-329.

Liu, D., I. B. Tager, J. R. Balmes & R. J. Harrison (1992) The effect of smoke inhalation on lung function and airway responsiveness in wildland fire fighters. *American Review of Respiratory Disease,* 146**,** 1469-1469.

Loboda, T., K. J. O'Neal & I. Csiszar (2007) Regionally adaptable dNBR-based algorithm for burned area mapping from MODIS data. *Remote Sensing of Environment,* 109**,** 429-442.

Lutz, J. A., C. H. Key, C. A. Kolden, J. T. Kane & J. W. van Wagtendonk (2011) Fire frequency, area burned, and severity: a quantitative approach to defining a normal fire year. *Fire Ecology,* 7**,** 51-65.

Malison, R. L. & C. V. Baxter (2010) The fire pulse: wildfire stimulates flux of aquatic prey to terrestrial habitats driving increases in riparian consumers. *Canadian Journal of Fisheries and Aquatic Sciences,* 67**,** 570-579.

Malmström, A. 2006. *Effects of wildfire and prescribed burning on soil fauna in boreal coniferous forests*.

Markham, B. L., J. C. Storey, D. L. Williams & J. R. Irons (2004) Landsat sensor performance: history and current status. *IEEE Transactions on Geoscience and Remote Sensing,* 42**,** 2691-2694.

Meigs, G. W., D. C. Donato, J. L. Campbell, J. G. Martin & B. E. Law (2009) Forest fire impacts on carbon uptake, storage, and emission: the role of burn severity in the Eastern Cascades, Oregon. *Ecosystems,* 12**,** 1246-1267.

Mercer, D. E. & J. P. Prestemon (2005) Comparing production function models for wildfire risk analysis in the wildland–urban interface. *Forest Policy and Economics,* 7**,** 782-795.

Miller, J. D., E. E. Knapp, C. H. Key, C. N. Skinner, C. J. Isbell, R. M. Creasy & J. W. Sherlock (2009a) Calibration and validation of the relative differenced Normalized Burn Ratio (RdNBR) to three measures of fire severity in the Sierra Nevada and Klamath Mountains, California, USA. *Remote Sensing of Environment,* 113**,** 645-656.

Miller, J. D. & H. Safford (2012) Trends in wildfire severity: 1984 to 2010 in the Sierra Nevada, Modoc Plateau, and southern Cascades, California, USA. *Fire Ecology,* 8**,** 41-57.

Miller, J. D., H. D. Safford, M. Crimmins & A. E. Thode (2009b) Quantitative Evidence for Increasing Forest Fire Severity in the Sierra Nevada and Southern Cascade Mountains, California and Nevada, USA. *Ecosystems,* 12**,** 16-32.

Miller, J. D. & A. E. Thode (2007) Quantifying burn severity in a heterogeneous landscape with a relative version of the delta Normalized Burn Ratio (dNBR). *Remote Sensing of Environment,* 109**,** 66-80.

Miller, M., W. Elliot, M. Billmire, P. Robichaud & K. Endsley (2016) Rapid-response tools and datasets for post-fire remediation: linking remote sensing and process-based hydrological models. *International Journal of Wildland Fire,* 25**,** 1061-1073.

Mitchell, M. & F. Yuan (2010) Assessing forest fire and vegetation recovery in the Black Hills, South Dakota. *Giscience & Remote Sensing,* 47**,** 276-299.

Murphy, K. A., J. H. Reynolds & J. M. Koltun (2008) Evaluating the ability of the differenced Normalized Burn Ratio (dNBR) to predict ecologically significant burn severity in Alaskan boreal forests. *International Journal of Wildland Fire,* 17**,** 490-499.

Nappi, A., P. Drapeau, M. Saint-Germain & V. A. Angers (2010) Effect of fire severity on long-term occupancy of burned boreal conifer forests by saproxylic insects and wood-foraging birds. *International Journal of Wildland Fire,* 19**,** 500-511.

New Jersey Department of the Treasury, O. o. M. a. B. 2006. State of New Jersey: The Governor's FY2007 Detailed Budget. D-123.

---. 2008. State of New Jersey: The Governor's FY2009 Detailed Budget. D-127.

---. 2010. State of New Jersey: The Governor's FY2011 Detailed Budget. D-113.

---. 2012. State of New Jersey: The Governor's FY2013 Detailed Budget. 563.

---. 2014. State of New Jersey: The Governor's FY2015 Detailed Budget. 586.

---. 2016. State of New Jersey: The Governor's FY2017 Detailed Budget. D-114.

NIFC (2016).

North, M. P. & M. D. Hurteau (2011) High-severity wildfire effects on carbon stocks and emissions in fuels treated and untreated forest. *Forest Ecology and Management,* 261**,** 1115-1120.

Parks, S., G. Dillon & C. Miller (2014) A New Metric for Quantifying Burn Severity: The Relativized Burn Ratio. *Remote Sensing,* 6**,** 1827-1844.

Parks, S. A., L. M. Holsinger, C. Miller & C. R. Nelson (2015) Wildland fire as a self-regulating mechanism: the role of previous burns and weather in limiting fire progression. *Ecological Applications*.

Parks, S. A., C. Miller, C. R. Nelson & Z. A. Holden (2013) Previous Fires Moderate Burn Severity of Subsequent Wildland Fires in Two Large Western US Wilderness Areas. *Ecosystems,* 17**,** 29-42.

Parson, A., P. R. Robichaud, S. A. Lewis, C. Napper & J. T. Clark (2010) Field guide for mapping post-fire soil burn severity.

Penman, T., F. Christie, A. Andersen, R. A. Bradstock, G. Cary, M. Henderson, O. Price, C. Tran, G. Wardle & R. J. Williams (2011) Prescribed burning: how can it work to conserve the things we value? *International Journal of Wildland Fire,* 20**,** 721-733.

Pereira, J. M. & Y. Govaerts (2001) Potential fire applications from MSG/SEVIRI observations. *Darmstadt, Eumetsat,* 41.

Perry, D. A., P. F. Hessburg, C. N. Skinner, T. A. Spies, S. L. Stephens, A. H. Taylor, J. F. Franklin, B. McComb & G. Riegel (2011) The ecology of mixed severity fire regimes in Washington, Oregon, and Northern California. *Forest Ecology and Management,* 262**,** 703-717.

Picotte, J. J., B. Peterson, G. Meier & S. M. Howard (2016) 1984–2010 trends in fire burn severity and area for the conterminous US. *International Journal of Wildland Fire,* 25**,** 413-420.

Prichard, S. J. & M. C. Kennedy (2012) Fuel treatment effects on tree mortality following wildfire in dry mixed conifer forests, Washington State, USA. *International Journal of Wildland Fire,* 21**,** 1004-1013.

--- (2014) Fuel treatments and landform modify landscape patterns of burn severity in an extreme fire event. *Ecological applications,* 24**,** 571-590.

Prichard, S. J., D. L. Peterson & K. Jacobson (2010) Fuel treatments reduce the severity of wildfire effects in dry mixed conifer forest, Washington, USA. *Canadian Journal of Forest Research,* 40**,** 1615-1626.

Reinhardt, E. D. 2003. Using FOFEM 5.0 to estimate tree mortality, fuel consumption, smoke production and soil heating from wildland fire. In *Proceedings of the 2nd International Wildland Fire Ecology and Fire Management Congress and 5th Symposium on Fire and Forest Meteorology*, 16-20.

Reinhardt, E. D. & M. B. Dickinson (2010) First-order fire effects models for land management: overview and issues.

Reinhardt, E. D., R. E. Keane & J. K. Brown (2001) Modeling fire effects. *International Journal of Wildland Fire,* 10**,** 373-380.

Robichaud, P. R., S. A. Lewis, D. Y. Laes, A. T. Hudak, R. F. Kokaly & J. A. Zamudio (2007) Postfire soil burn severity mapping with hyperspectral image unmixing. *Remote Sensing of Environment,* 108**,** 467-480.

Rocha, A. V. & G. R. Shaver (2009) Advantages of a two band EVI calculated from solar and photosynthetically active radiation fluxes. *Agricultural and Forest Meteorology,* 149**,** 1560-1563.

--- (2011) Burn severity influences postfire CO2 exchange in arctic tundra. *Ecological Applications,* 21**,** 477-489.

Rogers, B., S. Veraverbeke, G. Azzari, C. Czimczik, S. Holden, G. Mouteva, F. Sedano, K. Treseder & J. Randerson (2014) Quantifying fire-wide carbon emissions in interior Alaska using field measurements and landsat imagery. *Journal of Geophysical Research: Biogeosciences,* 119**,** 1608-1629.

Rose, E. T., T. R. Simons, R. Klein & A. J. McKerrow (2016) Normalized burn ratios link fire severity with patterns of avian occurrence. *Landscape Ecology***,** 1-14.

Rothermel, R. C. (1972) A mathematical model for predicting fire spread in wildland fuels.

Rothman, N., D. P. Ford, M. E. Baser, J. A. Hansen, T. O'Toole, M. S. Tockman & P. T. Strickland (1991) Pulmonary function and respiratory symptoms in wildland firefighters. *Journal of Occupational and Environmental Medicine,* 33**,** 1163-1167.

Schoennagel, T., T. T. Veblen & W. H. Romme (2004) The interaction of fire, fuels, and climate across Rocky Mountain forests. *BioScience,* 54**,** 661-676.

Soverel, N. O., D. D. B. Perrakis & N. C. Coops (2010) Estimating burn severity from Landsat dNBR and RdNBR indices across western Canada. *Remote Sensing of Environment,* 114**,** 1896-1909.

Stambaugh, M. C., L. D. Hammer & R. Godfrey (2015) Performance of burn-severity metrics and classification in oak woodlands and grasslands. *Remote Sensing,* 7**,** 10501-10522.

Strom, B. A. & P. Z. Fulé (2007) Pre-wildfire fuel treatments affect long-term ponderosa pine forest dynamics. *International Journal of Wildland Fire,* 16**,** 128-138.

Sunderman, S. O. & P. J. Weisberg (2011) Remote sensing approaches for reconstructing fire perimeters and burn severity mosaics in desert spring ecosystems. *Remote Sensing of Environment,* 115**,** 2384-2389.

Swiston, J. R., W. Davidson, S. Attridge, G. T. Li, M. Brauer & S. F. van Eeden (2008) Wood smoke exposure induces a pulmonary and systemic inflammatory response in firefighters. *European Respiratory Journal,* 32**,** 129-138.

Turner, M. G., W. W. Hargrove, R. H. Gardner & W. H. Romme (1994) Effects of fire on landscape heterogeneity in Yellowstone National Park, Wyoming. *Journal of Vegetation Science,* 5**,** 731-742.

van Eeden, S. F., A. Yeung, K. Quinlam & J. C. Hogg (2005) Systemic response to ambient particulate matter: relevance to chronic obstructive pulmonary disease. *Proceedings of the American Thoracic Society,* 2**,** 61-67.

Van Wagtendonk, J. W., R. R. Root & C. H. Key (2004) Comparison of AVIRIS and Landsat ETM+ detection capabilities for burn severity. *Remote Sensing of Environment,* 92**,** 397-408.

Veraverbeke, S., S. Lhermitte, W. W. Verstraeten & R. Goossens (2010) The temporal dimension of differenced Normalized Burn Ratio (dNBR) fire/burn severity studies: The case of the large 2007 Peloponnese wildfires in Greece. *Remote Sensing of Environment,* 114**,** 2548-2563.

--- (2011) A time-integrated MODIS burn severity assessment using the multi-temporal differenced normalized burn ratio (dNBRMT). *International Journal of Applied Earth Observation and Geoinformation,* 13**,** 52-58.

Veraverbeke, S., E. N. Stavros & S. J. Hook (2014) Assessing fire severity using imaging spectroscopy data from the Airborne Visible/Infrared Imaging Spectrometer (AVIRIS) and comparison with multispectral capabilities. *Remote Sensing of Environment,* 154**,** 153-163.

Verbyla, D. L., E. S. Kasischke & E. E. Hoy (2008) Seasonal and topographic effects on estimating fire severity from Landsat TM/ETM+ data. *International Journal of Wildland Fire,* 17**,** 527-534.

Wagner, C. V. (1973) Height of crown scorch in forest fires. *Canadian Journal of Forest Research,* 3**,** 373-378.

Warner, T. A., N. S. Skowronski & M. R. Gallagher (2017) High spatial resolution burn severity mapping of the New Jersey Pine Barrens with WorldView-3 near-infrared and shortwave infrared imagery. *International Journal of Remote Sensing,* 38**,** 598-616.

Whittier, T. R. & A. N. Gray (2016) Tree mortality based fire severity classification for forest inventories: A Pacific Northwest national forests example. *Forest Ecology and Management,* 359**,** 199-209.

Wiedinmyer, C. & J. C. Neff (2007) Estimates of CO 2 from fires in the United States: implications for carbon management. *Carbon Balance and Management,* 2**,** 10.

Williams, C. A., G. J. Collatz, J. Masek, C. Huang & S. N. Goward (2014) Impacts of disturbance history on forest carbon stocks and fluxes: Merging satellite disturbance mapping with forest inventory data in a carbon cycle model framework. *Remote Sensing of Environment,* 151**,** 57-71.

Wimberly, M. & M. Reilly (2007) Assessment of fire severity and species diversity in the southern Appalachians using Landsat TM and ETM+ imagery. *Remote Sensing of Environment,* 108**,** 189-197.

Table 1. Specifications of Sensors Useful for Calculating NIR (700 - 1400nm) and SWIR (1400 - 2500) Based Burn Severity Indices

Sensor	NIR Band	NIR band-width (nm)	Spatial Res.	SWIR band	SWIR band-width (nm)	Spatial Res.	Revisit Cycle	Domain	Availability
Terra MODIS	2	841 - 876	250m	7	2105 - 2155	500m	16 days	Public	12/18/99 - present
Aqua MODIS	2	841 - 876	250m	7	2105 - 2155	500m	16 days	Public	5/4/02 - present
Landsat 4 TM	4	760 - 900	30m	7	2080 - 2650	30m	18 days	Public	7/16/82 - 7/87
Landsat 5 TM	4	760 - 900	30m	7	2080 - 2650	30m	18 days	Public	4/1/84 - 12/21/12
Landsat 7 ETM+	4	770 - 900	30m	7	2090 - 2350	30m	16 days	Public	4/15/99 - present
Landsat 8	5	850 - 880	30m	7	2110 - 2290	30m	16 days	Public	2/2/11 - present
ASTER	3N	760 - 860	15m	4	1600 - 1700	30m	16 days	Public	12/18/99 - present
	3B	701 - 860	30m	5	2145 - 2185	30m			
				6	2185 - 2225	30m			
				7	2235 - 2285	30m			
				8	2295 - 2365	30m			
				9	2360 - 2430	30m			
World-view 3	6	705 - 745	7m[a]	10	1550 - 1590	7m[b]	By-request	Comm.	8/13/14 - present
	7	770 - 895	7m[a]	11	1640 - 1680	7m[b]			
	8	860 - 1040	7m[a]	12	1710 - 1750	7m[b]			
	9	1195 - 1225	7m[b]	13	2145 - 2185	7m[b]			
				14	2185 - 2225	7m[b]			
				15	2235 - 2285	7m[b]			
				16	2295 - 2365	7m[b]			

Quickbird	4	760 - 900	2.4m	(no SWIR band)		By-request	Comm.	10/15/01 - 12/17/14
AVIRIS	70 bands in 10nm increments between 700 - 1400nm		2.4m	90 bands in 10nm increments between 1400 - 2500nm	Up to 2.4m	By-request	Public	1987 - present

[a] *Data is collected with a 1.24m spatial resolution but served at a 7.00m resolution*
[b] *Data is collected with a 3.40m spatial resolution but served at a 7.00m resolution*

CHAPTER 2: Evaluation of Field and Remote Sensing Burn Severity Indices in a Northeastern Pine-dominated Landscape

Abstract

Remotely sensed burn severity maps have become an important tool for fire ecologists and managers, enabling them to estimate variability in fire effects more rapidly, safely, and effectively than field methods alone permit. The effectiveness of these maps, however is based on the strengths of relationships between the remotely sensed and field indices of burn severity from which they are derived. Despite the breadth of work validating the use of remotely sensed burn severity, differences in field indices, remotely sensed indices, and sensor types used to derive these relationships has made rigorous comparison of these indices difficult. This study evaluates the prediction of two field indices, CBI and WCBI, from a total of 15 candidate models each, varying by remote sensing index used as a predictor (NBR, dNBR, RdNBR, and RBR), and equation form (polynomial, exponential, and sigmoidal). Models were ranked based on AIC and RRS, providing means to choose an optimal model for this environment. Overall, the results of this study document strong relationships between field and remotely sensing burn severity indices derived from Landsat ETM+ data for the pitch pine dominated forests of New Jersey's Pinelands National Reserve (PNR), and provide evidence to support the selection of specific a specific methodology for predicting field indices from remotely sensed data. Models that predicted WCBI tended to have lower AICs and RSSs than those that predicted CBI, and the two highest ranking models predicted WCBI from single-date (post-fire) NBR, rather than indices generated from multi-temporal (pre- and post-fire) data.

Introduction

Remote sensing of burn severity can be used to monitor short and long term fire effects. Burn severity is defined as the magnitude of environmental change incurred and is measured

following fire, typically using satellite imagery that is calibrated to field data (Kolden, Smith and Abatzoglou 2015, Keeley 2009). Burn severity differs from fire intensity, which describes energetic properties of active fire (Byram 1959, Rothermel 1972, Ryan and Noste 1985, Cram, Baker and Boren 2006), although both burn severity and fire intensity are theoretically linked through the combustion and heat transfer processes that cause fire effects, however, little is known about the exact relationship between burn severity and fire intensity (Heward et al. 2013). When remotely sensed burn severity estimates are calibrated with other field observations of burn severity, or other fire effects, relationships can be defined that enable researchers and managers to draw inferences about fire effects where only remote sensing data is available. Not does this facilitate much faster analyses of fire effects than when only using field methods, but the spatial resolution and wall-to-wall coverage of remotely sensed burn severity data can provide highly comprehensive and spatially discrete maps of change resulting from fire (Chapter 1).

One common use of remotely sensed burn severity maps has been to estimate fire perimeters, including unburned interior areas that traditional mapping methods often miss (Kolden et al. 2012), however it has also been used to identify the locations of specific fire effects that are of interest to fire managers, researchers, and policy makers. For instance, a substantial breadth of research using burn severity has been conducted in boreal forest to be correlate fire activity with fuel consumption and emissions (Boby et al. 2010), mortality and regeneration patterns of dominant tree species (Johnstone and Kasischke 2005), post-fire avian occurrence (Rose et al. 2016, Latif et al. 2016), changes in soil hydraulics (Moody et al. 2016), the influence on vegetation characteristics and weather fire effects (Birch et al. 2015, Davies et al. 2016, Viedma et al. 2015), and patterns of vegetation recovery following fire (Crotteau et al.

2015, Chambers et al. 2016). Hence this tool is useful in many aspects of forestry and wildlife research and management.

The Composite Burn Index (CBI) is the most common field-based index for quantifying burn severity, and involves ranking burn severity indicators within specific forest strata at sample plots and summarizing them with a simple formula (Key and Benson 2006). A total of 24 vegetation and substrate indicators are ranked on a [0-3] scale on a field sheet, representing the range of "No Effect" to "High Effect" (Figure 1). Ranks are then used in equations to summarize, overstory, and total Composite Burn Index (CBI) for each plot. Several slight variants of this method have been introduced in the existing literature, which involve omitting indicators that are impractical to measure or are irrelevant in the sample plot. For example, the GeoCBI variant uses a weighting factor based on leaf area index for each strata of vegetation when summarizing results and has gained increasing attention (De Santis and Chuvieco 2009). Similarly, Weighted CBI (WCBI) uses a focal estimation of percent cover to weight burn index rankings in each stratum, before estimating Total CBI (Cansler and McKenzie 2012). In southern Appalachian pine and oak dominated forest, a vastly simplified version of CBI that included only crown scorch and shrub damage was found to be well correlated with remotely sensed burn severity (Wimberly and Reilly 2007). Similarly, Koivula et al. (2006) evaluated severity solely on scorch class in one study, which provided useful covariate for beetle population data.

A variety of remotely sensed burn severity indices have been proposed and are typically validated and rescaled to predict CBI values, using regression equations. This is necessary, because remotely sensed burn severity indices measure altered surface reflectance, and therefore indirectly estimates physical change to vegetation and substrates. The most common methods for estimating burn severity are derived from near infrared (NIR) and short-wave infra-red (SWIR) imagery, which is represented by the bandwidths of 700 – 1400nm and 1400 –

2500nm, respectively (Warner, Skowronski and Gallagher 2017). The Near Burn Ratio (NBR) is the simplest of these indices and is a precursor in methods used to estimate other NIR and SWIR based indices. NBR is typically calculated from Landsat Thematic Mapper bands 5 and 7 (Key and Benson 1999). While multiple bands of Landsat data are available, these bands are less are the most sensitive to burned vegetation and soils while also being less correlated to each other than bands (Garcia and Caselles 1991). NBR is calculated using single date imagery hence it is readily obtainable. However this also means it is also unable to differentiate between burn severity and other forest disturbances that could have altered reflectance prior to burning. This can be resolved, however, by differencing bi-temporal NBR images that represent pre- and post-fire vegetation conditions, making it robust under a wide variety of forest conditions (Key and Benson 2006). NBR and differenced NBR (dNBR) are both absolute measures of burn severity, however, meaning that they are subject to showing greater change where pre-burn vegetation is denser, even if a less dense area had greater consumption. As a result, a relative form of dNBR (RdNBR) and the relative burn ratio (RBR) have been developed as NBR-based bi-temporal alternatives which are normalized to pre-burn vegetation reflectance (Miller and Thode 2007). Although theoretical arguments have been made in support of each one of these indices over the others, inconsistent differences in the strengths of correlations between field data and these indices have made it impossible to determine the superiority of an optimal index. Thus the most appropriate method for any new site location should be selected based on a rigorous comparison with field data.

Although multiple studies have compared various NIR and SWIR-based remote sensing indices with CBI and WCBI, few studies have evaluated the entire suite of these indices for optimization purposes. Similarly, optimization should also consider the suite of sensors that collect NIR and SWIR data, which each have slightly different bandwidth specifications and

therefore will produce slightly different results. For instance, in eastern pine-dominated forests, dNBR has been evaluated using Landsat TM, ETM+ (Wimberly and Reilly 2007, Picotte and Robertson 2011), and OLI sensors (Unger, Hung and Zhangb 2016), and Worldview 3 sensors (Warner et al. 2017), however, other NIR and SWIR based indices that may have had stronger correlations have not been tested. For instance, one study in the southeast revealed that although dNBR frequently outperformed NBR (Picotte and Robertson 2011). Likewise, in the Pacific Northwest, multiple studies reported that RdNBR consistently outperformed dNBR (Miller et al. 2009, Newcomer et al. 2009). Still further, a separate study reported that RBR consistently outperformed both RdNBR and dNBR in mixed conifer forests of from southwestern US to the Northern Rockies (Parks, Dillon and Miller 2014). However, none of these studies compare each remote sensing index, and some use different sensors, making it difficult to truly determine which is actually optimal.

My study aims to evaluate the use of NBR, dNBR, RdNBR, and RBR for pine-oak vegetation, common to coastal plains and ridgetops of the eastern US. We examine correlations between field and remotely sensed burn severity across 110 plots burned in prescribed and wildfires in the New Jersey PNR that occurred between 2013 and 2015. In my examination, I evaluate which index is most correlated with field data and which index is most successful at differentiating burned from unburned area. Finally, the results are summarized terms of their implications in pine-oak forests, as well as the broader context of remotely sensed burn severity indices.

Methods

Site Description

Burn severity was studied within the New Jersey Forest Fire Service's Central Division primary response area, in the New Jersey Pinelands ecological area. The New Jersey Pinelands

experiences a higher frequency of fires than other areas in the northeastern US, and often experiences tens of thousands of burned hectares per year (Forman and Boerner 1981). This area remains the locale of the majority of the state's fire activity (La Puma 2012). Its landscape is home to a variety of upland and wetland forest ecosystems, many of which are fire dependent and have experienced a high frequency of fire since before European settlement (Forman 2012). Of this landscape, 62% is comprised of upland forests (Lathrop and Kaplan 2004), which are subjected to the greatest amount of fire activity. These upland forests are dominated by three major communities; 1) oak-dominated stands, consisting of black oak (*Quercus velutina* Lam.), chestnut oak (*Q. prinus* L.), white oak (*Q. alba* L.), pitch pine (*Pinus rigida* Mill.), and shortleaf pine (*P. echinata* Mill.), 2) mixed stands, with pitch pine and mixed oaks in the overstory, and 3) pitch pine-dominated stands, consisting of pitch pine with few overstory oaks and abundant scrub oaks (*Q. marilandica* Muenchh., *Q. ilicifolia* Wangenh.) in the understory (McCormick and Jones 1973). Understory communities in these forests are dominated by varying mixes of ericaceous shrubs, shrub oaks, and associated species, such as lowbush blueberry (*Vaccinium palladum* Aiton and *angustifolium* Aiton), black huckleberry (*Gaylussacia baccata* (Wangenh.) K. Koch.), scrub oak (*Q. ilicifolia*), black jack oak (*Q. marilandica*), inkberry holly (*Ilex glabra*).

Field data

Field data were collected in 110 plots in burned and unburned conditions of upland forest, dominated by pines, between 2013 and 2015 (Figure 2). 77 plots were spread among 23 prescribed burn units, 20 plots were spread across 5 wildfires, and 13 were located in 6 stands that did not burn (Table 1). Three of the unburned plots, located at Jenkins (see Table 1), were prescribe burned two years prior to the study. Plot locations were recorded using a Trimble GeoExplorer 6000 GPS unit, paired with a Tornado receiver (Trimble Inc., Sunnyvale, CA, USA).

Differential correction was performed on point data to estimate horizontal accuracy of measured coordinates to be within 3m or less of the actual field location.

CBI and WCBI field factors were measured within a 15m radius of the GPS points. In the New Jersey Pinelands, and other pitch pine barrens, overstory pines and the understory of predominantly deciduous shrubs senesce more than half of foliage for the dormant season, when prescribed burning is conducted. Given that most factors assessed with the CBI and WCBI protocols are linked to the amount of foliage, and vegetation effects from dormant season burns are not necessarily visible until the growing season, this data was collected during the growing season (Table 1). This timing differs somewhat from that described in other studies that have focused on growing season fire, however, few studies have included dormant season burning when both evergreen and deciduous foliage are factors.

Sampling was conducted as an extended assessment, using a modified form of the Composite Burn Index method (Key and Benson 2006), which involved omitting 4 of the possible 23 evaluation factors that did not apply to the Pinelands environment or were difficult to observe objectively. For instance, ranking effects to downed heavy fuel with a diameter greater than 20.32cm was omitted because fuels of that class were not found in any of the survey plots. Likewise, “colonizers” and “species relative abundance” were deemed a poor metric of severity, since pre-fire species typically re-colonize following fire through sprouting of subsurface rhizomes during the growing season following fire (Matlack, Gibson and Good 1993). Focally estimated percent cover of vegetation (FCOV), assessed for each strata as part of the CBI method, permitted calculation of WCBI.

Image processing and generation of burn severity maps

Maps of NBR, dNBR, RdNBR, and RBR were generated for each year, within the study area, as the results of a sequence of data processing steps (Figure 3). Landsat 7 ETM+ scenes of

path 32-33 and row 13-14, acquired through the USGS GLOVIS database (Table 2). Although many prior studies have based burn severity maps on data collected within ± 2 weeks of fires, to control for the amount of regeneration that occurs following fire, and to control for ambient pre- and post-fire reflectance, this approach does not control for seasonal variation in ambient reflectance that can occur between fires. Further, regeneration following dormant season fire in temperate-deciduous and temperate-mixed forests does not initiate until the growing season, although substantial regeneration following growing season fire can occur within weeks, making it difficult to compare both types of fire when using the typical ± 2 week window. Therefore the burn severity maps were generated data from the growing season following fire. I further constrained the timing of imagery to the period between Julian dates 176 and 288, which correspond to the period of full leaf expansion (Clark et al. 2012).

Standard raw image processing steps were necessary before imagery could be used to generate burn severity maps. First, pixel values were converted from digital numbers to top of atmosphere reflectance values to normalize for natural variation in solar angle and the distance between the sun and the Earth (Chander, Markham and Helder 2009). Next, pixels with incomplete information, which occur often at the edges of missing data swaths in SLC-off imagery, were selected and removed. Next, clouds and cloud shadows that obscured areas burned by fires were manually masked. Radiometric correction was then performed, by scaling reflectance values of regions dominated by evergreens that have little variation in reflectance between seasons and years under normal growing conditions (Isaacson, Serbin and Townsend 2012). For this purpose, Atlantic White Cedar (*Chameacyparis thyoides)* stands, present in all imagery, were chosen and used to calibrate all data to 2010 Landsat 5 TM imagery for being the clearest and most complete image of all years. This provided a selection of multiple calibrated growing season images for each year of the study, but that did not completely cover the area of

interest due to SLC-off missing data or masked clouds. I chose to fill gaps in data by mosaicking the calibrated imagery as necessary, to produce complete coverage of the fires monitored in this study (Veraverbeke et al. 2011). Mosaicked images were then used to compute burn severity coverages for each year. Burn severity indices were then computed as follows.

$NBR = \frac{NIR-SWIR}{NIR+SWIR}$, (Key and Benson 1999)

$dNBR = NBR_{pre} - NBR_{post}$, (Key and Benson 2006)

$RdNBR = \frac{dNBR}{\sqrt{ABS(\frac{NBR_{pre}}{1000})}}$, (Miller and Thode 2007)

$RBR = \frac{dNBR}{NBR_{pre}+1.001}$ (Parks et al. 2014)

For each CBI plot location, I extracted values or each burn severity index for GPS point described in the previous section. Since it is unlikely for CBI plots to be centered on Landsat pixels, due to horizontal error in GPS and Landsat datasets, it is common to extract indices either as an average of pixel values in a 3 x 3 window, surrounding the GPS point (Miller and Thode 2007), or by using bilinear interpolation to derive an average of the four nearest pixels that is weighted based on the distances of pixel centroids from the GPS point (Cansler and McKenzie 2012). Given the size of the field plots (30m diameter) and the size of pixels (30 x 30m), a 3 x 3 window would inevitably incorporate pixels that were not observed in the field, producing edge effects. I therefore used bilinear interpolation, which incorporated pixels on a more appropriate spatial scale given my field plots.

Evaluation of Remote Sensing Data with Field Data

Twelve models were developed to predict CBI and WCBI. Each model differed by the independent variable used (NBR, dNBR, RdNBR, and RBR) and the equation form (polynomial, exponential, sigmoidal). Similar variation in models can be observed in previous studies (Chen et al. 2011, Warner et al. 2017, Wimberly and Reilly 2007, Picotte and Robertson 2011). The

polynomial (Eqn. 1), exponential (Eqn. 2), and sigmoidal equations (Eqn. 3) used in this study are given in the following equations, where x and *y* represent remotely sensed and field burn severity indices, respectively, and other symbols represent coefficients.

$$y = \beta_0 + \beta_1 x + \beta_2 x^2 \quad \text{(Eqn. 1)}$$

$$y = \beta_0 + \beta_1(1 - e^{-\beta_2 x}) \quad \text{(Eqn. 2)}$$

$$y = \frac{\beta_0}{1+e^{-(\beta_1(x-\beta_2))}} \quad \text{(Eqn. 3)}$$

I used a two-step process to first identify the best models to predict CBI and WCBI, and second select which of those two resultant models was better. To select the best CBI and WCBI models, I used a k-fold leave one out cross validation approach to calculate Residual Sum of Square (RSS) and Akaike's Information Criterion (AIC) for each model and compared them within CBI and WCBI model groups. In each iteration of the k-fold process, the data was ordinated by CBI and split into 5 quantiles, from which 80% of plots in each quantile were selected and combined into a training dataset, and the remaining 20% of data was reserved for testing. This ensured that training and test data each represented the same range of the burn severity observed. Outputs for each group models (i.e. CBI and WCBI) were then evaluated using RSS as a primary criterion and AIC as a secondary criterion, when RSS values were similar, to select the top CBI and WCBI models. The two resulting models were then rerun using the entire dataset, and coefficient of determination and coefficient values were calculated for the observed values versus the model predicted values.

Results

A total of 110 field plots were assessed using CBI and WCBI methods. CBI values ranged from 0 – 2.68, representing 89% of the potential range of burn severity. In contrast, WCBI ranged of 0 – 2.49, representing only 83% of the possible range of burn severity. Mean CBI and WCBI across all plots were nearly identical, however, the variance of WCBI was much lower

(Table 3) and its distribution was much narrower (Figure 5). FCOV was substantially higher in the bottom two forest strata for nearly all fires than in the top 3 strata, indicating that WCBI is influenced by effects in the lower strata much more so than in the upper strata (Table 3).

Across all plots, ranges of NBR, dNBR, RdNBR, and RBR were [-7 – 799], [-6 – 760], [0 – 914], and [-3 – 450], respectively, defining the range from no effect to a high degree of effect. Means for each index were 473, 187, 233, and 112. Maps of remotely sensed burn severity are provided in Figure 6 to illustrate spatial of variability observed in prescribed fires and wildfires.

RSS and AIC of each candidate model are provided in Table 4. For models of the CBI group, those with polynomial and sigmoidal functions and tended to have more favorable RSS and AIC values than those with exponential functions. This was similarly observed among WCBI which also tended to have more favorable RSS values when NBR was the independent variable rather than a bi-temporal index. The best choice CBI model was that with a polynomial function and rdNBR as the independent variable, while the best choice WCBI model was the exponential model which used NBR as the independent variable. Coefficient estimates for all candidate models are provided in Table 5. Coefficients of determination of observed vs. predicted values for the top CBI and WCBI were 0.74 and 0.68, respectively, indicating the CBI model as the best choice model (Figure 7).

Discussion

This study evaluated the prediction of two field indices of burn severity, CBI and WCBI, in eastern pitch pine-dominated forests using commonly used NIR and SWIR-based burn severity indices and equation forms, to provide evidence for the selection of the optimal combination of field index, remote sensing index, and equation form. The results of this study suggest that that despite the similarities of approaches used in previous studies, differences in the derivations of field and remote sensing indices and equation forms used to describe relationships can impact

the level of information predicted by calibration models, and may limit the comparability of studies that with varying approaches.

On average, WCBI was more closely related to remote sensing indices of burn severity than CBI, as indicated by lower RRS and AIC values in Table 5. This result differs from that of Cansler and McKenzie (2012), who found that CBI had somewhat stronger correlations with both dNBR and RdNBR than GeoCBI (similar to WCBI) did in temperate coniferous forests of the Cascade Range of the Pacific Northwest. Interestingly, single date NBR was also a stronger independent variable for predicting WCBI than similar bi-temporal indices, thought to be more robust. Despite these overall trends in WCBI models, the a CBI model which used a polynomial equation and rdNBR as the independent variable was found to be best over all other candidate models (Figure 7).

The key difference between CBI and WCBI models is the inclusion of a forest density estimate used to weight severity data from each strata. In the case of this study, WCBI was largely influenced by patterns in FCOV, which manifest as homogenously dense conditions in understory strata, below 1m, and substantially sparser conditions in the overstory. This effectively diminishes the importance of the overstory strata in WCBI calculations, and augmenting those of the understory, to the extent that understory variability dwarfed that factors >1m in WCBI calculations (Table 3). The consistency of this pattern across widely dispersed plots suggest this pattern is likely a landscape scale trend in the vegetation, which may diminish the value of WCBI in this environment, although it remains unclear whether this trend is natural, or due to historic or recent forest management strategies (such as even aged regeneration from previous landscape scale clear cutting or landscape scale fire activity). Similarly, FCOV is a 'rough' estimate of the vertical distribution of forest structure, given that is focally estimated, and, more rigorous evaluations of the connection between forest structure

and remotely sensed burn severity estimates, such as LiDAR, would produce better input data for WCBI estimates. Although LiDAR data has historically been expensive and complicated to acquire, the advent of new, easier to use off-the shelf LiDAR devices may aid in FCOV estimation in the near future.

It was also interesting that WCBI was best predicted by NBR in all cases. Since NBR is a single-date index, and therefore not an estimate of change, one would expect that any of the bi-temporal indices would have been more strongly related to field data. For instance, bi-temporal indices account for pre-fire deviations in reflectance that NBR does not. This finding challenges the convention that bi-temporal remote sensing indices of change, such as dNBR, rdNBR, and RBR, are implicitly better than the simpler NBR. Although NBR was once used exclusively, few if any studies continue to present remotely sensed burn severity data in terms of NBR, in favor of bi-temporal indices which are expected to be more robust. One explanation for why NBR was able to do this is because of the rapid recovery of leaf area within the first two years of disturbance that occurs in this environment after non-stand replacing events (Clark et al. 2012, Schafer et al. 2014).

Finally, a key difference between this study and other similar studies is the use of mosaicked imagery, from the period of maximum leaf area to produce burn severity indices for multiple fires within a given year. Compared to other studies, which have produced maps for individual fires using data from a ±2 week post-fire window of time for image acquisition. While this convention may be sufficient for regions with discrete fire seasons which coincide with the growing season, this poses challenges for regions where fires are not constrained to the growing season or dormant season. Seasonal variation in reflectance can confound the comparability of results between different fires (Kolden et al. 2015). For instance, remotely sensed burn severity indices derived from dormant season don't account for damage to deciduous plants, although

they make up an important part of the forest's leave area during the growing season and are impacted by both dormant season and growing season fire. If comparing fire effects throughout the year is important, then using the period with the greatest potential for spectral change and change of cues observable in the field is optimal (e.g. the growing season). My approach demonstrates that using a more standardized baseline of reflectance, by using growing season only data, is a robust way to evaluate severity in a way that is consistent between both growing season and dormant season reflectance conditions.

Conclusions

This study evaluated different approaches to modeling field indices of burn severity from common remote sensing indices and provides a basis for using a polynomial equation to predict CBI, as a preferable field index of severity over WCBI, using rdNBR as a dependent variable. However, WCBI provided still had a strong positive correlation with remote sensing data, particularly with simple, single-date NBR data. The results of this study also suggest that landscape scale patterns in forest structure could strongly influence WCBI data, and that better techniques for acquiring forest structure data, such as LiDAR, should be used to better more rigorously examine WCBI. Finally, this study also provides evidence for using growing season data to derive remotely sensed burn severity for both dormant and growing season fires.

References

Birch, D., P. Morgan, C. Kolden, J. Abatzoglou, G. Dillon, A. Hudak & A. Smith. 2015. Vegetation, topography and daily weather influenced burn severity in central Idaho and western Montana forests. Ecosphere 6 (1): 17.

Boby, L. A., E. A. Schuur, M. C. Mack, D. Verbyla & J. F. Johnstone (2010) Quantifying fire severity, carbon, and nitrogen emissions in Alaska's boreal forest. *Ecological Applications,* 20**,** 1633-1647.

Byram, G. M. (1959) Combustion of forest fuels. *Forest fire: control and use,* 1**,** 61-89.

Cansler, C. A. & D. McKenzie (2012) How robust are burn severity indices when applied in a new region? Evaluation of alternate field-based and remote-sensing methods. *Remote sensing,* 4**,** 456-483.

Chambers, M. E., P. J. Fornwalt, S. L. Malone & M. A. Battaglia (2016) Patterns of conifer regeneration following high severity wildfire in ponderosa pine–dominated forests of the Colorado Front Range. *Forest Ecology and Management,* 378**,** 57-67.

Chander, G., B. L. Markham & D. L. Helder (2009) Summary of current radiometric calibration coefficients for Landsat MSS, TM, ETM+, and EO-1 ALI sensors. *Remote sensing of environment,* 113**,** 893-903.

Chen, X., J. E. Vogelmann, M. Rollins, D. Ohlen, C. H. Key, L. Yang, C. Huang & H. Shi (2011) Detecting post-fire burn severity and vegetation recovery using multitemporal remote sensing spectral indices and field-collected composite burn index data in a ponderosa pine forest. *International Journal of Remote Sensing,* 32**,** 7905-7927.

Clark, K. L., N. Skowronski, M. Gallagher, H. Renninger & K. Schäfer (2012) Effects of invasive insects and fire on forest energy exchange and evapotranspiration in the New Jersey pinelands. *Agricultural and Forest Meteorology,* 166-167**,** 50-61.

Cram, D. S., T. T. Baker & J. C. Boren (2006) Wildland fire effects in silviculturally treated vs. untreated stands of New Mexico and Arizona.

Crotteau, J. S., M. W. Ritchie, J. M. Varner & J.-P. Berrill (2015) Quercus kelloggii (Newb.) sprout response to fire severity in northern California.

Davies, G., R. Domenech-Jardi, A. Gray & P. Johnson (2016) Vegetation structure and fire weather influence variation in burn severity and fuel consumption during peatland wildfires. *Biogeosciences,* 12**,** 15737-15762.

De Santis, A. & E. Chuvieco (2009) GeoCBI: A modified version of the Composite Burn Index for the initial assessment of the short-term burn severity from remotely sensed data. *Remote Sensing of Environment,* 113**,** 554-562.

Forman, R. 2012. *Pine Barrens: ecosystem and landscape*. Elsevier.

Forman, R. T. & R. E. Boerner (1981) Fire frequency and the pine barrens of New Jersey. *Bulletin of the Torrey Botanical Club***,** 34-50.

Garcia, M. L. & V. Caselles (1991) Mapping burns and natural reforestation using Thematic Mapper data. *Geocarto International,* 6**,** 31-37.

Heward, H., A. M. S. Smith, D. P. Roy, W. T. Tinkham, C. M. Hoffman, P. Morgan & K. O. Lannom (2013) Is burn severity related to fire intensity? Observations from landscape scale remote sensing. *International Journal of Wildland Fire,* 22**,** 910.

Isaacson, B. N., S. P. Serbin & P. A. Townsend (2012) Detection of relative differences in phenology of forest species using Landsat and MODIS. *Landscape ecology,* 27**,** 529-543.

Johnstone, J. F. & E. S. Kasischke (2005) Stand-level effects of soil burn severity on postfire regeneration in a recently burned black spruce forest. *Canadian Journal of Forest Research,* 35**,** 2151-2163.

Keeley, J. E. (2009) Fire intensity, fire severity and burn severity: a brief review and suggested usage. *International Journal of Wildland Fire,* 18**,** 116-126.

Key, C. H. & N. C. Benson (1999) The Normalized Burn Ratio (NBR): A Landsat TM radiometric measure of burn severity. *United States Geological Survey*.

Key, C. H. & N. C. Benson (2006) Landscape assessment (LA). *FIREMON: Fire effects monitoring and inventory system. Gen. Tech. Rep. RMRS-GTR-164-CD, Fort Collins, CO: US Department of Agriculture, Forest Service, Rocky Mountain Research Station*.

Kolden, C. A., J. A. Lutz, C. H. Key, J. T. Kane & J. W. van Wagtendonk (2012) Mapped versus actual burned area within wildfire perimeters: characterizing the unburned. *Forest Ecology and Management,* 286**,** 38-47.

Kolden, C. A., A. M. Smith & J. T. Abatzoglou (2015) Limitations and utilisation of Monitoring Trends in Burn Severity products for assessing wildfire severity in the USA. *International Journal of Wildland Fire,* 24**,** 1023-1028.

La Puma, I. P. 2012. Fire in the pines: a landscape perspective of human-induced ecological change in the pinelands of New Jersey. Rutgers University-Graduate School-New Brunswick.

Lathrop, R. & M. Kaplan (2004) New Jersey land use/land cover update: 2000–2001. *New Jersey Department of Environmental Protection,* 35.

Latif, Q. S., J. S. Sanderlin, V. A. Saab, W. M. Block & J. G. Dudley (2016) Avian relationships with wildfire at two dry forest locations with different historical fire regimes. *Ecosphere,* 7.

Matlack, G., D. Gibson & R. Good (1993) Clonal propagation, local disturbance, and the structure of vegetation: ericaceous shrubs in the pine barrens of New Jersey. *Biological Conservation,* 63**,** 1-8.

McCormick, J. & L. Jones. 1973. *The Pine Barrens: Vegetation Geography*. New Jersey State Museum.

Miller, J. D., E. E. Knapp, C. H. Key, C. N. Skinner, C. J. Isbell, R. M. Creasy & J. W. Sherlock (2009) Calibration and validation of the relative differenced Normalized Burn Ratio (RdNBR) to three measures of fire severity in the Sierra Nevada and Klamath Mountains, California, USA. *Remote Sensing of Environment,* 113**,** 645-656.

Miller, J. D. & A. E. Thode (2007) Quantifying burn severity in a heterogeneous landscape with a relative version of the delta Normalized Burn Ratio (dNBR). *Remote Sensing of Environment,* 109**,** 66-80.

Moody, J. A., B. A. Ebel, P. Nyman, D. A. Martin, C. Stoof & R. McKinley (2016) Relations between soil hydraulic properties and burn severity. *International Journal of Wildland Fire,* 25**,** 279-293.

Newcomer, M., D. Delgado, C. Gantenbein, T. Wang, S. Prichard, C. Schmidt & J. Skiles. 2009. Burn severity assessment in the Okanogan-Wenatchee forest using NASA satellite missions. In *Proceedings of the ASPRS Annual Conference*.

Parks, S., G. Dillon & C. Miller (2014) A New Metric for Quantifying Burn Severity: The Relativized Burn Ratio. *Remote Sensing,* 6**,** 1827-1844.

Picotte, J. J. & K. M. Robertson (2011) Validation of remote sensing of burn severity in south-eastern US ecosystems. *International Journal of Wildland Fire,* 20**,** 453-464.

Rose, E. T., T. R. Simons, R. Klein & A. J. McKerrow (2016) Normalized burn ratios link fire severity with patterns of avian occurrence. *Landscape Ecology***,** 1-14.

Rothermel, R. C. (1972) A mathematical model for predicting fire spread in wildland fuels.

Ryan, K. C. & N. V. Noste (1985) Evaluating prescribed fires.

Schafer, K. V., H. J. Renninger, N. J. Carlo & D. W. Vanderklein (2014) Forest response and recovery following disturbance in upland forests of the Atlantic Coastal Plain. *Front Plant Sci,* 5**,** 294.

Unger, D., I.-K. Hung & Y. Zhangb (2016) Landsat 8 OLI Imagery Classification Accuracy of Hardwood versus Pine Forest: A Cautionary Tale. *Journal of Forestry***,** 201.

Veraverbeke, S., S. Lhermitte, W. W. Verstraeten & R. Goossens (2011) A time-integrated MODIS burn severity assessment using the multi-temporal differenced normalized burn ratio (dNBRMT). *International Journal of Applied Earth Observation and Geoinformation,* 13**,** 52-58.

Viedma, O., J. Quesada, I. Torres, A. De Santis & J. M. Moreno (2015) Fire severity in a large fire in a Pinus pinaster forest is highly predictable from burning conditions, stand structure, and topography. *Ecosystems,* 18**,** 237-250.

Warner, T. A., N. S. Skowronski & M. R. Gallagher (2017) High spatial resolution burn severity mapping of the New Jersey Pine Barrens with WorldView-3 near-infrared and shortwave infrared imagery. *International Journal of Remote Sensing,* 38**,** 598-616.

Wimberly, M. & M. Reilly (2007) Assessment of fire severity and species diversity in the southern Appalachians using Landsat TM and ETM+ imagery. *Remote Sensing of Environment,* 108**,** 189-197.

Table 1. Burned and unburned locations of 110 CBI and WCBI field plots. A total of 77 plots were located in prescribed fires, 20 were located in wildfires, and 13 were located in unburned areas. See also to Figure 2.

Prescribed Fires	Date	Fire Size (ha)	Field Plots (n)
AT&T Line	3/3/2013	29	3
Dan's Bridge	3/5/2013	118	3
Experiment 1	3/5/2013	7	12
Fish & Wildlife	3/10/2013	103	1
Cedar Bridge	3/15/2013	162	3
Dead Pheasant	3/15/2013	55	1
Burnt Schoolhouse	3/6/2014	5	1
Experiment 2	3/11/2014	5	12
Bulltown Road	3/14/2014	132	3
Tylertown	3/14/2014	76	3
3 Foot Road	3/15/2014	78	3
Carranza Skit	3/15/2014	53	3
East Sandy Ridge	3/15/2014	56	3
Lacey	3/15/2014	89	3
Rattler Rd North	3/15/2014	65	3
Rattler Rd South	3/15/2014	76	1
Snuffy's Turnpike	3/16/2014	62	1
Whiting East	3/16/2014	14	3
Whiting Middle	3/16/2014	43	3
Whiting West	3/16/2014	67	3
Burn Experiment	3/23/2014	2	3
Bloody Ridge Rd	3/24/2014	58	3
Bodine Field	3/24/2014	39	3

Wildfires	Date	Fire Size (ha)	Field Plots (n)
Crossroads Wildfire	4/24/2014	81	3
Continental Wildfire	4/24/2014	128	3
Springers Brook Wildfire	4/25/2014	104	3
Bodine Field Wildfire	7/7/2014	11	3
Atsion Wildfire	5/7/2015	277	8

Unburned Areas	Most Recent Burn Date	Field Plots (n)
Brendan T. Byrne SF		1
Butterworth Rd North		3
Butterworth Rd South		3
Jenkins	2011	3
Nugentown	1983	3

Table 2. Identification information about of Landsat scenes used to develop growing season mosaics. Data for 2012-2013 were calibrated to the 2010 data, which was the most complete and clear of growing season data available from 2010-2014.

Year	Date	Path	Row	Image ID
2010	28-Aug	14	32	lt50140322010240
2012	2-Jul	13	32	le70130322012183
	20-Sep	13	32	le70130322012263
	3-Aug	13	32	le70130322012215
2013	25-Jun	14	32	le70140322013176
	5-Aug	13	32	le70130322013217
	6-Sep	13	32	le70130322013249
	15-Oct	14	32	le70140322013288
2014	28-Jun	14	32	le70140322014179
	7-Jul	13	32	le70130322014188
	30-Jul	14	33	le70140332014211
	30-Jul	14	33	le70140332014211
	8-Aug	13	32	le70130322014220
	15-Aug	14	32	le70140322014227
2015	24-Jun	13	32	le70130322015175
	17-Jul	14	32	le70140322015198
	26-Jul	13	32	le70130322015207
	18-Aug	14	32	le70140322015230

Table 3. Summary of field-based burn severity assessments (excluding unburned plots which had severities of 0)

Forest Stratum	Pre-Fire Percent Cover (Mean ± 1 Standard Deviation)	CBI	WCBI
Substrates	98 ± 4		
Low Shrubs, Herbs, Trees < 1m	90 ± 13	1.41 ± 0.46	1.40 ± 0.48
Tall Shrubs and Trees 1 to 5m	23 ± 21		
Intermediate Trees	14 ± 11	1.41 ± 0.83	1.41 ± 0.82
Big Trees	19 ± 12		
Total	49 ± 5	1.41 ± 0.63	1.39 ± 0.50

Table 4. AIC and RSS for candidate models of CBI and WCBI. Models were evaluated using residual sum of squares (RSS) as a primary criterion and Akaike's Information Criterion (AIC) as a second criterion where RSS values were similar between models. The best model of each group is indicated in bold. Values were generated using a k-fold leave one out cross validation approach, in which data was ordinated by CBI and split into 5 quantiles, from which 80% of each quantile were randomly selected to populate a training dataset in each fold, while the remaining 20% of data was reserved for cross validation. AIC and RSS values represent averages across all models from the cross validation segment of each fold.

Dependent Variable	Eqn. Form	Independent Variable	RSS	AIC
CBI	**Pol**	NBR	4.4	87.6
		dNBR	4.1	82.6
		rdNBR	**4.1**	**82.5**
		RBR	4.2	82.4
	Exp	NBR	4.4	87.5
		dNBR	4.9	100.9
		rdNBR	5.0	100.9
		rbr	4.9	99.3
	Sig	NBR	4.2	80.9
		dNBR	4.2	81.8
		rbr	4.3	82.0
		rdNBR	4.4	82.0
WCBI	Pol	NBR	3.9	77.0
		dNBR	4.0	79.7
		rdNBR	4.1	79.3
		RBR	4.0	79.5
	Exp	NBR	3.9	76.8
		dNBR	4.8	95.3
		rdNBR	4.8	95.3
		rbr	4.7	94.1
	Sig	NBR	4.1	80.3
		rbr	4.1	80.0
		dNBR	4.2	79.8
		rdNBR	4.3	80.3

Table 5. Maximum likelihood estimates and 2 standard errors (2 SE) for coefficients of models predictive of field indices of burn severity from remotely sensed indices of burn severity. Values for the best choice model are given in bold.

Predicted Index (Field)	Eqn. Form	Predictor Index (Remote Sensing)	β_0	2 SE	β_1	2 SE	β_2	2 SE
CBI	**Pol**	NBR	1.242	0.005	-5.619	0.034	-1.152	0.017
		dNBR	1.245	0.005	5.584	0.031	-1.648	0.02
		rdNBR	**1.24**	**0.006**	**5.536**	**0.03**	**-1.67**	**0.02**
		RBR	1.24	0.005	5.583	0.031	-1.568	0.02
	Exp	NBR	2.486	0.004	1	0.043	0.002	2.57E-05
		dNBR	0.625	0.004	-161.448	1.667	2.07E-05	1.69E-07
		rdNBR	0.607	0.005	-115.223	2.157	2.48E-05	2.89E-07
		rbr	0.62	0.004	-185.639	1.978	3.03E-05	2.56E-07
	Sig	NBR	2.182	0.007	0.011	0.001	1.42E+02	1.02E+01
		dNBR	2.358	0.007	0.01	9.59E-05	148.17	0.96
		rbr	2.34	0.007	0.016	0	88.39	0.59
		rdNBR	2.329	0.007	0.008	8.62E-05	179.40	1.18
WCBI	Pol	NBR	1.234	0.005	-4.734	0.03	-1.165	0.019
		dNBR	1.232	0.004	4.624	0.027	-1.528	0.021
		rdNBR	1.229	0.005	4.62	0.028	-1.523	0.021
		RBR	1.229	0.005	4.638	0.027	-1.439	0.02
	Exp	NBR	2.215	0.003	0.552	0.054	2.00E-03	2.99E-05
		dNBR	0.72	0.004	-145.908	1.734	1.91E-05	1.92E-07
		rdNBR	0.702	0.004	-111.658	2.507	2.18E-05	3.18E-07
		rbr	0.713	0.005	-167.233	1.857	2.80E-05	2.44E-07
	Sig	NBR	2.17	0.006	0.11	0.001	143.49	10.48
		rbr	2.166	0.006	0.014	1.53E-04	73.82	0.52
		dNBR	2.161	0.006	0.009	9.51E-05	120.75	0.83
		rdNBR	2.147	0.007	0.007	5.91E-05	150.25	1.06

Figure 1. The Composite Burn Index Field Sheet (Key and Benson 2006).

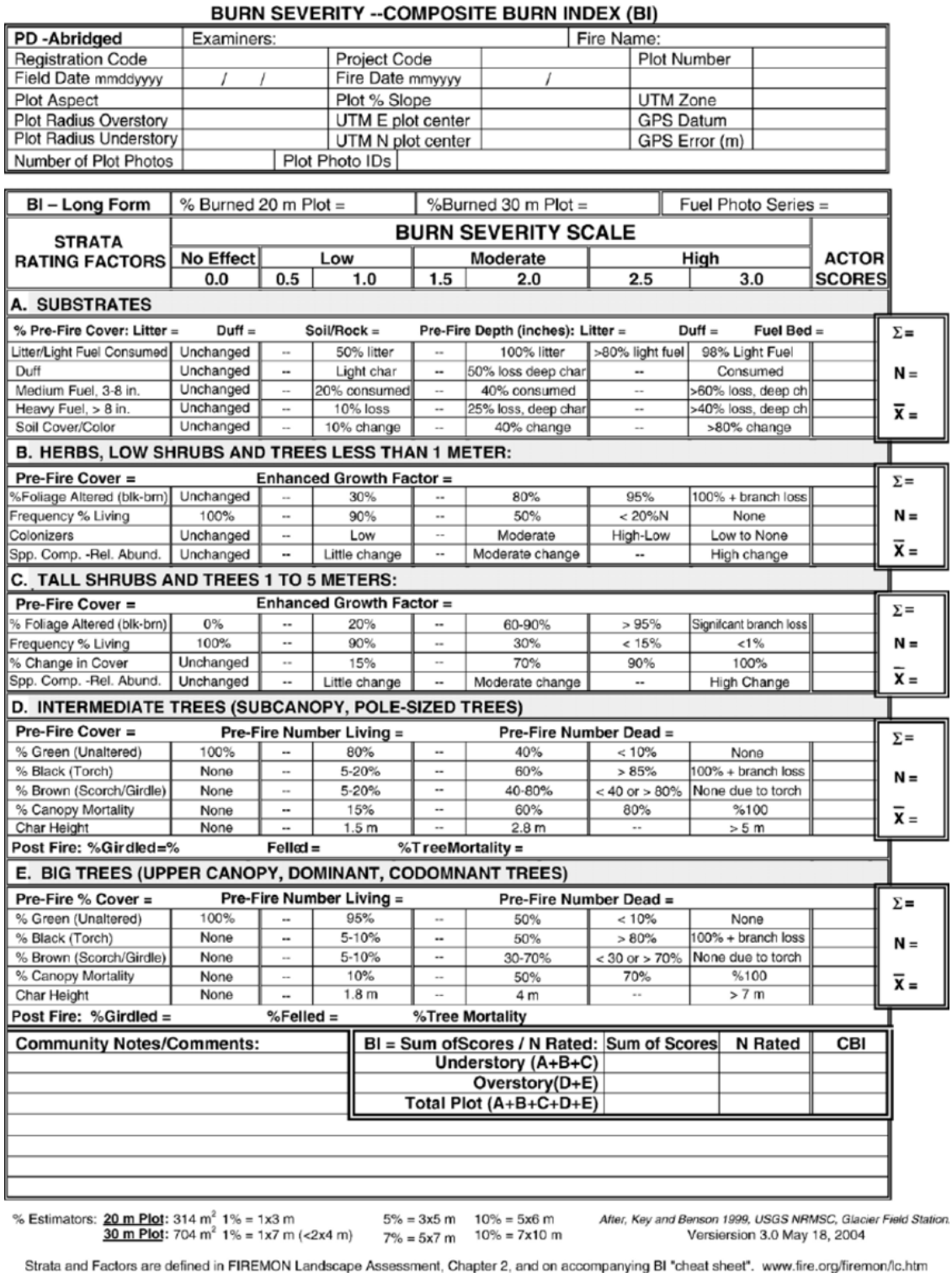

BURN SEVERITY --COMPOSITE BURN INDEX (BI)

PD -Abridged	Examiners:			Fire Name:		
Registration Code		Project Code		Plot Number		
Field Date mmddyyyy	/ /	Fire Date mmyyyy	/			
Plot Aspect		Plot % Slope		UTM Zone		
Plot Radius Overstory		UTM E plot center		GPS Datum		
Plot Radius Understory		UTM N plot center		GPS Error (m)		
Number of Plot Photos		Plot Photo IDs				

BI – Long Form	% Burned 20 m Plot =	%Burned 30 m Plot =	Fuel Photo Series =

STRATA RATING FACTORS	BURN SEVERITY SCALE							ACTOR SCORES
	No Effect	Low		Moderate		High		
	0.0	0.5	1.0	1.5	2.0	2.5	3.0	
A. SUBSTRATES								
% Pre-Fire Cover: Litter =	**Duff =**		**Soil/Rock =**		**Pre-Fire Depth (inches): Litter =**		**Duff =** **Fuel Bed =**	
Litter/Light Fuel Consumed	Unchanged	--	50% litter	--	100% litter	>80% light fuel	98% Light Fuel	
Duff	Unchanged	--	Light char	--	50% loss deep char	--	Consumed	
Medium Fuel, 3-8 in.	Unchanged	--	20% consumed	--	40% consumed	--	>60% loss, deep ch	
Heavy Fuel, > 8 in.	Unchanged	--	10% loss	--	25% loss, deep char	--	>40% loss, deep ch	
Soil Cover/Color	Unchanged	--	10% change	--	40% change	--	>80% change	
B. HERBS, LOW SHRUBS AND TREES LESS THAN 1 METER:								
Pre-Fire Cover =	**Enhanced Growth Factor =**							
%Foliage Altered (blk-brn)	Unchanged	--	30%	--	80%	95%	100% + branch loss	
Frequency % Living	100%	--	90%	--	50%	< 20%N	None	
Colonizers	Unchanged	--	Low	--	Moderate	High-Low	Low to None	
Spp. Comp. -Rel. Abund.	Unchanged	--	Little change	--	Moderate change	--	High change	
C. TALL SHRUBS AND TREES 1 TO 5 METERS:								
Pre-Fire Cover =	**Enhanced Growth Factor =**							
% Foliage Altered (blk-brn)	0%	--	20%	--	60-90%	> 95%	Significant branch loss	
Frequency % Living	100%	--	90%	--	30%	< 15%	<1%	
% Change in Cover	Unchanged	--	15%	--	70%	90%	100%	
Spp. Comp. -Rel. Abund.	Unchanged	--	Little change	--	Moderate change	--	High Change	
D. INTERMEDIATE TREES (SUBCANOPY, POLE-SIZED TREES)								
Pre-Fire Cover =	**Pre-Fire Number Living =**				**Pre-Fire Number Dead =**			
% Green (Unaltered)	100%	--	80%	--	40%	< 10%	None	
% Black (Torch)	None	--	5-20%	--	60%	> 85%	100% + branch loss	
% Brown (Scorch/Girdle)	None	--	5-20%	--	40-80%	< 40 or > 80%	None due to torch	
% Canopy Mortality	None	--	15%	--	60%	80%	%100	
Char Height	None	--	1.5 m	--	2.8 m	--	> 5 m	
Post Fire: %Girdled=%		**Felled =**		**%TreeMortality =**				
E. BIG TREES (UPPER CANOPY, DOMINANT, CODOMNANT TREES)								
Pre-Fire % Cover =	**Pre-Fire Number Living =**				**Pre-Fire Number Dead =**			
% Green (Unaltered)	100%	--	95%	--	50%	< 10%	None	
% Black (Torch)	None	--	5-10%	--	50%	> 80%	100% + branch loss	
% Brown (Scorch/Girdle)	None	--	5-10%	--	30-70%	< 30 or > 70%	None due to torch	
% Canopy Mortality	None	--	10%	--	50%	70%	%100	
Char Height	None	--	1.8 m	--	4 m	--	> 7 m	
Post Fire: %Girdled =		**%Felled =**		**%Tree Mortality**				

Σ = N = $\bar{X}$ =

Community Notes/Comments:	BI = Sum ofScores / N Rated:	Sum of Scores	N Rated	CBI
	Understory (A+B+C)			
	Overstory(D+E)			
	Total Plot (A+B+C+D+E)			

% Estimators: **20 m Plot:** 314 m^2 1% = 1x3 m 5% = 3x5 m 10% = 5x6 m
30 m Plot: 704 m^2 1% = 1x7 m (<2x4 m) 7% = 5x7 m 10% = 7x10 m

After, Key and Benson 1999, USGS NRMSC, Glacier Field Station.
Versiersion 3.0 May 18, 2004

Strata and Factors are defined in FIREMON Landscape Assessment, Chapter 2, and on accompanying BI "cheat sheet". www.fire.org/firemon/lc.htm

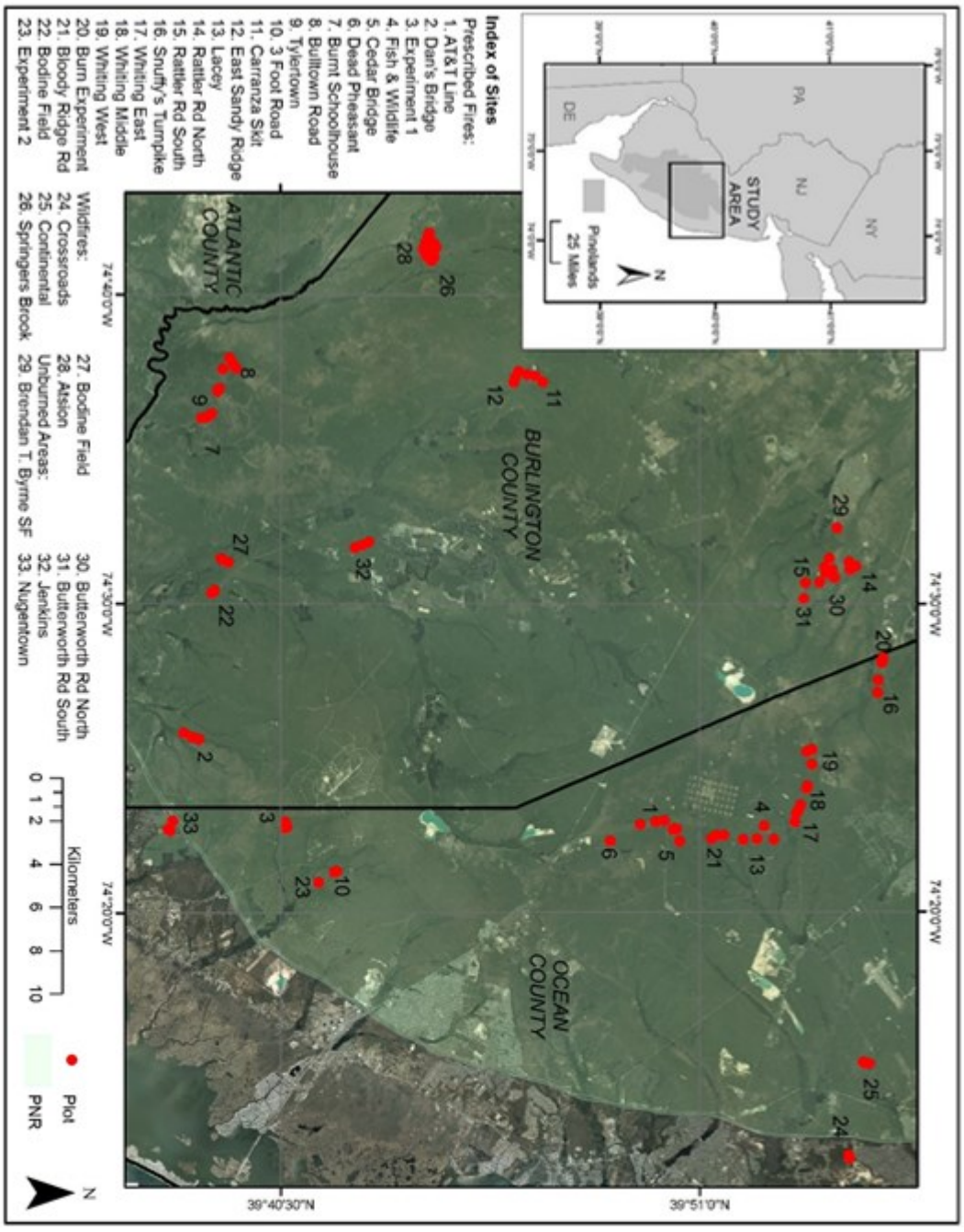

Figure 1. Area map of 33 study sites and 110 plot locations. See also Table 1.

Figure 2. Data processing workflow used to generate NBR, dNBR, rdNBR, and RBR.

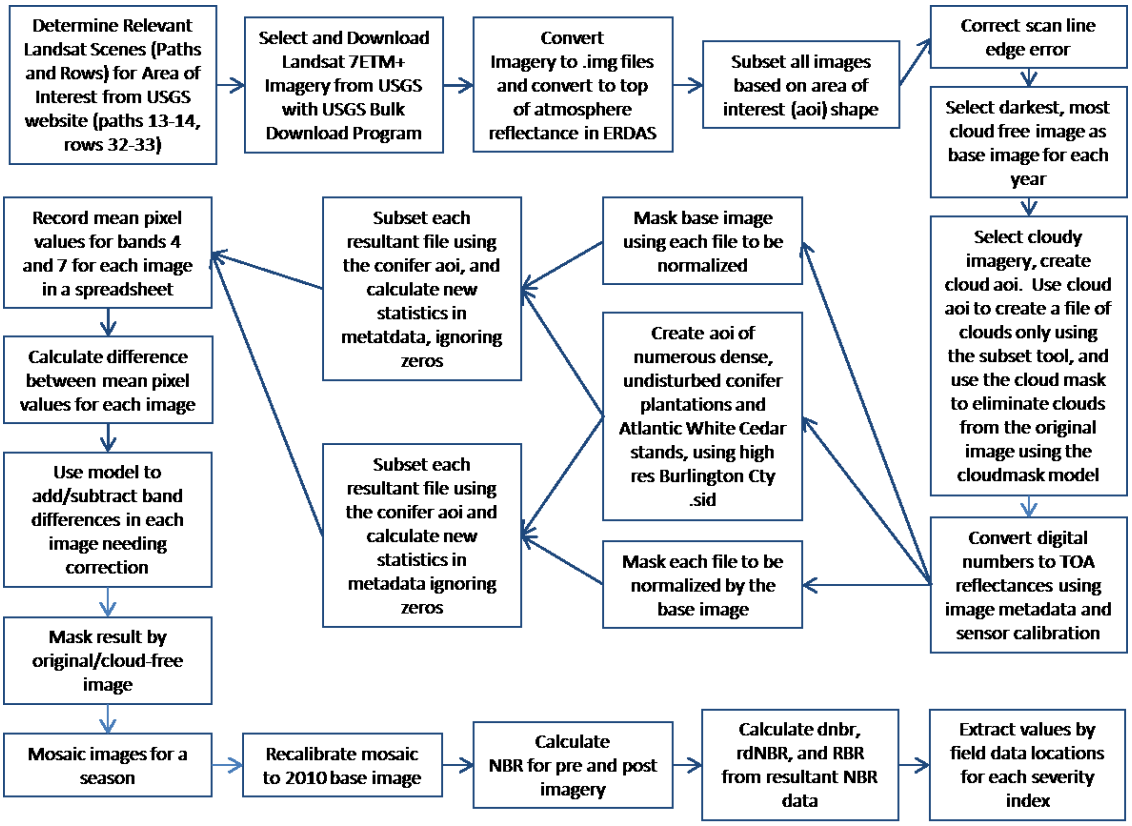

Figure 1. Growing season photos, following the Experiment 1 prescribed fire (left; CBI = 0.84) and Springers Brook Wildfire (right; CBI = 2.68) capture many differences of low and high severity fire. The fires occurred on March 5, 2013 and April 25, 2014, respectively, and were photographed in August of the same years.

Figure 3. Histogram of the distribution of burn severity at research plots burned in prescribed fire and wildfire, using CBI and alternative form of CBI weighted by focally observed percent cover in each forest strata (WCBI).

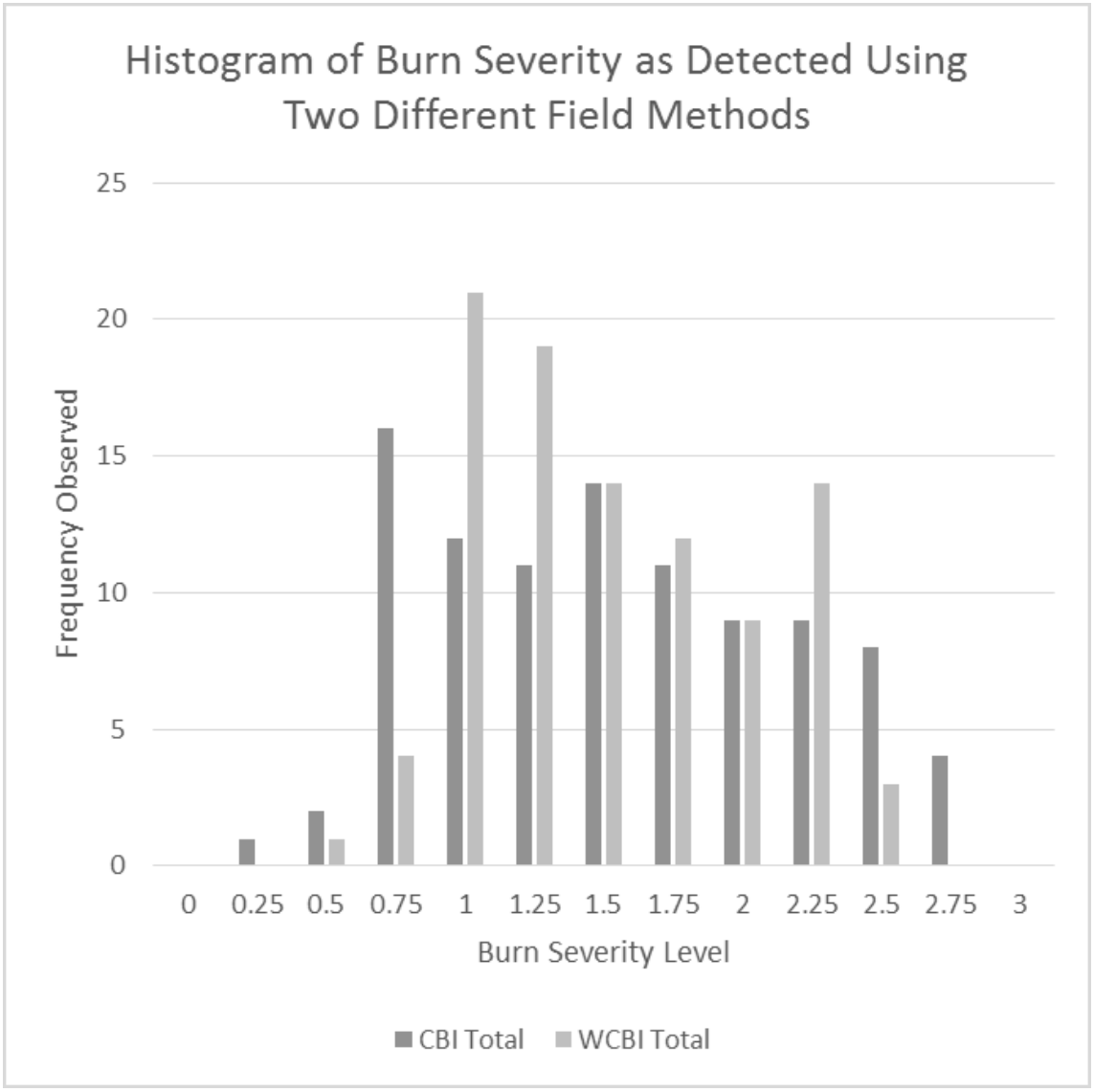

Figure 4. Maps of depicting field survey locations and relative differenced normalized burn ratio (rdNBR) at the 2013 Dan's Bridge Prescribed Fire, the 2014 Springers Brook Wildfire, and the 2014 Bodine Field Wildfire.

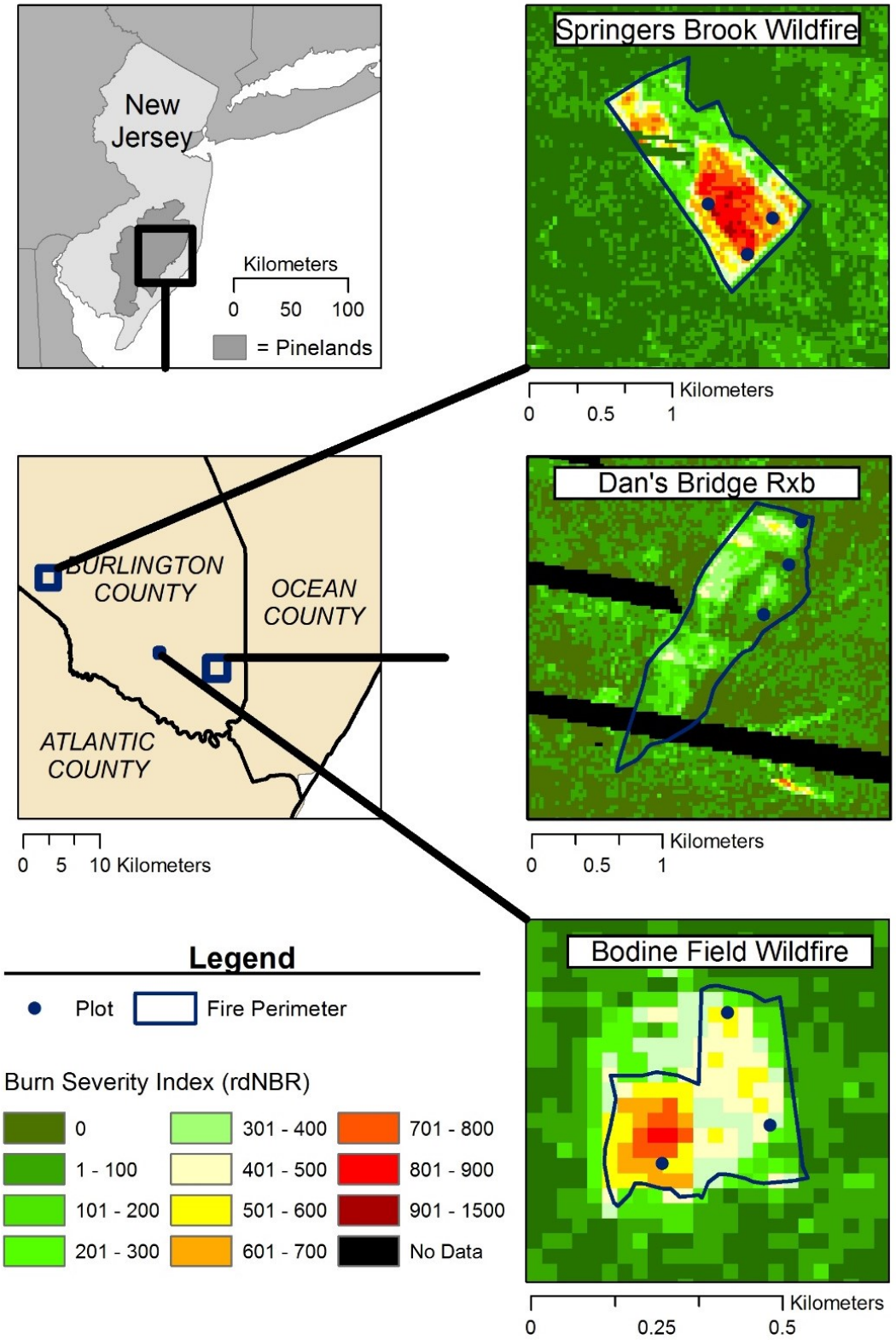

Figure 5. Top candidate models from the CBI and WCBI groups were re-run using the entire dataset. Coefficients of determination for observed vs. predicted values were calculated and used to select final model. The resulting model used CBI as the dependent variable, rdNBR as the independent variable, and a polynomial equation form (given in Eqn.1).

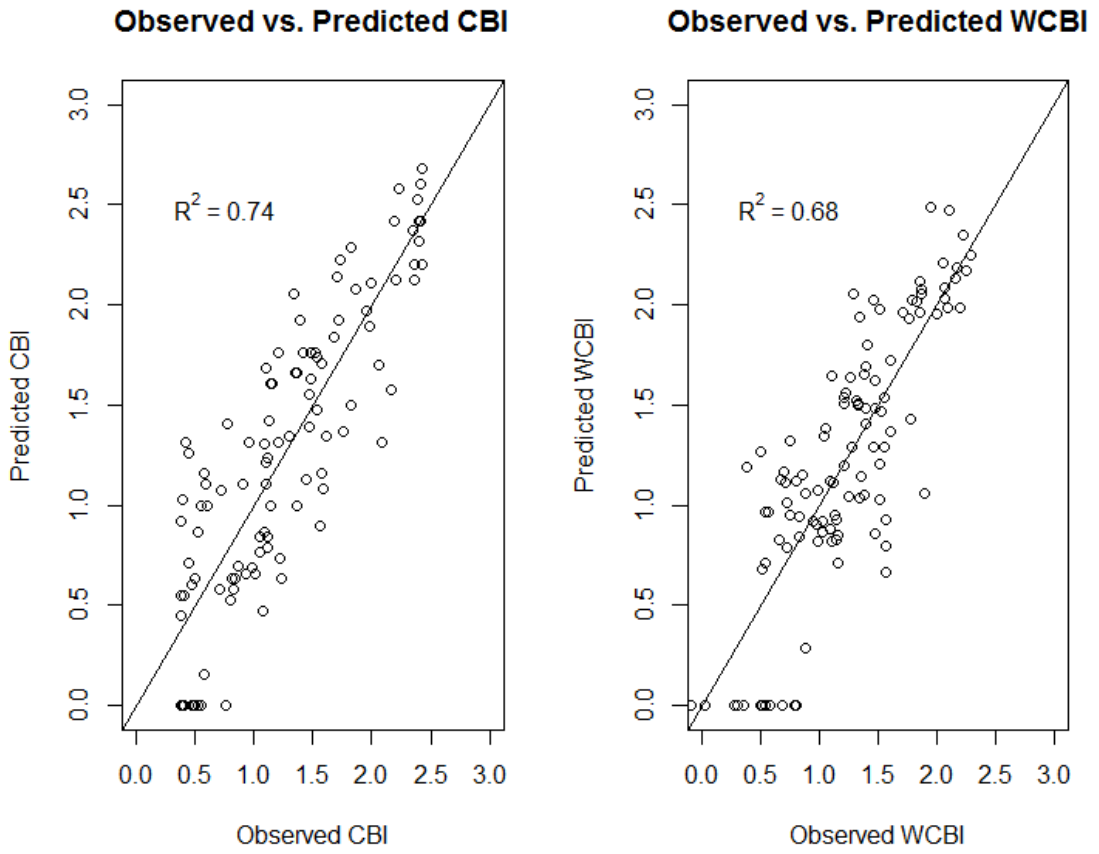

CHAPTER 3: The Use of Forest Census and Remotely Sensed Burn Severity Data to Estimate Tree Mortality

Abstract

Current tools for predicting fire induced tree mortality rely on post fire field surveys that provide limited information on the spatial variability mortality rates, and are also costly, tedious, and dangerous to obtain. Alternatively, rapid field and remote sensing approaches have proven useful for generating spatially comprehensive predictions of burn severity across burned forests, or the magnitude of ecological change, as well as other more nuanced ecological responses, but have not yet been incorporated into models of fire-induced tree mortality. I developed three logistic regression models to determine whether burn severity data could be incorporated with pre-burn forest census data to improve predictions of mortality among pitch pine following prescribed fire and wildfire events, and, whether field or remotely sensed burn severity data provided the most improvement among predictions. The first model incorporated only tree dimensions as parameters, while the second and third models also included field estimated burn severity and remotely sensed burn severity, respectively. I found that while both models that included burn severity parameters produced substantially better results than the model which did not, the model that incorporated remotely sensed burn severity produced the best results. I also provide an equation for estimating pitch pine (*Pinus rigida* Mill.) bark thickness, developed from an independent dataset, which I included in my models as it is a common parameter in other models of fire induced tree mortality. I then discuss local management implications of the results, along with the broader implications for the improvement of fire induced tree mortality estimation.

Introduction

Monitoring ecological impacts of fires is essential for evaluating net changes on forest ecosystem processes and the degree to which forest management goals are bolstered or set back by fire events. Ecosystem processes of concern can include water and nutrient cycling, regeneration, and carbon storage, while goals may include impacting stand density to promote forest health, timber quality, or regeneration, or to reduce hazardous fuels. A commonality among these processes and goals, are that they scale closely the attributes of the forest tree populations, and are therefore estimated from forest census data, collected at the tree-level through forest inventory programs, such as the US Forest Service's Forest Inventory and Analysis Program (https://www.fia.fs.fed.us/). Thus, evaluating fire impacts on forest tree populations, in a way that relates to inventory data is necessary to estimate broader stand-level changes in forests in relation to management objects. Fire-induced tree mortality is among the most rudimentary of impacts to forest tree populations, relates directly to even the most basic forest inventories, and is therefore is an essential fire effect to capture with post-fire monitoring.

Fire-induced tree mortality

The mechanisms by which fire kills trees have been well studied, especially in the western United States. Physiologically, fire can cause immediate mortality in trees in three ways: through bole damage, crown damage, and root damage (Michaletz and Johnson 2007). Short of combustion, lethal damage to these tissues is believed to begin when tissues reach temperatures of 50-60®C, at which protein denaturation occurs (Michaletz and Johnson 2006, Rosenberg et al. 1971, Van Wagner 1973). Girdling of the bole can impact the phloem and xylem, or just the phloem, which is exterior to the xylem. When only phloem is girdled, canopy growth can still continue, but the channel that enables nutrient and photosynthate flow between roots and the crown has been broken, postponing the death of crown and root tissues until they have expended

water and nutrient reserves(Michaletz and Johnson 2007). Bark provides insulation to the bole, slowing the rate of heat transfer to the cambium (Dickinson and Johnson 2004, Lawes et al. 2011). Bark thickness and density depend on species and tree size and explain differences in the rates of heat transfer to the cambium among different trees (Bauer et al. 2010, Hengst and Dawson 1994, Lawes et al. 2011). Crown damage, may occur from consumption of foliage and apical meristem tissue or damage to these tissues from heat transfer from the combustion of other nearby materials (Michaletz and Johnson 2007). Root damage can occur from flaming surface fire or smoldering combustion (flameless) of organic material within the soil. Damage from surface fire involves heat transfer from the fire environment to the soil surface, through the soil, and finally from soil to root bark, cambium, and meristem tissue (Michaletz and Johnson 2008). Through smoldering combustion, root material may be consumed or damaged through the transfer of heat from combusting subsurface materials (Stephens and Finney 2002, Watts 2013).

While mechanisms of tree mortality are well understood, direct measurements of specific damages remain inadequate, and may be unnecessary when the objective is simply estimating mortality rates. Indirect estimates, such as percent crown damage or scorch height, are highly correlated with physiological damage for many species. Further, the characteristics of individual species, such as the insulating value of bark, carbon reserves available to recover from disturbance, ability to compartmentalize damage and resist decay, and the ability to re-sprout, are relatively well understood. Thus, by incorporating factors indicative of a tree's ability to resist fire damage into logistic regression models, researchers have produced equations that accurately predict mortality and survival of individual trees which can be tailored to individual species (Ryan and Reinhardt 1988, Ryan and Amman 1994, Stephens and Finney 2002, Hood et al. 2008).

Classic models of fire-induced tree mortality

In classic models of fire-induced tree mortality, individual tree size, bark thickness (typically based on species-specific height and diameter relationships), and species are used as base-level inputs. These data can be gathered from pre-fire forest inventories, however commonly used models also incorporate post-fire damage surveys of individual trees to improve estimates. The damage most commonly used in these predictions is some metric of crown scorch percentage. Patterns of mortality derived from such models, such as those from the Ryan - Amman model, have been incorporated into modeling tools, such as FVS, FOFEM and FARSITE, allowing managers to estimate the likely impacts of fuel treatments and wildfire on mortality rates (Reinhardt 2003, Reinhardt and Dickinson 2010). Hood et.al. (2008) conducted the first evaluation of many species-specific coefficients for the Ryan-Amman model and found modeled stand-level mortality to be within 20% of actual values for subalpine fir (*Abies lasiocarpa* (Hook.) Nutt.), white fir (*A. concolor* (Gord. & Glend.) Lindl.), Douglas fir (*Pseudotsuga menziesii* (Mirb.) Franco), incense cedar (*Calocedrus decurrens* (Torr.) Florin), Engelmann spruce (*Picea engelmannii* Parry), whitebark pine (*Pinus albicaulis* Engelm.), lodgepole pine (*P. contorta* Dougl.), ponderosa pine (*P. ponderosa* Dougl. ex Laws.), Jeffrey pine (*P. jeffreyi* Balf.), and sugar pine (*P. lambertiana* Dougl.). While the Ryan-Amman model is the most widely used, Finney and Steven (2002) provided an alternate logistic regression form that also uses percent crown volume scorched and dbh to predict mortality of a similar suite of conifers of the western United States. This approach has been used in multiple subsequent studies to relate in fire-induced tree mortality to the degree of fire impacts on individual trees (Hély, Flannigan and Bergeron 2003, Kobziar, Moghaddas and Stephens 2006, Regelbrugge and Conard 1993).

Remote Sensing Alternatives

Remote sensing methods represent an alternative strategy for estimating fire effects, and offer the possibility of enhancing (or even changing) the way fire-induced tree mortality is

measured. Over the past decade, managers and researchers have begun to record and study the spatial distribution of fire effects, using methods of estimating burn severity, an index of the overall magnitude of ecological damage caused by wildland fire (Keeley 2009). Federal programs, such as Burned Area Emergency Response (BAER, http://www.fs.fed.us/eng/rsac/baer/), the Rapid Assessment of Vegetation Condition after Wildfire (RAVG, http://www.fs.fed.us/postfirevegcondition/index.shtml), and the Monitoring Trends in Burn Severity (MTBS, http://www.mtbs.gov/methods.html), now provide burn severity map products that are freely available to managers and the general public. These estimates are essentially measures of the change in reflectance of vegetation and soil that result from fire, as derived by differencing pre- and post-fire imagery, using selected bands of light, typically the mid-infrared (MIR) and near-infrared (NIR) bands. While data of many other bandwidths of light are also available, recent work by Warner, Skowronski, and Gallagher (2017) has further demonstrated the higher utility of MIR and NIR for detecting burn severity in a conifer dominated forest. While a variety of sensors can be used to collect these data, the most commonly used are the (freely available) imagery available through the US Geological Survey from Landsat 5, Landsat 7, and Landsat 8, which have a relatively high pixel resolution of 30 x 30m. While numerous indices of remotely sensed burn severity have been presented, those generated from NIR and MIR data, such as the Differenced Normalized Burn Ratio (dNBR) and Relative dNBR (rdNBR), have yielded the highest correlations with field observations (Chen et al. 2011, Key and Benson 2006, Miller and Thode 2007, Miller et al. 2009, Whittier and Gray 2016). Both dNBR and rdNBR are calculated from pre- and post-burn NIR and MIR imagery, such as bands 4 and 7 collected by Landsat 7. While dNBR has been used in more studies than rdNBR, the latter has mathematical and standardization merits that make it an attractive alternative (Miller and Thode 2007).

Calibrating remote sensing indices with field observations is necessary to produce realistic estimates of surface change. In the western United States, the Composite Burn Index (CBI) and its geometrically structured form (GeoCBI) have been used extensively to translate raw dNBR and rdNBR values into ecologically meaningful outputs (Chen et al. 2011, De Santis and Chuvieco 2009, Key and Benson 2006, Miller et al. 2009). CBI is an index of burn severity that is calculated as the composite of several severity indicators (e.g. % Crown scorch, amount of litter consumption, etc.) where each are scored on a scale of [0 - 3] (Key and Benson 2006). Observations are ranked according to guidelines on the CBI field sheet, such that those with the highest degrees of change are ranked as 3, while those of no fire effect are ranked as 0. These criteria, are then summarized into stratum-specific Burn Indices (BI), and are finally combined to obtain an overall Composite Burn Index. These evaluation criteria are known to be correlated with altered reflectance, and include estimates of crown damage. As crown damage is known to be an indicator of stem mortality, these results suggest that dNBR or rdNBR values might provide suitable alternative to estimates of mortality model inputs of post-fire tree damage, providing broader spatial coverage, without the need to conduct costly and tedious post-fire field surveys, at least where pre-burn inventory data are available.

Focus of this Study

The focus of this study was to determine whether incorporating post-fire burn severity data with pre-fire inventory data in logistic regression models could yield accurate predictions of fire-induced tree mortality, using pitch pine (*Pinus rigida* Mill.) as a test species. Further, I evaluated whether field or remote sensing estimates of burn severity produced the greatest improvement, as opposed to using pre-fire inventory alone. With consideration of the physiological basis for tree mortality and existing models of fire-induced tree mortality, I included tree height, diameter, and bark thickness as model parameters for the first model. I also included

CBI and rdNBR data as parameters in the second and third models, respectively. Current models typically estimate bark thickness as a function of species, diameter, and height, however this function was not previously published for pitch pine. Therefore, I provide a function to estimate pitch pine bark, which I evaluated from an independent dataset of pitch pines. I then used these functions to explore the question of whether post-fire rdNBR or CBI data could be used to develop accurate estimates of mortality from pre-fire inventory data.

Methods

Site description

This research was conducted in Burlington and Ocean Counties, New Jersey, within the 445,000 ha Pinelands National Reserve (PNR). The PNR is a landscape of upland forests dominated by oak and pine and lowland forests dominated by cedar, pine, and maple (Forman 2012, Robichaud and Anderson 1994). Upland forests account for approximately 62% of the forested area of the PNR and experience a high frequency of both wild and prescribed fire. They are made up of 3 distinct communities, all of which contain Pitch Pine (*Pinus rigida*): (1) oak-dominated stands, comprised of chestnut oak (*Quercus. prinus* L.), black oak (*Q. velutina* Lam.), white oak (*Q. alba* L.), scarlet oak (*Q. coccinea* Muenchh.), with scattered shortleaf pine (*P. echinata* Mill.) and Pitch Pine, (2) mixed pine-oak stands, with an overstory of pitch pine and mixed oaks, and (3) pitch pine-dominated stands, containing few overstory oaks, but with an understory of abundant scrub oaks (*Q. marlandica* Münchh and *Q. ilicifolia* Wangenh.) (Boerner and Forman 1982, Forman and Boerner 1981, Forman 2012, Lathrop and Kaplan 2004, Robichaud 1973). Of these species, pitch pine is likely the most adapted to resisting fire, with specialized thick, flakey bark, and the ability to sprout new growth rapidly (epicormic buds) after canopy consuming fires. Such adaptions make pitch pine a representative species to evaluate the candidate models over a range of fire conditions (Ledig and Little 1998, Little and Moore 1945, Little and Somes 1956).

Bark Thickness Model

Height and dbh data were coupled with bark thickness obtained from basal transverse sections of the primary growth axis for 266 harvested pitch pines (e.g. stump slices). These data were collected via destructive harvest within five 400m^2 forest plots between 2010-2012, originally measured for Joint Fire Sciences Program Project 10-1-02-14 The plots were split between two distinct management areas in the PNR, with three plots located in Stafford Forge Wildlife Management Area and two located in Brendan T. Byrne State Forest, approximately 25 miles to the northwest. None of the plots had a history of prescribed burning within their immediate vicinities, but the plots in Stafford Forge Wildlife Management Area had experienced wildfires in 1971 and 2007, and those Brendan T. Byrne State Forest had burned in 1963.

Height and dbh's of trees included in this segment of the study ranged from 2.5-18.5 m and 4.1-36.3 cm, respectively, representing the size class distribution of approximately 99% of the living pitch pine volume in New Jersey's Ocean and Burlington Counties, as well as across the entire state (FIA 2015). Basal transverse sections were cut with a thickness of 2 – 4 cm, flush with the ground, and stored for later analysis. Of the 266 sections collected, 153 were suitable for analysis. Bark thickness was measured manually to the nearest millimeter at 5 random locations on each section, using a ruler.

A linear regression model was developed to predict bark thickness (Eqn. 1). In this equation, Y_i is the log transformed mean of basal bark thickness of tree *i*, and follows a normal distribution described by a mean, derived from regression model parameters, and a variance, described by tau, τ. In the equation it assumed that x_{1i} and x_{2i} r the log height in meters and dbh in centimeters of tree *i*, ($x_{1i} \cdot x_{2i}$) represents an interactive term for log height and dbh, and e represents an error term,

$$Y_i \sim \text{Normal}\ (\beta_0 + \beta_1 x_{1i} + \beta_2 x_{2i} + \beta_{12} x_{1i} x_{2i} + e\ ,\ \tau) \qquad \text{(Eqn. 1)}$$

Model coefficients are represented (β_0, β_1, β_2 and β_{12}). Prediction accuracy was assessed using R^2.

Mortality Models and Model Selection

93 fixed area forest census plots were installed across 26 pitch pine dominated stands to collect tree mortality immediately following prescribed fire and wildfire events in 2013 and 2014. Plots burned in prescribed fires were surveyed prior to March burns, providing a preliminary determination of live and dead trees (pre- fire), as part of Joint Fire Sciences Program Project 12-1-03-11 (Skowronski et al. 2016). Mortality rates in wildfire plots, which burned during the period of April - July, were only surveyed following the fire, because it was impossible to predict and sample prior to wildfires. For these plots, I assumed a background mortality rate of approximately 1.4% for pitch pine for the area of study (FIA 2015), given the absence of southern pine beetle damage, storm damage, or other indicators that there had been mortality prior to the wildfires. Census plots were circular in shape and had a radius of 7.3m, to match that of a standard US Forest Service FIA subplot, yielding a total area of 167m^2. Plot center locations were recorded, using a Trimble GeoExplorer 6000 GPS unit, paired with a Tornado receiver (Trimble Inc., Sunnyvale, CA, USA). Differential correction was performed on point data to estimate horizontal accuracy of measured coordinates to be within 3m or less of the actual field location. Height and dbh of all trees > 2m tall were measured using a hypsometer (Haglof VL400, Haglof Sweden AB, Langsele, Sweden) and a diameter tape. Bark thickness was estimated from tree height and diameter data with Eqn. 1.

Satellite imagery was then used to estimate burn severity for all plots by calculating the relative differenced normalized burn ratio (rdNBR). The steps to estimate burn severity as rdNBR can be broken into four phases: (1) pre-processing of raw data, (2) generating Normalized Burn Ratio (NBR) coverages, (3) generating the differenced Normalized Burn Ratio (dNBR) coverages,

and finally (4) generating rdNBR coverages. In the pre-processing phase, pixel values are first converted from digital numbers to top of atmosphere reflectance and radiometric correction is performed. Clouds and cloud shadows which are frequently present even in relatively cloud-free data, are then masked. Finally, I accounted for scan line error gaps in the data (see Markham et al. 2004) and those caused by clouds by gap filling with error-free data from overlapping flight paths on the same or similar dates. In the second phase, raw pre- and post-fire imagery is processed with an algorithm to produce normalized burn ratio (NBR) values.

$$NBR = (NIR - MIR) / (NIR+MIR)$$ (Key and Benson 1999)

In the third phase, NBR is used to calculate dNBR.

$$dNBR = (NBR_{pre\text{-}fire} - NBR_{post\text{-}fire})$$ (Key and Benson 2006)

Finally, in the fourth phase rdNBR is calculated from dNBR.

$$rdNBR = 1000 \cdot (NBR_{pre} - NBR_{post}) \div \sqrt{|NBR_{pre}|}$$ (Miller and Thode 2007)

The New Jersey Pinelands conveniently falls at the intersection of multiple flight paths of this satellite. While no single image covers the entire extent of the area of interest of the study area, multiple paths overlap the core of the area. I therefore used Landsat 7 ETM+ data from paths 13 and 14 and rows 32 and 33 collected between Julian dates 176 and 288 (Table 1). This reflects the period when leaf area is at an annual maximum. Digital reflectance values were converted to top of atmosphere reflectance and radiometric correction was performed for all data. Clouds were then manually masked, as done by Isaacson (2012). Multi-temporal imagery from different row/path combinations within growing seasons was then mosaicked to fill gaps and produce full coverage leaf-on datasets of NIR and MIR reflectance. Resulting data were then used to calculate normalized burn ratio (NBR) coverages for 2012, 2013 and 2014. Resultant NBR was used to calculate dNBR for 2013 and 2014, and finally rdNBR. I then extracted rdNBR for the field plot

coordinates, described earlier in this section. Concurrent CBI data was collected in each plot using the CBI field sheet from the FIREMON manual (Key and Benson 2006).

I developed a three logistic regression models for estimating tree mortality, using different combinations of pre-fire census plot data and post-fire burn severity estimates to explore the question of whether field or remotely sensed burn severity estimates produced better predictions than pre-fire census plot data alone. The first model included only diameter at breast height, height, and basal bark thickness as parameters, while the second and third models also included CBI and rdNBR, respectively. Each model was run in SAS and cross-validated using a k-fold leave-one out approach, with plots as replicates.

Accuracies of the tree mortality predictions for each model were assessed using three methods, including overall accuracy, Akaike Information Criterion (AIC), and Saveland and Neuenschwander's signal detection approach for evaluating tree mortality predictions (1990). Overall accuracy is simply calculated as the ratio of correct predictions to total predictions. AIC is a system of ranking candidate model's, based on the amount of information lost when they are used to predict data, and factors in the trade-off of added model complexity by penalizing models for the number of parameters it includes (Akaike 1974). However, since AIC is provides a measure of model quality relative to other candidate models, but not an absolute description of quality, it is typically used in conjunction with other measures of model quality to improve the model selection process. Finally, the signal detection is approach, described by Saveland and Neuenschwander, is useful for assessing the prediction of binary outcomes, in which the investigator is concerned with the probability of four types of possible outcomes: true-positive, true-negative, false-positive, and false-negative. In the case of this study these are analogous to the outcomes: accurately predicted live, accurately predicted dead, falsely predicted live, and falsely predicted dead. In this framework, the problem is interpreted as having 3 parts, including

(1) the actual state of nature, (2) the response, and (3) the outcome. Whether the outcome results in a true-positive, true-negative, false-positive, false-negative, and can be visualized by drawing a (2 x 2) matrix of state of nature and response (Figure 1). Bayesian decision analysis is incorporated by combining the probabilities of the states of nature, with that of the response given the state of nature, to produce a posterior probability of each possible prediction outcome.

Results

Bark Thickness Model

Bark thickness was positively correlated with both height and diameter. Average basal bark thickness ranged between 0.2 and 2.2cm for individual trees, while minimum and maximum thicknesses observed were 0.1 cm and 3.2 cm. Estimates for Eqn. 1 coefficients were ($\beta_0 = -1.097$), ($\beta_1 = 0.299$), ($\beta_2 = 0.088$), and ($\beta_{12} = -0.026$), and were all significant with a 95% credible interval. A regression of predicted basal bark thickness values and actual bark thickness values had an ($r^2 = 0.52$), indicating a moderate fit (Figure 2).

Mortality Models and Model Selection

The independent set of plot data used in this segment of the study included a total of 2639 trees from 93 plots spread across 26 burn units. 17% of the stems died as a direct result of fire across the burned plots. Height and dbh ranged from 2 – 22.3m and 1.0 – 48.3cm, respectively. Average height and diameter were 7.8 ± 4.2m and 11.26 ± 7.7 cm (mean ± 1 standard deviation), respectively, reflecting over 99% of the size distribution of pitch pines in these counties as well as across the entire state (FIA 2015). rdNBR ranged from 0 – 891 while CBI ranged from 0 – 2.68, representing ranges from no-effect to high severity according to both indices. Overall accuracy, AIC, and posterior probabilities of prediction outcomes generated with Saveland and Neuenschwander's signal detection method all agreed that the models that incorporated rdNBR

and CBI produced substantially better estimates than the model that only used pre-fire census data, and that the model that incorporated rdNBR produced slightly better results than that which incorporated CBI. Overall classification accuracy of the severity exclusive model, the CBI inclusive model, and the rdNBR inclusive model were 0.82, 0.86, and 0.88, respectively, while posterior probabilities of correct predictions of mortality, generated using Saveland and Neuenschwander's method were 0.57, 0.68, and 0.72 (Table 2). Parameter estimates for each model are provided in Table 3.

Discussion

Estimating fuel treatment and wildfire use effectiveness remains a global challenge to fire managers. The identification of relationships between fire effects and remote sensing indices of burn severity, however, have opened the door to improving upon evaluating the balance of positive and negative outcomes of operational fire management choices. One goal of fire management is regulate the rates of tree mortality, either by limiting mortality to reduce effects, such as in mature timber stands, or to increase mortality, perhaps when reducing stand density or promoting certain types of habitat are management objectives. Current tools that predict tree mortality require inputs from post-fire surveys of damages to individual trees, which put technicians directly in hazardous environments, are tedious to collect, and may be spatially limited by the number of plots that can be collected during a field campaign.

The results of this study support that incorporating plot level post-fire burn severity estimates with pre-fire census data into logistic regression models produces substantially better results than when pre-fire census data is used alone in similar models. The rates of correct predictions found in this study are comparable to published accuracies of more tedious and less spatially precise field assay methods, that are widely used today by fire managers for other conifer species (Hood et al. 2008). Further, this novel approach to tree mortality estimation provides

strong evidence for the utility of remotely sensed burn in a region where few studies have demonstrated its use (Stambaugh, Hammer and Godfrey 2015, Warner et al. 2017). Despite the broad use of burn severity estimates, few studies have conducted rigorous physical measurements of ecological change as they relate to rdNBR or dNBR (Kolden, Smith and Abatzoglou 2015, Morgan et al. 2014). Finally, while previous studies have evaluated tree mortality primarily as an effect often exclusively in wildfires, the results of this study have been cross-validated using a combination of both prescribed and wildfire data, supporting the utility of this approach in either management scenario.

I observed that when rdNBR was incorporated into the logistic regression models, prediction accuracies were slightly better than when CBI was incorporated. This is interesting, because CBI is typically thought to be a more accurate and direct observation of burn severity than rdNBR, is therefore often used as a calibration standard for rdNBR data in new vegetation types, and therefore should be more effective at aiding in the prediction of tree mortality. However, CBI is also thought to be prone to observer bias and inconsistent reporting (Morgan et al. 2014). Alternatively, rdNBR also has error stemming from mismatch in spatial resolution of reflectance data and fire effects, as well as positional mismatch between GPS locations of field plots and remote sensing datasets. I used medium spatial resolution data collected by the publicly available Landsat TM and ETM+ sensor platforms to derive rdNBR, however, recent burn severity research with the new, commercially available high resolution data collected by the Worldview3 platform is may produce even higher accuracy results (Warner et al. 2017). Standards for evaluating error in CBI data remain to be agreed upon and therefore this error is unaccounted for, however, these results suggest that bias in CBI data likely outweighs error in rdNBR. My study suggests that bias in CBI data should be further evaluated by the research community, and that

tree mortality rates or that other directly measurable fire effects may actually serve as better standards for evaluating burn severity.

In addition to providing more accurate predictions of tree mortality and survivorship, rdNBR is safer, more spatially comprehensive, and less time consuming to obtain, making it an ideal input for fire effects models such as those aimed to estimate fire-induced tree mortality. However, rdNBR requires the investment of software, computational hardware, and technical expertise that may be beyond the means of some managers. CBI data requires substantially less training to acquire, and adequate datasets can be collected quickly by field crews, therefore remains a suitable alternative when the use of rdNBR data is not practical.

The results of this study can also be used as a basis by which to improve existing mortality models, particularly the Ryan and Amman model, used in the majority of fire management software packages that predict mortality, which have many similarities to the model I developed. The Ryan and Amman model incorporates the same pre-fire tree-level census plot data, a species specific coefficient, and a canopy damage parameter for each tree, assessed post-fire in the field. These models have traditionally been evaluated by their rates of accuracy, but report little data about the rates of false predictions among live and dead classes. Future work could improve these studies by replacing the post-fire tree-level damage parameter with plot-level rdNBR data and include posterior probabilities of model prediction rates generated using Saveland and Neuenschwander's approach, as done in this study.

Conclusions

This study demonstrates that rapid assessments of post-fire burn severity, either in the field or via remote sensing methods, can be incorporated with pre-fire census plot data to estimate tree mortality in prescribed fire and wildfire scenarios, and provide potentially more spatially comprehensive assessment of mortality without requiring the input of field data that is

dangerous to collect. This study demonstrates this using pitch pine in the southern New Jersey Pine Barrens as a test species, with a dataset that represents 99% of the distribution of pitch pine in the state. The results of this study suggest that while incorporating CBI into logistic regression models can provide good results, rdNBR can provide stronger results without the need for field work. This finding was counterintuitive, and suggests that the observer bias in rdNBR data may produce more error than spatial inconsistencies in rdNBR data. The results should be used in planning to identify the level of burn severity necessary to accomplish forest management goals in pitch pine dominated stand. In the broader arena, this work should be used as a framework to parameterize fire-induced tree mortality models for additional species.

References

Akaike, H. (1974) A new look at the statistical model identification. *IEEE transactions on automatic control,* 19**,** 716-723.

Bauer, G., T. Speck, J. Blömer, J. Bertling & O. Speck (2010) Insulation capability of the bark of trees with different fire adaptation. *Journal of Materials Science,* 45**,** 5950-5959.

Boerner, R. E. & R. Forman (1982) Hydrologic and mineral budgets of New Jersey Pine Barrens upland forests following two intensities of fire. *Canadian Journal of Forest Research,* 12**,** 503-510.

Chen, X., J. E. Vogelmann, M. Rollins, D. Ohlen, C. H. Key, L. Yang, C. Huang & H. Shi (2011) Detecting post-fire burn severity and vegetation recovery using multitemporal remote sensing spectral indices and field-collected composite burn index data in a ponderosa pine forest. *International Journal of Remote Sensing,* 32**,** 7905-7927.

De Santis, A. & E. Chuvieco (2009) GeoCBI: A modified version of the Composite Burn Index for the initial assessment of the short-term burn severity from remotely sensed data. *Remote Sensing of Environment,* 113**,** 554-562.

Dickinson, M. B. & E. A. Johnson (2004) Temperature-dependent rate models of vascular cambium cell mortality. *Canadian Journal of Forest Research,* 34**,** 546-559.

FIA. 2015. Forest Inventory and Analysis Data Online. St. Paul, MN: U.S. Department of Agriculture, Forest Service, Northern Research Station.

Forman, R. 2012. *Pine Barrens: ecosystem and landscape*. Elsevier.

Forman, R. T. & R. E. Boerner (1981) Fire frequency and the pine barrens of New Jersey. *Bulletin of the Torrey Botanical Club***,** 34-50.

Hély, C., M. Flannigan & Y. Bergeron (2003) Modeling tree mortality following wildfire in the southeastern Canadian mixed-wood boreal forest. *Forest Science,* 49**,** 566-576.

Hengst, G. E. & J. O. Dawson (1994) Bark properties and fire resistance of selected tree species from the central hardwood region of North America. *Canadian Journal of Forest Research,* 24**,** 688-696.

Hood, S. M., C. W. McHugh, K. C. Ryan, E. Reinhardt & S. L. Smith (2008) Evaluation of a post-fire tree mortality model for western USA conifers. *International Journal of Wildland Fire,* 16**,** 679-689.

Hurteau, M. D., J. B. Bradford, P. Z. Fulé, A. H. Taylor & K. L. Martin (2014) Climate change, fire management, and ecological services in the southwestern US. *Forest Ecology and Management,* 327**,** 280-289.

Isaacson, B. N., S. P. Serbin & P. A. Townsend (2012) Detection of relative differences in phenology of forest species using Landsat and MODIS. *Landscape ecology,* 27**,** 529-543.

Keeley, J. E. (2009) Fire intensity, fire severity and burn severity: a brief review and suggested usage. *International Journal of Wildland Fire,* 18**,** 116-126.

Key, C. H. & N. C. Benson (1999) The Normalized Burn Ratio (NBR): A Landsat TM radiometric measure of burn severity. *United States Geological Survey*.

Key, C. H. & N. C. Benson (2006) Landscape assessment (LA). *FIREMON: Fire effects monitoring and inventory system. Gen. Tech. Rep. RMRS-GTR-164-CD, Fort Collins, CO: US Department of Agriculture, Forest Service, Rocky Mountain Research Station*.

Kobziar, L., J. Moghaddas & S. L. Stephens (2006) Tree mortality patterns following prescribed fires in a mixed conifer forest. *Canadian Journal of Forest Research,* 36**,** 3222-3238.

Kolden, C. A., A. M. Smith & J. T. Abatzoglou (2015) Limitations and utilisation of Monitoring Trends in Burn Severity products for assessing wildfire severity in the USA. *International Journal of Wildland Fire,* 24**,** 1023-1028.

Lathrop, R. & M. Kaplan (2004) New Jersey land use/land cover update: 2000–2001. *New Jersey Department of Environmental Protection,* 35.

Lawes, M. J., A. Richards, J. Dathe & J. J. Midgley (2011) Bark thickness determines fire resistance of selected tree species from fire-prone tropical savanna in north Australia. *Plant Ecology,* 212**,** 2057-2069.

Ledig, F. T. & S. Little. 1998. Pitch pine (Pinus rigida Mill.): ecology, physiology and genetics. In *Pine Barrens Ecosystem and Landscape,* ed. R. T. T. Forman, 347-372. New Brunswick, NJ: Rutgers University Press.

Little, S. & E. Moore (1945) Controlled burning in South Jersey's oak-pine stands. *Journal of Forestry,* 43**,** 499-506.

Little, S. & H. A. Somes (1956) Buds enable pitch and shortleaf pines to recover from injury.

Markham, B. L., J. C. Storey, D. L. Williams & J. R. Irons (2004) Landsat sensor performance: history and current status. *IEEE Transactions on Geoscience and Remote Sensing,* 42**,** 2691-2694.

Michaletz, S. & E. Johnson (2006) A heat transfer model of crown scorch in forest fires. *Canadian Journal of Forest Research,* 36**,** 2839-2851.

Michaletz, S. T. & E. A. Johnson (2007) How forest fires kill trees: A review of the fundamental biophysical processes. *Scandinavian Journal of Forest Research,* 22**,** 500-515.

Michaletz, S. T. & E. A. Johnson (2008) A biophysical process model of tree mortality in surface fires. *Canadian Journal of Forest Research,* 38**,** 2013-2029.

Miller, J. D., E. E. Knapp, C. H. Key, C. N. Skinner, C. J. Isbell, R. M. Creasy & J. W. Sherlock (2009) Calibration and validation of the relative differenced Normalized Burn Ratio (RdNBR) to three measures of fire severity in the Sierra Nevada and Klamath Mountains, California, USA. *Remote Sensing of Environment,* 113**,** 645-656.

Miller, J. D. & A. E. Thode (2007) Quantifying burn severity in a heterogeneous landscape with a relative version of the delta Normalized Burn Ratio (dNBR). *Remote Sensing of Environment,* 109**,** 66-80.

Morgan, P., R. E. Keane, G. K. Dillon, T. B. Jain, A. T. Hudak, E. C. Karau, P. G. Sikkink, Z. A. Holden & E. K. Strand (2014) Challenges of assessing fire and burn severity using field measures, remote sensing and modelling. *International Journal of Wildland Fire,* 23**,** 1045-1060.

Moritz, M. A., M.-A. Parisien, E. Batllori, M. A. Krawchuk, J. Van Dorn, D. J. Ganz & K. Hayhoe (2012) Climate change and disruptions to global fire activity. *Ecosphere,* 3**,** art49.

Regelbrugge, J. C. & S. G. Conard (1993) Modeling tree mortality following wildfire in Pinus ponderosa forests in the central Sierra-Nevada of California. *International Journal of Wildland Fire,* 3**,** 139-148.

Reinhardt, E. D. 2003. Using FOFEM 5.0 to estimate tree mortality, fuel consumption, smoke production and soil heating from wildland fire. In *Proceedings of the 2nd International Wildland Fire Ecology and Fire Management Congress and 5th Symposium on Fire and Forest Meteorology*, 16-20.

Reinhardt, E. D. & M. B. Dickinson (2010) First-order fire effects models for land management: overview and issues.

Robichaud, B. 1973. *Vegetation of New Jersey*. New Brunswick, NJ: Rutgers University Press.

Robichaud, B. & K. Anderson. 1994. *Plant communities of New Jersey: a study in landscape diversity*. New Brunswick, NJ: Rutgers University Press.

Rosenberg, B., G. Kemeny, R. C. Switzer & T. C. Hamilton (1971) Quantitative evidence for protein denaturation as the cause of thermal death.

Ryan, K. C. & G. D. Amman (1994) Interactions between fire-injured trees and insects in the Greater Yellowstone Area.

Ryan, K. C. & E. D. Reinhardt (1988) Predicting postfire mortality of seven western conifers. *Canadian Journal of Forest Research,* 18**,** 1291-1297.

Saveland, J. M. & L. F. Neuenschwander (1990) A signal detection framework to evaluate models of tree mortality following fire damage. *Forest Science,* 36**,** 66-76.

Skowronski, N., A. Simeoni, K. Clark, W. Mell, R. Hadden, R. Kremens, A. Filkov, W. Edwards, J. Dusha, A. Evans-House, E. Mueller, M. Gallagher, J. C. Thomas, M. El Houssami & S. Santamaria. 2016. Evaluation and Optimization of Fuel Treatment Effectiveness with an Integrated Experimental/Modeling Approach Final Report: JFSP Project Number 12-1-03-11. 24. Joint Fire Sciences Program.

Stambaugh, M. C., L. D. Hammer & R. Godfrey (2015) Performance of burn-severity metrics and classification in oak woodlands and grasslands. *Remote Sensing,* 7**,** 10501-10522.

Stephens, S. L. & M. A. Finney (2002) Prescribed fire mortality of Sierra Nevada mixed conifer tree species: effects of crown damage and forest floor combustion. *Forest Ecology and Management,* 162**,** 261-271.

Van Wagner, C. (1973) Height of crown scorch in forest fires. *Canadian Journal of Forest Research,* 3**,** 373-378.

Warner, T. A., N. S. Skowronski & M. R. Gallagher (2017) High spatial resolution burn severity mapping of the New Jersey Pine Barrens with WorldView-3 near-infrared and shortwave infrared imagery. *International Journal of Remote Sensing,* 38**,** 598-616.

Watts, A. C. (2013) Organic soil combustion in cypress swamps: moisture effects and landscape implications for carbon release. *Forest Ecology and Management,* 294**,** 178-187.

Whittier, T. R. & A. N. Gray (2016) Tree mortality based fire severity classification for forest inventories: A Pacific Northwest national forests example. *Forest Ecology and Management,* 359**,** 199-209.

Williams, R. J., R. A. Bradstock, G. J. Cary, N. J. Enright, A. M. Gill, A. Leidloff, C. Lucas, R. J. Whelan, A. N. Andersen & D. J. Bowman (2009) Interactions between climate change, fire regimes and biodiversity in Australia: a preliminary assessment.

Table 1. Identification codes of Landsat imagery used to develop growing season mosaics. Data for 2012-2013 were calibrated to the 2010 data, which was the most complete and clear of growing season data available from 2010-2014.

Year	Landsat Image ID
2010	lt50140322010240
2012	le70130322012183, le70130322012263, le70130322012215
2013	le70140322013288, le70130322013217, le70130322013249, le70140322013176
2014	le70140332014211, le70130322014188, le70140332014211, le70140322014179, le70140322014227, le70130322014220

Table 2. Parameter coefficient estimates and standard errors (SE) for three candidate logistic regression models of fire-induced tree mortality. The first model excludes a severity parameter, and only uses parameters sourced from pre-fire census plot, while the second two models incorporate a burn severity parameter, either CBI or rdNBR.

	Severity exclusive model		*CBI inclusive model*		*rdNBR inclusive model*	
Parameter	Estimate	SE	Estimate	SE	Estimate	SE
Intercept	-0.6568	0.1299	2.6583	0.2211	0.8052	0.1626
Height	0.1246	0.0317	0.1152	0.0379	0.1693	0.0401
dbh	0.386	0.0343	0.6679	0.0466	0.6121	0.0463
Bark thickness	-2.9796	0.3106	-5.0474	0.3858	-4.571	0.3941
Burn severity index	-	-	-2.672	0.1434	-0.00849	0.000429

Table 3. Statistics for model fit of three candidate logistic regression models of fire-induced tree mortality. The model that incorporated rdNBR had the best overall fit, the lowest AIC, and the lowest rate of both false negative and false positive predictions, making it the best model of the three.

Statistic	Severity exclusive model	CBI inclusive model	rdNBR inclusive model
AIC	2197	1646	1545
Overall fit Saveland and Neuenschwander's Signal Detection Method	0.82	0.86	0.88
P(L|I)	0.91	0.93	0.94
P(D|I)	0.09	0.07	0.06
P(D|d)	0.57	0.68	0.72
P(D|I)	0.43	0.32	0.28

Figure 1. 2x2 matrix of illustrating the framework for predicting a state of nature given the actual state of nature, in this case tree survivorship, adapted from Saveland and Neuenschwander (1990).

		State of Nature	
		Living (l)	Dead (d)
Response	Living (L)	True-Positive P(L|l)	False-Positive P(L|d)
	Dead (D)	False-Negative P(D|l)	True-Negative P(D|d)

$$P(L|l) + P(D|l) = 1.0$$
$$P(L|d) + P(D|d) = 1.0$$

Figure 2. Regression of average bark thickness vs. bark thickness predicted from using Eqn. 4 (r2 = 0.52).

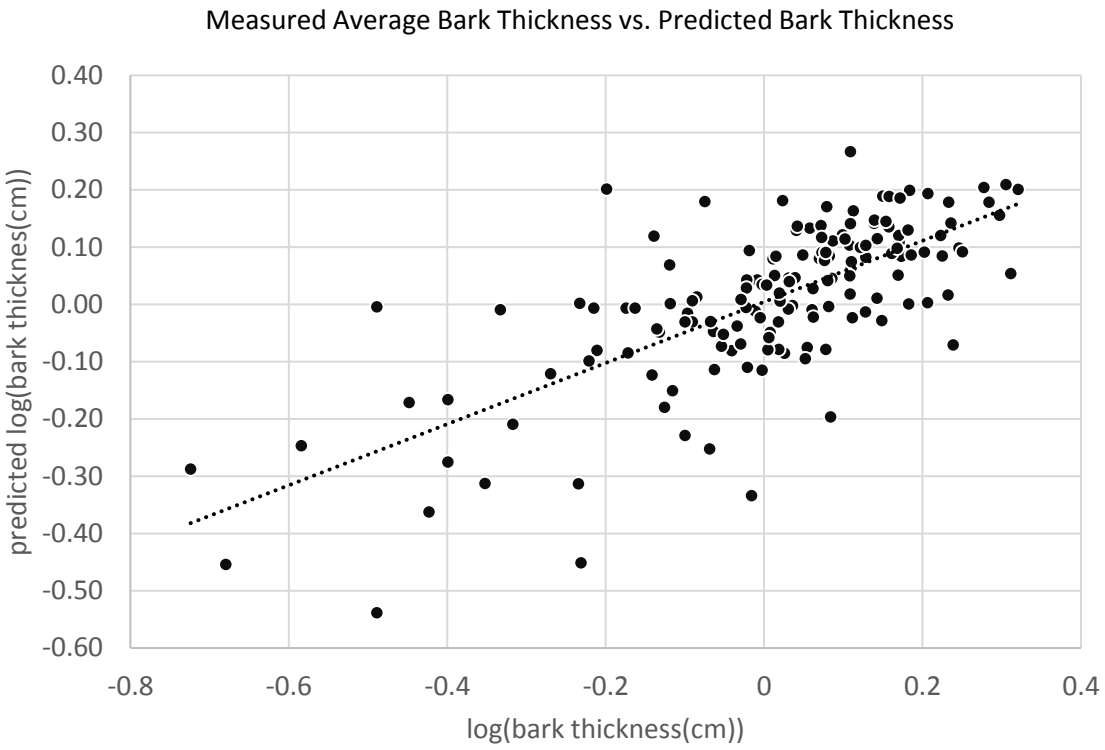

CHAPTER 4: Estimation fuel consumption with field and burn severity methods in the New Jersey Pinelands National Reserve

Abstract

The fuels consumed by wildland fires and prescribed burns are proportional to both reduced risk and carbon emissions, and therefore, accurately estimating fuel consumption is essential to evaluate management options and their success rates. Accurate estimates of fuel consumption are challenging, and often prohibitively tedious, and can be dangerous for field technicians working in post-fire conditions. This study focused on the calibration and validation of surface fuel consumption in the New Jersey Pinelands National Reserve to estimates of field and remotely sensed burn severity, using the Composite Burn Index (CBI) and the Normalized Burn Ratio (NBR). The results of this study suggest that absolute consumption cannot be directly predicted from burn severity data alone, however, relative consumption increases predictably with burn severity and can therefore be used to estimate absolute fuel consumption when pre-burn fuel loading is known. This study provides equations for estimating the relative consumption of surface fuel types in the New Jersey Pinelands National Reserve, which can then be used in conjunction with pre-fire fuel loading data to estimate consumption. This study tests the effectiveness of this method, by validating predictions generated using the approach presented in this manuscript at 6 independent prescribed burns with field estimates of consumption. Finally, I compare consumption rates determined for the PNR with those observed in other conifer dominated forest types, where similar studies have been conducted.

Introduction

Forest ecosystem processes play vital roles in the global carbon cycle, driving accumulation of carbon into pools of live and dead biomass, while simultaneously causing carbon release through natural decomposition and metabolic processes (Waring and Running

2010). A breadth of research suggests that forest disturbances and extreme weather events that damage vegetation are occurring with increasing frequency and alter these processes, causing rapid, transient releases of stored carbon, and subsequent shifts of carbon accumulation rates (Dale et al. 2000, Nemani et al. 2003). Among these disturbances is wildland fire, which releases broadly varying amounts of sequestered carbon into the atmosphere depending on fuel loads and fire characteristics, and causing short- to long-term effects on net ecosystem production. While wildland fire may impact a relatively small percentage of the worlds landmass each year, the effects of fire have an appreciable impact of the global carbon cycle requires monitoring and proactive management to control (Schimel and Baker 2002).

The impacts of fire on ecosystem carbon exchange and aboveground carbon stocks have been studied in a broad range of vegetation types present in North America, including boreal forests (Boby et al. 2010, Bond-Lamberty et al. 2007), temperate coniferous, deciduous, and mixed forests (Campbell et al. 2007, Clark, Skowronski and Gallagher 2015, Hurteau et al. 2014, North and Hurteau 2011), and tundra (Jiang et al. 2015, Rocha and Shaver 2011); however, uncertainty about the spatial heterogeneity of fuels, the magnitude of fire effects, and the actual extent of area burned limits the accuracy of biomass consumption from fires and associated changes in the carbon cycle (Kolden et al. 2012, Meigs et al. 2009, Rogers et al. 2014). Overall, fire consumes biomass, modifies the vertical and horizontal distributions of biomass, redistributes the proportions of live and dead biomass, and alters the balance of carbon exchange with the atmosphere (Amiro et al. 2010, Waring and Running 2010). Magnitude and duration of these impacts on the global C cycle, however, can vary greatly by vegetation types, level of fire intensity. For instance, following wildfires, boreal and temperate coniferous forests are likely remain carbon sinks until about 10 years (Amiro et al. 2010), however, recovery following prescribed fires may only require 4-5 years (Clark et al. 2015). Similarly, stand

replacing fire can substantially alter subsequent ecosystem processes linked to regeneration and carbon exchange rates in temperate forests, if fire effects include shifts in vegetation type (Kashian et al. 2006).

Traditional estimates of biomass consumption across individual fires are based on estimates of consumption rates multiplied by the estimated area burned. Consumption rates are estimated by measuring pre- and post-burn load of specific fuel types and calculating the amount of fuel consumed. However, sampling fuels before and after fire requires technical expertise, lab facilities, and dedication of technical personnel to the field for each fire, which most institutions cannot afford. Further, adequate characterizations of pre-burn fuel conditions are rarely available for wildfires, limiting the applicability of this approach for a large proportion of fire events. Inaccurate delineations of area burned and failure to incorporate heterogeneity in fire effects across burned areas can also lead to error in consumption estimates, and associated emissions estimates. Inaccurate wildfire mapping may be more common than many researchers and managers believe. For instance, Kolden et al. (2012) found that fire perimeters in Yosemite, Glacier, and Yukon-Charley National Parks overestimated actual area burned by 37%, 17%, and 14%, respectively, mainly because they failed to exclude interior unburned area.

Well calibrated remote sensing indices, however, can greatly improve the delineation of fire perimeters and unburnt interior areas, while also serving to map spatial variability in fire effects. Recent studies have begun using a combination of biometric plots and remote sensing indices that account for spatial variability in the magnitude of fire effects, to produce more accurate estimates of carbon emissions from fire (Meigs et al. 2009, Rogers et al. 2014). A specific class of remote sensing indices, known a burn severity indices, are sensitive to change in forest reflectance patterns and reflect the magnitude of change in photosynthetically active vegetation and soil conditions across burned areas as high resolution maps, and have been

found to be proportional to physical change in vegetation and consumption. Meigs et al. (2009) and Rogers et al. (2014) used this approach to estimate carbon emissions in ponderosa pine, mixed conifer stands, and coniferous boreal forest in western North America by estimating emissions factors in the field for specific severity classes and then multiplying factors by the total number of pixels in each severity class. Although both of these studies found that remote sensing indices of burn severity were most correlated with relative consumption (e.g. percent consumed), each also provides emissions factors in absolute form to be used with remotely sensing indices when pre-burn fuel conditions are not known. The use of this technique remains geographically isolated to these two forest types, and has not been validated with independent data.

Managed fire is crucial for the perpetuity of Pine Barrens ecosystems and the ecological diversity, environmental services, carbon storage, and natural beauty they provide (Forman 2012, Ribic et al. 2016), however, the use of fire to preserve these environments, and many others, is increasingly challenged by a lack of monitoring required to evaluate outcomes (Harden 2016, Loehman, Reinhardt and Riley 2014). Carbon accumulation and recovery patterns related to fires have been well studied in Pine Barrens ecosystems (Clark, Skowronski and Gallagher 2014) and the use of remotely sensed burn severity has shown much promise (Warner, Skowronski and Gallagher in press), however the two have not yet been incorporated in this forest type. The scope of this study was to test the ability of remotely sensed data to predict 1) relative fuel consumption when pre-burn fuel loading was known, and 2) absolute consumption when pre-burn fuel loading was not known. To accomplish this, fuel consumption was estimated using traditional, destructive sampling methods at 83 plots that burned in wildfires and prescribed fires, and relationships with remote sensing indices were evaluated. The best resulting model was then validated with data from 6 prescribed burns, ranging from low to high

intensity, where pre- and post-burn fuel loading had been measured across burn units. Model results were then compared to empirical estimates of consumption at the six burns, and the utility of this method for monitoring fuel consumption, is discussed.

Methods

Site Description

The Pinelands National Reserve (PNR), located in southern New Jersey, represents approximately 450,000 ha of contiguous forest where fire management plays a key role in public safety, water and nutrient cycles, and the ecology of both common and endangered forest species. This landscape is home to a variety of upland and wetland forest ecosystems, many of which are fire dependent (Forman 2012). Of this landscape, 62% is comprised of upland forests (Lathrop and Kaplan 2004), which are subjected to the greatest amount of fire activity. These upland forests are dominated by three major communities; 1) oak-dominated stands, consisting of black oak (*Quercus velutina* Lam.), chestnut oak (*Q. prinus* L.), white oak (*Q. alba* L.), pitch pine (*Pinus rigida* Mill.), and shortleaf pine (*P. echinata* Mill.), 2) mixed stands, with pitch pine and mixed oaks in the overstory, and 3) pitch pine-dominated stands, consisting of pitch pine with few overstory oaks and abundant scrub oaks (*Q. marilandica* Muenchh., *Q. ilicifolia* Wangenh.) in the understory (McCormick and Jones 1973). Understory communities in these forests are dominated by varying mixes of ericaceous shrubs, shrub oaks, and associated species, such as lowbush blueberry (*Vaccinium palladum* Aiton and *angustifolium* Aiton), black huckleberry (*Gaylussacia baccata* (Wangenh.) K. Koch.), scrub oak (*Q. ilicifolia*), black jack oak (*Q. marilandica*), inkberry holly (*Ilex glabra*). The PNR has historically experienced a higher frequency of fires than other areas in the northeastern US (Forman and Boerner 1981). Over the past 10 years, approximately 63,000 ha in have burned in prescribed fire and 34,000 ha have burned in wildfire across public lands in the state (Bien 2016, New Jersey Department of the

Treasury 2006, 2008, 2010, 2012, 2014, 2016, Stevenson 2016). Over the past century, fire prevention and suppression efforts, aimed at reducing public risk, have been quite successful, and have likely also maintained a reduction in fire emissions and an increase in carbon storage over this timescale (Clark et al. 2010, Clark et al. 2015, Forman and Boerner 1981). However, with an average of over 1,000 wildfire ignitions each year and semi-frequent large fires in a continually wildland-urban interface setting, the need for continued adaptation of fire management strategies to meet developing public safety and environmental needs remains critical.

Fuel Consumption Sampling

71 forest census plots were installed across 21 prescribe burn units, prior to burning, as part of an independent study to assess fuel treatment effectiveness in 2012, 2013, and 2014 (Skowronski et al. 2016). Plots were circular, with a radius of 15 m, and were spread broadly across burn units with a minimum distance of 30m from fire perimeters. At each plot, forest floor and shrub biomass was destructively harvested in three $1m^2$ areas, prior to burning, and again at three new locations after burning. Forest floor material was harvested down to, but not including, the soil organic matter layer, which does not frequently burn and was easily differentiated by a lack of entire or distinguishable fuel particles (e.g. leaves, twigs, fruiting bodies). An additional 12 pairs plots were installed following 4 wildfires in 2014. Paired plots were located 60 m apart, on opposite sides of control lines, where pre-burn fire histories and fuel conditions had been similar prior to burning, according to local fire managers who worked the burns. It was assumed that the unburnt fuels are representative of pre-burn conditions of these burn areas, however, there is no way to directly measure pre-burn fuel loading in the field environment once it has been consumed. Locations of all burned plots were recorded with a Trimble GeoExplorer 6000 GPS unit, paired with a Tornado receiver (Trimble Inc., Sunnyvale, CA,

USA). Differential correction was performed on all points and resulted in an estimated horizontal accuracy of within 3m or less of the actual field locations of all points. All samples were dried in laboratory convection ovens at 60® C for a minimum of 2 days, sorted into fuel classes and weighed. Pre- and post-burn masses were differenced for each plot to generate estimates of consumption.

Field Estimation of Burn Severity

Field estimates of burn severity were assessed at all burned calibration plots, using the Composite Burn Index, described by Key and Benson (2006). This method involves ranking fire effects factors, using pre-defined criteria, on a scale of [0 – 3], following fires. Assessments were conducted during the growing season following each fire, within the original 15m plot radii. Minor modifications to this method were made, according the suggestions in the method's original description, which including omitting certain irrelevant factors(Key and Benson 2006). For instance, changes in species composition were not evaluated because this data was unavailable at the spatial resolution of this study, and previous work has suggested that understory shrub components are unlikely to change, due to prolific sprouting traits, following prescribed fires (Matlack, Gibson and Good 1993). Likewise, coarse woody debris greater than 8 inches in diameter was disregarded as a factor following fieldwork, as it is uncommon on this landscape and was absent from almost all plots.

CBI estimates are generated on a continuous range of [0 – 3], however it is common to classify these estimates as "No Effect", "Low Severity", "Moderate Severity", and "High Severity" for simplified comparison with other environmental data (Key and Benson 1999). These classifications essentially represent the ranges of [0.0 – 0.5], [0.5 – 1.5], [1.5 – 2.5], and [2.5 – 3.0], respectively, and it is this form of CBI that has been used in other studies to estimate

carbon emissions from fire, rather than the continuous form (Boby et al. 2010, Meigs et al. 2009, Rogers et al. 2014). Therefore, classified CBI was also calculated for each plot.

Remote Sensing of Burn Severity

Remotely sensed burn severity was estimated with the Normalized Burn Ratio (NBR) index of burn severity for all fires involved in the study, using Landsat TM and ETM+ imagery. This index is estimated from reflectance data of the earth's surface, visible in NIR and SWIR data, and which is captured in Landsat TM and ETM+ bands 4 (NIR) and 7 (SWIR). These bands are highly sensitive to changes in forest leaf area and the char that is produced by fire, and are the least correlated of Landsat TM and ETM+ bands (Garcia and Caselles 1991), making them a sensible data source from which to derive NBR. Therefore this study is focused on the use of NBR. NBR is estimated by subtracting NIR pixel values from SWIR pixel values, and dividing by the sum of the NIR and SWIR pixel values (Key and Benson 1999). Resultant NBR values are typically multiplied by 1000, to convert from decimal form to integer form, for easier interpretation. Although a variety of methods for deriving burn severity from other reflectance data have been suggested in some other regions, strong correlations between NIR and SWIR bands and field data imagery have been observed in the New Jersey Pinelands (Warner et al. in press). Although Warner et al. (in press) used NIR and SWIR data from a different sensor to estimate dNBR, rather than NBR, in the Pinelands, other work that has compared these estimates suggests that NBR may be more robust in the on this landscape, at least when using LANDSAT data (Chapter 2).

Level 1 Landsat TM and ETM+ data was acquired through the USGS Global Visualization Viewer (GLOVIS) utility for the PNR in years 2010 – 2016. Since the PNR falls between multiple flight paths of Landsat satellites, with none catching the complete study area, imagery for paths 13 - 14 and rows 32 – 33 were used to make complete images of each year. While previous

studies in temperate conifer forests have suggested the use of imagery collected ±2 weeks from burn dates, previous work in the PNR suggests that growing season imagery, pre- and post-burn, collected when LAI is at a maximum, is still similarly correlated with both dormant and growing season fire effects in temperate deciduous and mixed forests, and reduces the need for data, processing, and has higher similarity in pre-burn reflectance (Chapter 2). In accordance with the suggestions of this previous study, satellite data collected between the 176th and 288th days of the year were used in this study.

Multiple processing steps are required to convert raw Landsat imagery into useful NBR data. First, Landsat data, which is served in a digital format to decrease file size, must be converted to top of atmosphere reflectance values. Clouds and pixels missing band 4 or 7 values in Landsat ETM+ SLC-off data (see Markham et al. (2004)) were masked from images as necessary. Variation in atmospheric conditions requires that data be then normalized to a single clear image. For this step, I chose an image from 2010 collect by the Landsat TM sensor, which was the clearest and most complete (e.g. cloud-free and without missing data) of all the available growing season imagery for 2010 – 2016. Each subsequent image was normalized to dense, mature Atlantic White Cedar forests (*Chamaecyparis thyoides* (L.) Britton, Sterns & Poggenb.), and are a good normalization feature because they are evergreen, and tend to have consistent reflectances through time (Isaacson, Serbin and Townsend 2012). Finally, images within given years were mosaicked to produce complete, growing season images for each year (Howard and Lacasse 2004). NBR was estimated for each year using the mosaicked imagery.

GPS data, collected during the field component, was then used to extract burn severity data for each plot. Since it is unlikely that plot centers of field plots and Landsat pixels will overlap, and therefore field plots may partially overlap into multiple pixels, it is common to derive plot NBR values with a sampling method that incorporates values of neighboring pixels. I

followed the previous work of Warner et al. (in press) in the PNR, using a bilinear interpolation that produces a weighted average pixel value, that incorporates the distances of the four nearest pixel centroids to the GPS point location (e.g. plot center). The resulting set of NBR data was then classified into No Effect, Low Effect, Moderate Effect, and High Effect classes following the calibration described in Chapter 2. Wall to wall burn severity maps were also extracted for the 5 validation burns, which burned entire units to easily defined natural boundaries.

Calibration of Burn Severity Indices to Fuel Consumption Data

Continuous and classified CBI and NBR were calibrated to the absolute and relative estimates of surface fuel consumption, using linear regression, and were evaluated based on goodness of fit to produce a total of 4 calibrations. Relative and absolute consumption data were also pooled by classified NBR and CBI severity classes, and averages and standard deviations were determined, as has been previous studies in conifer forests of the Pacific Northwest and the Alaska (Boby et al. 2010, Meigs et al. 2009, Rogers et al. 2014). This produced an additional 4 calibrations. The utility of the all calibrations were compared and the best CBI and best NBR calibrations were selected.

Validation

Pre- and post- burn fuels were sampled at six additional prescribed fires that were conducted in similar forest types between 2008 and 2015, where fire intensity was also recorded during burns, for Joint Fire Sciences Program Project 09-1-04-1 and Joint Fire Sciences Project 12-1-03-11. Fuels from each of these fires were dried, sorted, and weighed as described previously in this section, however unlike the 2011 burn, plot data was geo-located, allowing me to collect post-burn data near pre-burn samples. Fuels of each of these fires were differenced and multiplied by the area of each burn to estimate overall consumption. Fire intensity estimates were based on temperature and turbulent kinetic energy measurements from similar

custom meteorological arrays, deployed in each burn unit (See Clark et al. (2010), Heilman et al. (2013), Kiefer et al. (2014), Skowronski et al. (2016)). While these intensity estimates are not used in any calculations in this analysis, they provide a useful context for whether the model performs under the range of possible fire intensities, typical of prescribed burns in the PNR. With both methods, fuel consumption was estimated in terms of foliage, fine, wood, and stems, and were then summed for total consumption. Using the same approach as described earlier in this chapter, NBR burn severity coverages were mapped for each burn. Pixel frequency in each severity class was determined for each fire, and used to estimate the absolute consumption by multiplying the relative consumption associated with each severity class, determined in the calibration phase, by the average fuel loading of each fire, and then weighting the sum of consumption in all classes by the proportion of area they represented in each fire. This process was conducted for each fuel type (e.g. fine, wood, stems, foliage), and resultant NBR-based consumption estimates were compared to field-based consumption estimates for each fuel type with linear regression to evaluate how well this method predicts consumption within each fuel class. Absolute fire-wide consumption was also estimated using both methods.

Results

Fuel Consumption Sampling

Overall fuel loading of surface and ground fuels across all plots was 16.13 ± 4.19 T ha^{-1} (mean ± 1 standard deviation). Fine, Wood, Stem, and Foliage material made up approximately 52%, 23%, 25%, and >1%, respectively (Table 1). Pre-burn loading had a slightly lower average than a previously published study reports, which found pre-burn pine-scrub oak forest loading to be 21.58 ± 7.02 T ha^{-1} and fine, wood, and stem components to comprise 51%, 12%, and 37% of overall material (Clark et al. 2015). Fuel consumption was largely a function of pre-burn fuel loading and fire type (Figure 1). Overall, relative consumption was 63 ± 21%, at prescribed fires

whereas relative consumption at wildfires was 72 ± 16% (mean ± 1 standard deviation). This difference was expected given prescribed fires in this area are typically conducted in a manner intended to produce less of an effect than wildfires. Absolute consumption, was very similar between sites. A total of 10.7 ± 5.13 T ha^{-1} was consumed across prescribed fires while 10.57 ± 4.36 T ha^{-1} were consumed in the wildfire plots. Upon closer look at consumption in individual fuel classes, it is apparent that wildfires do consistently consume more of all fuels than prescribed fires, except wood, which seems to be produced in some circumstances (Table 1). This is counterintuitive, although, Clark et al. (2015) also found very high standard deviations among wood consumption observed at other prescribed burns in the PNR.

Field Estimation of Burn Severity

Across all field plots, continuous CBI ranged from 0.20 – 2.55, and had an average of 1.26 ± 0.54 (average ± 1 standard deviation). In prescribed fire plots, CBI was significantly lower than in wildfire plots (mean ± 1 standard deviation 1.13 ± 0.45; 2.07 ± 0.35). Classified CBI for all prescribed fire and wildfire plots produced a total of 3 No Effect plots, 54 Low Severity plots, 25 Moderate Severity plots, and 1 High Severity plot. Since only 1 High Severity plot was found, this observation was omitted from analysis using classified CBI.

Remote Sensing of Burn Severity

Across all field plots, continuous NBR ranged from [-30 - 714], and had an average of 453 ± 165 (average ± 1 standard deviation). In prescribed fire plots, NBR was significantly higher than in wildfire plots (mean ± 1 standard deviation 504 ± 103; 151 ± 139), which was to be expected given the inverse relationship between NBR and severity. The variance of burn severity among prescribed fire plots was similar with both NBR and CBI, although among wildfire plots burn severity assessed with NBR had a much greater variance than it did when estimated with CBI. When NBR was classified using the classification scheme developed in Chapter 2 of

this thesis, there were a total of 3 No Effect plots, 54 Low Severity plots, 25 Moderate Severity plots, and 1 High Severity Plot.

Calibration of Burn Severity Indices to Consumption Data

Continuous CBI was poorly correlated with both absolute and relative consumption, although relative consumption had a notably higher coefficient of correlation ($R^2 = 0.01$; $R^2 = 0.07$) (Figure 2). When fuel consumption was pooled by classified CBI, total consumption values increased with severity. Fine fuel consumption had low variances within all classes, while variances of other fuel types were considerably higher. Variance of wood consumption was notably high in Low Severity plots, in contrast to that of No Effect and Moderate Severity plots. Overall, relative consumption had lower variances than absolute consumption, which was to be expected given the higher correlation of continuous CBI and relative consumption. Continuous NBR was poorly correlated with absolute and relative consumption (Figure 2). When fuel consumption was pooled by severity classes derived from NBR, total consumption values increased with severity as would be expected. Relative consumption averages had substantially lower variances than absolute severity. Overall, classified CBI and NBR produced the most sensible estimates, which were of relative consumption.

Validation

Among the 6 fires used in the validation component of this study, fire size ranged from 4.3ha to 161 ha. The prescribed burns at Turkey Buzzard Bridge, Acorn Hill, and Experiment 1 were described as having generally low intensity, while Cedar Bridge, Experiment 1, and Experiment 2, were described as having high intensity (Table 3), providing a representative range of prescribed fire intensity for context of validation results. In each of these fires, a mix of backing, flanking, and head fire were used to burn fuels, however the lower intensity fires were

dominated by backing fire, while the Cedar Bridge fire was dominated by a combination of backing and flanking fire, and Experiments 1 and 2 were dominated by head fire.

Although CBI was the best of the three burn severity indices tested, no additional validation dataset was available with which to validate estimates of consumption. I therefore only validated the method which used classified NBR to estimate relative consumption. NBR estimates of burn severity were within range of those observed in the calibration phase of this study (Figure 3). No pixels were classified as having high severity in any of these fires.

Fuel loading and consumption at validation plots was similar to that found in calibration plots (Tables 1 and 4). Three of the fires, which had not been burned in at least 30 years, had substantially higher fuel loads than the other three, which had been burned sometime within the previous 15 years. Half of the validation burns as being of generally low intensity, while the other half were of generally high intensity (Table 3).

Average fuel consumption, estimated using both field and remote sensing methods, was compared in terms of Mg ha^{-1} for each fuel type. Regressions of field and remote sensing-based consumption estimates show that the results of each burn were highly correlated for fine fuels ($R^2 = 0.78$), however other shrub and wood estimates had worse correlations (Figure 4). This was expected, however, given the high standard deviations on the estimates of shrub and wood consumption for each burn severity class (Table 2). Wood and shrubs represent minor components of total consumption, relative to fine fuel consumption, and therefore, correlations between each method's estimates of total consumption were very high ($R^2 = 0.90$) (Figure 4).

Of all of the fires, the Cedar Bridge fire consumed the most fuel both per hectare and had the highest total consumption of any fire. The Butler Place fire, on the other hand, had higher total fuel consumption than the Turkey Buzzard Bridge Fire, which was larger. Similarly,

the Experiment 1 consumed approximately twice the fuel than Experiment 3 did, which was conducted two years after Experiment 1 in the same burn unit.

Discussion

The scope of this study was to calibrate and validate a remote sensing burn severity index for assessing fuel consumption in the New Jersey Pinelands National Reserve. The PNR was chosen as a large, contiguously forested area, with a high fire frequency (over 1,000 fires annually) and an active prescribed and wildfire management program (La Puma, Lathrop and Keuler 2013, Skowronski et al. 2016). Based on previous research, I chose to use NBR, which was found to be highly correlated with other field observations (Chapter 2), and is similar to dNBR, which is also highly correlated with field observations (Warner et al. in press). We first calibrated NBR, as well as a simple field method for estimating burn severity that may be useful to practitioners on small, low-value burns, with field estimates of consumption at prescribed fires and wildfires, and validated the calibrations with and independent dataset.

During the calibration phase of this study, it was found that total fuel consumption at prescribed fires was largely proportional to the amount of pre-burn fuel loading, and that an average of 66% was consumed (Figure 2). Overall wildfire consumption was determined to be 72%, however this was likely lower than the actual consumption due to an inability to differentiate consumption from standing woody material that was only partially burned and then fell to the forest floor after the flame front passed. Actual fuel consumption was likely to be much higher, and future work should aim to differentiate these effects. Fine fuels, which make up an average of 78% of the consumed material in prescribed fires and 67% of consumed material in wildfires was the most correlated with pre-burn fuel loading estimates (Figure 2), following foliage, which was the most minor contributing fueltype, and was the most predictable with burn severity estimates (Figure 4). Fine fuels were also the most homogenous

of the fuel groups, in terms of pre-burn loading, post-burn loading, and consumption in both the calibration and validation datasets (Tables 1 and 4). On the other hand wood consumption was the poorest measurement of the study, and was undoubtedly a large source of error in the study. The results suggest that in prescribed burn plots, wood actually contributed an average 9% in material and less than 1% of overall consumption in wildfire plots. This clearly misrepresents consumption, through a movement of woody material to the forest floor that was not accounted for, and was subsequently the fuel type with the worst predictions (Figure 4). Shrub stem material represented an average of 30% and 28% of prescribed fire and wildfire consumption respectively, but were also somewhat variable (Table 1). Although foliage consumption was high and consistent between both prescribed fires and wildfires, it represented less than 1% of prescribed fire consumption and only 3% of wildfire consumption, and was therefore relatively insignificant, in terms of overall consumption.

Initial comparisons between continuous burn severity indices and continuous consumption estimates (both absolute and relative) revealed poor correlations in all cases, although CBI was more correlated with relative consumption than NBR (Figure 2). When classified CBI and NBR and consumption data was averaged by class, relative consumption clearly increased with burn severity (Table 2). CBI also had lower variances about averages of relative consumption, than NBR, which was to be expected given the better correlation that CBI data had with consumption in Figure 2. Absolute consumption had high variances in both cases. These results support those of previous studies using CBI and dNBR, which is similar to NBR, that burn severity indices are substantially better at estimating relative consumption than absolute consumption. Further, the study at hand suggests that estimates of relative consumption produced using CBI are slightly more accurate than those estimated with remote sensing (Table 2). As a remote sensing method, however, NBR can be used across a broader area and more

rapidly than the field estimated CBI, and is more repeatable (Morgan et al. 2014), making it a preferable option to managers.

Relative rates of fuel consumption, determined for specific burn severity classes with NBR, were validated 6 independent prescribed fires, where field estimates of fuel loading had been collected, pre- and post-burn, and consumption had been calculated. We estimated actual per hectare consumption of surface and ground fuels, by multiplying consumption rates for specific burn severities by the number of pixels of that severity. Overall, field and remote sensing estimates of consumption were highly correlated ($R^2 = 0.90$), which was largely dependent on the predictability of fine fuels, which make up the majority of consumed material (Figure 4).

Several limitations about the results of this study should be considered. First, this study only accounted for fuels in the forest understory, and did not quantify impacts to soil or tree biomass pools. Soil organic matter and below ground biomass, such as tree roots and soil organisms, are typically not consumed during the dormant season when prescribed fires are conducted in this landscape. Further, multiple studies using LiDAR have illustrated that canopy fuels can represent an important component of overall consumption in prescribed fires in the PNR (Skowronski et al. 2011, Skowronski et al. 2007). Therefore, this study represents only a portion of the overall consumption that occurs during prescribed fires, but sets a framework for future studies aimed at quantifying canopy fuel change should build on. Second, the results of study did not incorporate high burn severity data, which would be expected from wildfires, and therefore are limited in terms of the range of severity for which they should be used to make predictions. However, the paired plot approach used in this study to capture data in 4 wildfires produced good results, and could be easily conducted at more future wild fires to produce a more comprehensive calibration. The data show that wildfire plots consumed greater

proportions of fuels than prescribed fires, but did not represent the entire range of wildfire conditions present on this landscape. Further, the results of both wild and prescribed fire consumption reveal an important challenge to estimating wood consumption that occurs when stems fall from vegetation to the forest floor. I suspect that this effect would be most pronounced and low to moderate severity fires, where fire behavior may be great enough to weaken fuel at the base, such that it falls into the burned area shortly after fire passes, whereas high severity fire would likely consume any of this fuel. A third limitation is the relatively small number of fires used in the validation segment of this study. Overall, this did not account for variations in ignition patterns, fuel moisture conditions, or weather conditions during these burns, which all can have important effects on fire behavior and associated consumption in this environment (Mueller et al. 2014).

Wildland fire is an important component of the global carbon cycle which causes rapid releases of stored carbon, as well the potential for subsequent vegetation growth that can outpace pre-fire carbon accumulation rates. The balance at which carbon accumulation outpaces carbon release, however, is largely related to the severity and frequency of fire events. Climate and human activity over at least the past 500 years have together dominated the control of fire regimes in the northeastern United States, and have dictated the role of fire and the global carbon cycle. The global carbon cycle is also strongly linked to climate, through its role in the greenhouse effect, ocean chemistry, and ocean currents, and has produced weather conducive for large and severe fires, and at times has given climate a greater role in defining this balance.

Under a climate conducive to fire activity, strategic elimination of hazardous fuels, through mechanical thinning, prescribed fire, and wildland fire use operations, is the only way to manage the severity of fires, but also creates an important juxtaposition between carbon and

risk management, as well as the need to accurately estimate consumption in order to evaluate the effectiveness of management for either goal. Estimating fuel consumption has remained a key challenge for fire management for many years, because consumption rates are often highly variable across broad spatial extents, however, recent research suggests that new remote sensing methods can enhance the estimation of spatial variability in consumption rates. These results of this study provide a new calibration and validation of a method that can improve the estimation of fuel consumption during prescribed burning, by integrating field estimates of fuel loading with easily calculated remote sensing indices. Managers can use this method to evaluate the effectiveness of treatments, in terms of meeting fuel reduction goals, and can use results to contrast the benefits and limitations of different management strategies that involve prescribed burning.

Conclusions

This study found that relative fuel consumption varies with fire type for fine, wood, shrub stem, and foliage fuel types, and that fine fuels are the most homogenous in terms of fuel loading and relative consumption. Overall, fine fuels represented 67% of total consumption in prescribed burns, and 78% of total consumption in wildfires, whereas other fuels made up lesser components. These relationships are correlated with NBR burn severity data, which can be derived from satellite imagery, and can be used to efficiently predict absolute fuel consumption when pre-burn fuel loading is known. These results were validated with an independent dataset. Although these results are limited to making predictions about surface and ground fuel consumption in the PNR for prescribed fires only, this tool can greatly increase the ability of managers to evaluate fuel consumption at fuel treatments and justify management strategies. Further, this study provide a framework and guidance that can be employed in future studies aimed at producing similar estimates under a wider range of conditions and fuel types.

Acknowledgements

This work was made possible through the availability of data collected for Joint Fire Sciences Program Projects 09-1-04-1 and 12-1-03-11; the invaluable guidance and technical support of Dr. Nicholas Skowronski, Dr. Kenneth Clark, and Dr. Warren Heilman of the US Forest Service Northern Research Station; the support from New Jersey Forest Fire Service section fire wardens Tom Gerber, Shawn Judy, Samuel Moore, John Earlin, Scott Knauer, Ashley House, and Brian Corvinis, and former division warden James Dusha, and former State Firewarden Maris Gabliks; and for the help of Michael Farrell, Melanie Maghirang, Nick Carlo, and Joseph Rua.

References

Amiro, B., A. Barr, J. Barr, T. Black, R. Bracho, M. Brown, J. Chen, K. Clark, K. Davis & A. Desai (2010) Ecosystem carbon dioxide fluxes after disturbance in forests of North America. *Journal of Geophysical Research: Biogeosciences,* 115.

Bien, W. F. 2016. (Personal Communication).

Boby, L. A., E. A. Schuur, M. C. Mack, D. Verbyla & J. F. Johnstone (2010) Quantifying fire severity, carbon, and nitrogen emissions in Alaska's boreal forest. *Ecological Applications,* 20**,** 1633-1647.

Bond-Lamberty, B., S. D. Peckham, D. E. Ahl & S. T. Gower (2007) Fire as the dominant driver of central Canadian boreal forest carbon balance. *Nature,* 450**,** 89-92.

Campbell, J., D. Donato, D. Azuma & B. Law (2007) Pyrogenic carbon emission from a large wildfire in Oregon, United States. *Journal of Geophysical Research: Biogeosciences,* 112.

Clark, K. L., N. Skowronski & M. Gallagher. 2014. The fire research program at the Silas Little Experimental Forest, New Lisbon, New Jersey. In *USDA Forest Service experimental forests and ranges*, 515-534. Springer.

Clark, K. L., N. Skowronski & M. Gallagher (2015) Fire Management and Carbon Sequestration in Pine Barren Forests. *Journal of Sustainable Forestry,* 34**,** 125-146.

Clark, K. L., N. Skowronski, M. Gallagher, W. Heilman & J. Hom. 2010. Fuel consumption and particulate emissions during fires in the New Jersey Pinelands. In *Proceedings of the 3rd Fire Behavior and Fuels Conference*, 19.

Dale, V. H., L. A. Joyce, S. McNulty & R. P. Neilson (2000) The interplay between climate change, forests, and disturbances. *Science of the Total Environment,* 262**,** 201-204.

Forman, R. 2012. *Pine Barrens: ecosystem and landscape*. Elsevier.

Forman, R. T. & R. E. Boerner (1981) Fire frequency and the pine barrens of New Jersey. *Bulletin of the Torrey Botanical Club***,** 34-50.

Garcia, M. L. & V. Caselles (1991) Mapping burns and natural reforestation using Thematic Mapper data. *Geocarto International,* 6**,** 31-37.

Harden, G. 2016. Audit Report: Forest Service Wildland Fire Activities – Hazardous Fuels Reduction. 42. US Department of Agriculture.

Heilman, W. E., S. Zhong, L. John & J. J. Charney (2013) Development of modeling tools for predicting smoke dispersion from low-intensity fires.

Howard, S. M. & J. M. Lacasse (2004) An evaluation of gap-filled Landsat SLC-off imagery for wildland fire burn severity mapping. *Photogrammetric Engineering and Remote Sensing,* 70**,** 877-880.

Hurteau, M. D., J. B. Bradford, P. Z. Fulé, A. H. Taylor & K. L. Martin (2014) Climate change, fire management, and ecological services in the southwestern US. *Forest Ecology and Management,* 327**,** 280-289.

Isaacson, B. N., S. P. Serbin & P. A. Townsend (2012) Detection of relative differences in phenology of forest species using Landsat and MODIS. *Landscape ecology,* 27**,** 529-543.

Jiang, Y., E. B. Rastetter, A. V. Rocha, A. R. Pearce, B. L. Kwiatkowski & G. Shaver (2015) Modeling carbon–nutrient interactions during the early recovery of tundra after fire. *Ecological Applications,* 25**,** 1640-1652.

Kashian, D. M., W. H. Romme, D. B. Tinker, M. G. Turner & M. G. Ryan (2006) Carbon storage on landscapes with stand-replacing fires. *BioScience,* 56**,** 598-606.

Key, C. H. & N. C. Benson (1999) The Normalized Burn Ratio (NBR): A Landsat TM radiometric measure of burn severity. *United States Geological Survey*.

Key, C. H. & N. C. Benson (2006) Landscape assessment (LA). *FIREMON: Fire effects monitoring and inventory system. Gen. Tech. Rep. RMRS-GTR-164-CD, Fort Collins, CO: US Department of Agriculture, Forest Service, Rocky Mountain Research Station*.

Kiefer, M. T., W. E. Heilman, S. Zhong, J. J. Charney, X. Bian, N. S. Skowronski, J. L. Hom, K. L. Clark, M. Patterson & M. R. Gallagher (2014) Multiscale Simulation of a Prescribed Fire Event in the New Jersey Pine Barrens Using ARPS-CANOPY. *Journal of Applied Meteorology and Climatology,* 53**,** 793-812.

Kolden, C. A., J. A. Lutz, C. H. Key, J. T. Kane & J. W. van Wagtendonk (2012) Mapped versus actual burned area within wildfire perimeters: characterizing the unburned. *Forest Ecology and Management,* 286**,** 38-47.

La Puma, I. P., R. G. Lathrop & N. S. Keuler (2013) A large-scale fire suppression edge-effect on forest composition in the New Jersey Pinelands. *Landscape Ecology,* 28**,** 1815-1827.

Lathrop, R. & M. Kaplan (2004) New Jersey land use/land cover update: 2000–2001. *New Jersey Department of Environmental Protection,* 35.

Loehman, R. A., E. Reinhardt & K. L. Riley (2014) Wildland fire emissions, carbon, and climate: Seeing the forest and the trees–A cross-scale assessment of wildfire and carbon dynamics in fire-prone, forested ecosystems. *Forest Ecology and Management,* 317**,** 9-19.

Markham, B. L., J. C. Storey, D. L. Williams & J. R. Irons (2004) Landsat sensor performance: history and current status. *IEEE Transactions on Geoscience and Remote Sensing,* 42**,** 2691-2694.

Matlack, G., D. Gibson & R. Good (1993) Clonal propagation, local disturbance, and the structure of vegetation: ericaceous shrubs in the pine barrens of New Jersey. *Biological Conservation,* 63**,** 1-8.

McCormick, J. & L. Jones. 1973. *The Pine Barrens: Vegetation Geography*. New Jersey State Museum.

Meigs, G. W., D. C. Donato, J. L. Campbell, J. G. Martin & B. E. Law (2009) Forest fire impacts on carbon uptake, storage, and emission: the role of burn severity in the Eastern Cascades, Oregon. *Ecosystems,* 12**,** 1246-1267.

Morgan, P., R. E. Keane, G. K. Dillon, T. B. Jain, A. T. Hudak, E. C. Karau, P. G. Sikkink, Z. A. Holden & E. K. Strand (2014) Challenges of assessing fire and burn severity using field measures, remote sensing and modelling. *International Journal of Wildland Fire,* 23**,** 1045-1060.

Mueller, E., N. Skowronski, A. Simeoni, K. Clark, R. Kremens, W. Mell, M. Gallagher, J. Thomas, A. Filkov & M. El Houssami (2014) Fuel treatment effectiveness in reducing fire intensity and spread rate-An experimental overview.

Nemani, R. R., C. D. Keeling, H. Hashimoto, W. M. Jolly, S. C. Piper, C. J. Tucker, R. B. Myneni & S. W. Running (2003) Climate-driven increases in global terrestrial net primary production from 1982 to 1999. *science,* 300**,** 1560-1563.

New Jersey Department of the Treasury, O. o. M. a. B. 2006. State of New Jersey: The Governor's FY2007 Detailed Budget. D-123.

---. 2008. State of New Jersey: The Governor's FY2009 Detailed Budget. D-127.

---. 2010. State of New Jersey: The Governor's FY2011 Detailed Budget. D-113.

---. 2012. State of New Jersey: The Governor's FY2013 Detailed Budget. 563.

---. 2014. State of New Jersey: The Governor's FY2015 Detailed Budget. 586.

---. 2016. State of New Jersey: The Governor's FY2017 Detailed Budget. D-114.

North, M. P. & M. D. Hurteau (2011) High-severity wildfire effects on carbon stocks and emissions in fuels treated and untreated forest. *Forest Ecology and Management,* 261**,** 1115-1120.

Ribic, C. A., D. J. Rugg, D. M. Donner, A. J. Beck & B. J. Byers (2016) The Moquah Barrens Research Natural Area: Loss of a pine barrens ecosystem.

Rocha, A. V. & G. R. Shaver (2011) Burn severity influences postfire CO2 exchange in arctic tundra. *Ecological Applications,* 21**,** 477-489.

Rogers, B., S. Veraverbeke, G. Azzari, C. Czimczik, S. Holden, G. Mouteva, F. Sedano, K. Treseder & J. Randerson (2014) Quantifying fire-wide carbon emissions in interior Alaska using field measurements and landsat imagery. *Journal of Geophysical Research: Biogeosciences,* 119**,** 1608-1629.

Schimel, D. & D. Baker (2002) Carbon cycle: the wildfire factor. *Nature,* 420**,** 29-30.

Skowronski, N., K. Clark, R. Nelson, J. Hom & M. Patterson (2007) Remotely sensed measurements of forest structure and fuel loads in the Pinelands of New Jersey. *Remote Sensing of Environment,* 108**,** 123-129.

Skowronski, N., A. Simeoni, K. Clark, W. Mell, R. Hadden, R. Kremens, A. Filkov, W. Edwards, J. Dusha, A. Evans-House, E. Mueller, M. Gallagher, J. C. Thomas, M. El Houssami & S. Santamaria. 2016. Evaluation and Optimization of Fuel Treatment Effectiveness with an Integrated Experimental/Modeling Approach Final Report: JFSP Project Number 12-1-03-11. 24. Joint Fire Sciences Program.

Skowronski, N. S., K. L. Clark, M. Duveneck & J. Hom (2011) Three-dimensional canopy fuel loading predicted using upward and downward sensing LiDAR systems. *Remote Sensing of Environment,* 115**,** 703-714.

Stevenson, M. 2016. (Personal Communication).

Waring, R. H. & S. W. Running. 2010. *Forest ecosystems: analysis at multiple scales*. Elsevier.

Warner, T. A., N. S. Skowronski & M. R. Gallagher (in press) High spatial resolution burn severity mapping of the New Jersey Pine Barrens with WorldView-3 near infrared and shortwave infrared imagery. *International Journal of Remote Sensing and Remote Sensing Letters*.

Table 1. Summary of fuel loading and consumption (T/ha), estimated at 74 prescribed burn plots and 12 wildfire plots in pine dominated forest of the Pinelands National Reserve. Stems and wood figures represent a total of 1 - 100 hr material, which was a combination of undifferentiated live and dead material for stems.

	Prescribed Fire			***Wildfire***		
	Pre-burn	Post-burn	Consumed	Pre-burn	Post-burn	Consumed
Fine	8.64 ± 1.96	1.95 ± 1.09	6.40 ± 2.46	6.56 ± 1.76	0.15 ± 0.36	6.41 ± 1.64
Wood	3.82 ± 2.02	2.04 ± 1.71	1.63 ± 2.62	2.80 ± 1.32	2.30 ± 2.31	0.49 ± 2.06
Stems	3.87 ± 2.05	1.46 ± 1.10	2.56 ± 2.17	4.90 ± 3.29	1.67 ± 2.40	3.23 ± 2.52
Foliage	0.04 ± 0.18	0.0 ± 0.01	0.1 ± 0.18	0.44 ± 0.63	0.01 ± 0.02	0.44 ± 0.63
Total	**16.37 ± 4.02**	**5.46 ± 2.72**	**10.70 ± 5.13**	**14.7 ± 5.13**	**4.13 ± 2.94**	**10.57 ± 4.36**

Table 2. Summary of absolute and relative consumption of surface and ground fuels in relation to field (CBI) and remote sensing (NBR) indices of burn severity.

	CBI			*NBR (Calibrated with CBI)*		
	No Effect	Low Severity	Moderate Severity	No Effect	Low Severity	Moderate Severity
n	*3*	*54*	*25*	*3*	*52*	*28*
			Absolute Consumption (T/ha)			
Fine	5.65 ± 2.88	6.49 ± 2.27	6.58 ± 2.35	6.97 ± 0.43	6.43 ± 2.43	6.54 ± 2.12
Wood	1.74 ± 1.65	1.48 ± 2.57	2.10 ± 2.45	2.35 ± 0.96	1.87 ± 2.52	1.14 ± 2.56
Stems	-0.55 ± 2.24	2.61 ± 1.83	3.26 ± 2.57	3.37 ± 4.14	2.26 ± 1.86	3.37 ± 2.40
Foliage	0.00 ± 0.00	0.03 ± 0.11	0.27 ± 0.52	0.07 ± 0.13	0.02 ± 0.08	0.26 ± 0.51
Total	6.84 ± 1.31	10.61 ± 4.90	12.21 ± 4.37	12.77 ± 3.10	10.58 ± 4.86	11.31 ± 7.76
			Relative Consumption (%)			
Fine	58 ± 16	75 ± 16	82 ± 14	74 ± 3	57 ± 16	81 ± 15
Wood	43 ± 43	29 ± 74	34 ± 58	51 ± 10	37 ± 65	16 ± 77
Stems	-11 ± 86	58 ± 36	63 ± 38	33 ± 44	55 ± 38	63 ± 44
Foliage	0 ± 0	9 ± 29	39 ± 49	33 ± 58	8 ± 27	37 ± 47
Total	47 ± 7	64 ± 19	72 ± 13	63 ± 1	64 ± 18	68 ± 18

Table 3. Size and counts of pixels in different severity classes for 6 prescribed burns.

Fire Name	Size (ha)	No Effect Pixels	Low Severity Pixels	Moderate Severity Pixels	Fire Intensity Characterization
Turkey Buzzard Bridge	99	539	567	0	Low (Heilman et al. 2013)
Acorn Hill	107	23	945	283	Low (Kiefer et al. 2014)
Cedar Bridge	161	0	0	1801	High (Clark et al. 2010)
Experiment 1	6.7	55	20	0	High (Skowronski et al. 2016)
Experiment 2	4.3	7	44	0	High (Skowronski et al. 2016)
Experiment 3	6.7	52	23	0	Low (Skowronski et al. 2016)

Table 4. Fuel loading and consumption for 6 prescribed fires.

Fire Name	Fuel Type	*Pre-burn* mean ± 1SD	*Post-burn* mean ± 1SD	*Consumption* mean ± 1SD
Acorn Hill	Foliage	0.03 ± 0.04	0.00 ± 0.00	0.03 ± 0.04
	Fine	5.38 ± 2.78	4.01 ± 1.97	1.39 ± 3.41
	Wood	1.04 ± 0.65	0.68 ± 0.86	0.36 ± 1.08
	Stems	6.49 ± 3.60	2.50 ± 1.79	4.03 ± 3.96
Turkey Buzzard Bridge	Foliage	0.00 ± 0.00	0.00 ± 0.00	0.00 ± 0.00
	Fine	7.47 ± 1.16	3.10 ± 0.78	4.38 ± 1.40
	Wood	2.32 ± 1.46	1.86 ± 0.95	0.47± 1.72
	Stems	1.69 ± 1.32	1.27 ± 0.56	0.42 ± 1.44
Cedar Bridge	Foliage	0.00 ± 0.00	0.00 ± 0.00	0.00 ± 0.00
	Fine	15.4 ± 3.55	7.12 ± 1.78	8.32 ± 1.94
	Wood	2.61 ± 2.09	1.82 ± 1.36	0.81 ± 2.48
	Stems	4.45 ± 1.02	3.78 ± 2.02	0.65 ± 1.12
EX1	Foliage	0.16 ± 0.36	0.00 ± 0.00	0.14 ± 0.69
	Fine	6.93 ± 1.91	2.37 ± 0.68	5.03 ± 0.85
	Wood	4.92 ± 2.42	2.23 ± 0.78	2.86 ± 2.96
	Stems	3.69 ± 2.06	0.99 ± 0.70	2.82 ± 2.57
EX2	Foliage	0.00 ± 0.00	0.00 ± 0.00	0.00 ± 0.00
	Fine	9.70 ± 2.90	2.72 ± 0.69	7.54 ± 2.28
	Wood	3.17 ± 1.63	2.67 ± 2.74	0.61 ± 3.30
	Stems	4.40 ± 1.59	1.25 ± 0.80	3.38 ± 1.48
EX3	Foliage	0.01 ± 0.02	0.00 ± 0.00	0.01 ± 0.02
	Fine	2.22 ± 1.15	0.90 ± 0.49	3.56 ± 1.06
	Wood	5.49 ± 1.78	2.24 ± 0.71	-0.08 ± 1.17
	Stems	2.53 ± 1.72	2.66 ± 1.53	1.40 ± 1.26

Table 5. Total consumption estimates for 6 prescribed fires using the field and NBR methods.

	Field Method			*NBR Method*		
Fire	Mg/ha	Mg	St.Dev.	Mg/ha	Mg	St.Dev.
Acorn Hill	5.75	569.49		7.39	731.61	21%
Turkey Buzzard Bridge	5.52	590.64		6.39	683.73	21%
Cedar Bridge	16.92	2724.12	19%	15.7	2527.70	2%
EX1	10.85	72.72	65%	8.65	57.96	36%
EX2	11.52	49.55	61%	9.25	39.78	30%
EX3	4.88	32.72	72%	5.84	39.13	35%

Figure 1. Fuel consumption in relation to pre-burn fuel loading for wild and prescribed fires in the New Jersey Pinelands National Reserve. Average fuel consumption ± 1 standard deviation for fine, wood, stems, and foliage was 72 ± 17%, 30 ± 69%, 51 ± 47%, 100 ± 0% in prescribed burns and 98 ± 4%, 18 ± 58%, 64 ± 31%, 100 ± 0%. Note the lower apparent consumption of wood in wildfires, likely to do a relocation of canopy and shrub wood to the forest floor during moderate severity fire. Overall consumption was 67 ± 14% in prescribed fires and 72 ± 16% at wildfires, however the consumption rate of wildfires is likely low due to the fact that this study was not able to differentiate consumption at the forest floor and transport of similar material from shrubs or trees that had been partially burned and fell.

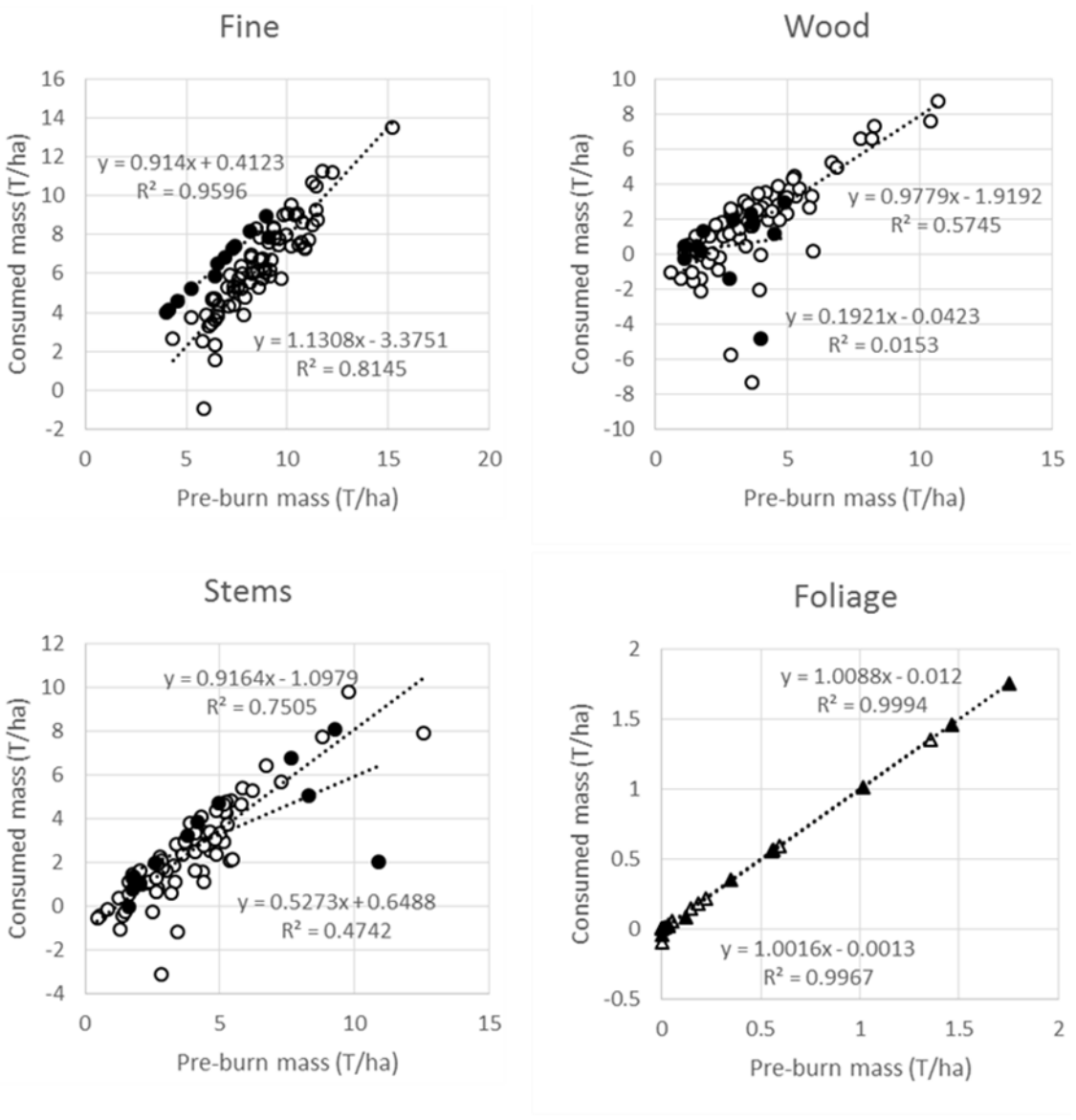

Figure 2. Relationships between fuel consumption and burn severity. Consumption was considered in terms of absolute consumption, or mass consumed, as well as relative consumption, or the percentage of mass consumed. A field (CBI) remote sensing index (NBR) are compared.

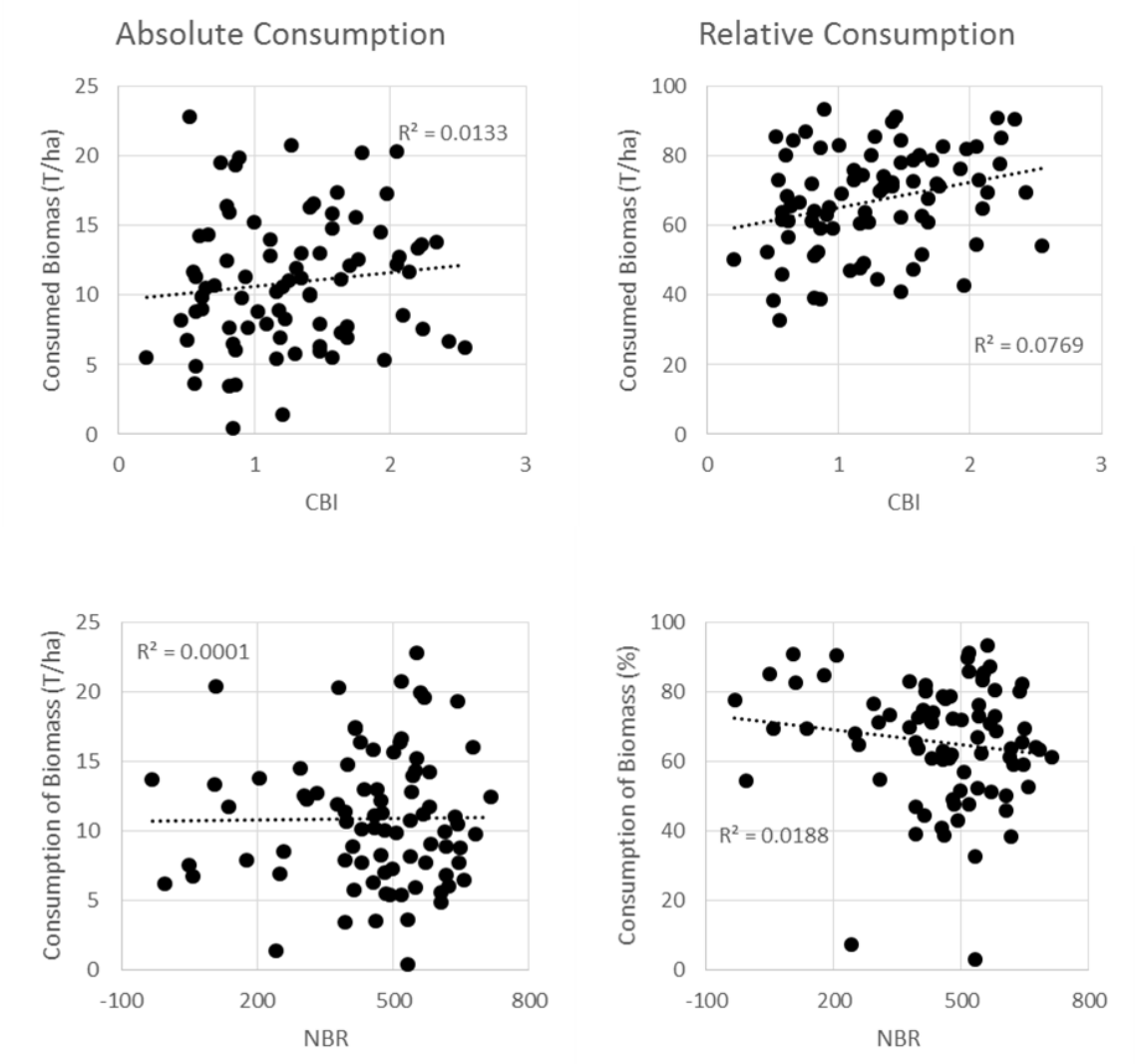

Figure 3. Burn severity maps of three large and three small prescribed burns, conducted in the New Jersey Pinelands between 2008 and 2015. Experiment 1 and Experiment 3 represent 2013 and 2015 burns of the same unit. Burn severity is measured in terms of the NBR.

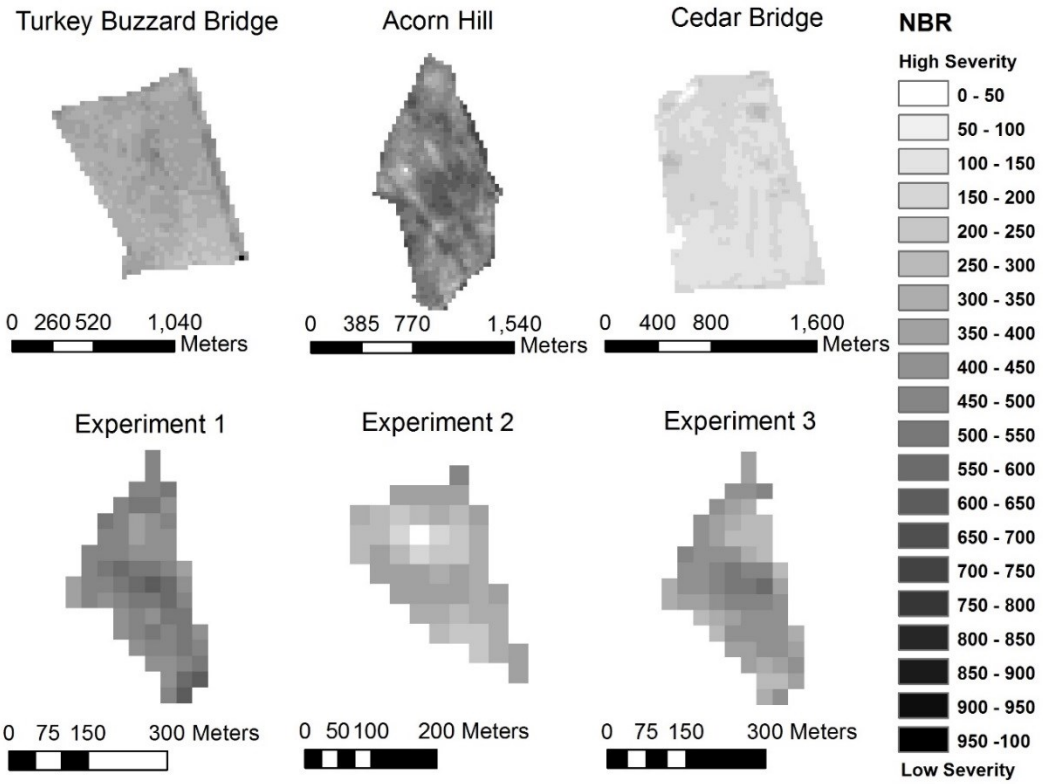

Figure 4. Regression of fuel consumption estimated from NBR and fuel consumption estimated from destructive sampling pre- and post-fire for 6 prescribed burns in the NJ Pinelands. Total and fine fuel consumption had high coefficients of determination, while shrub and wood consumption was substantially lower, but also represent a small amount of the overall consumption in prescribed burns.

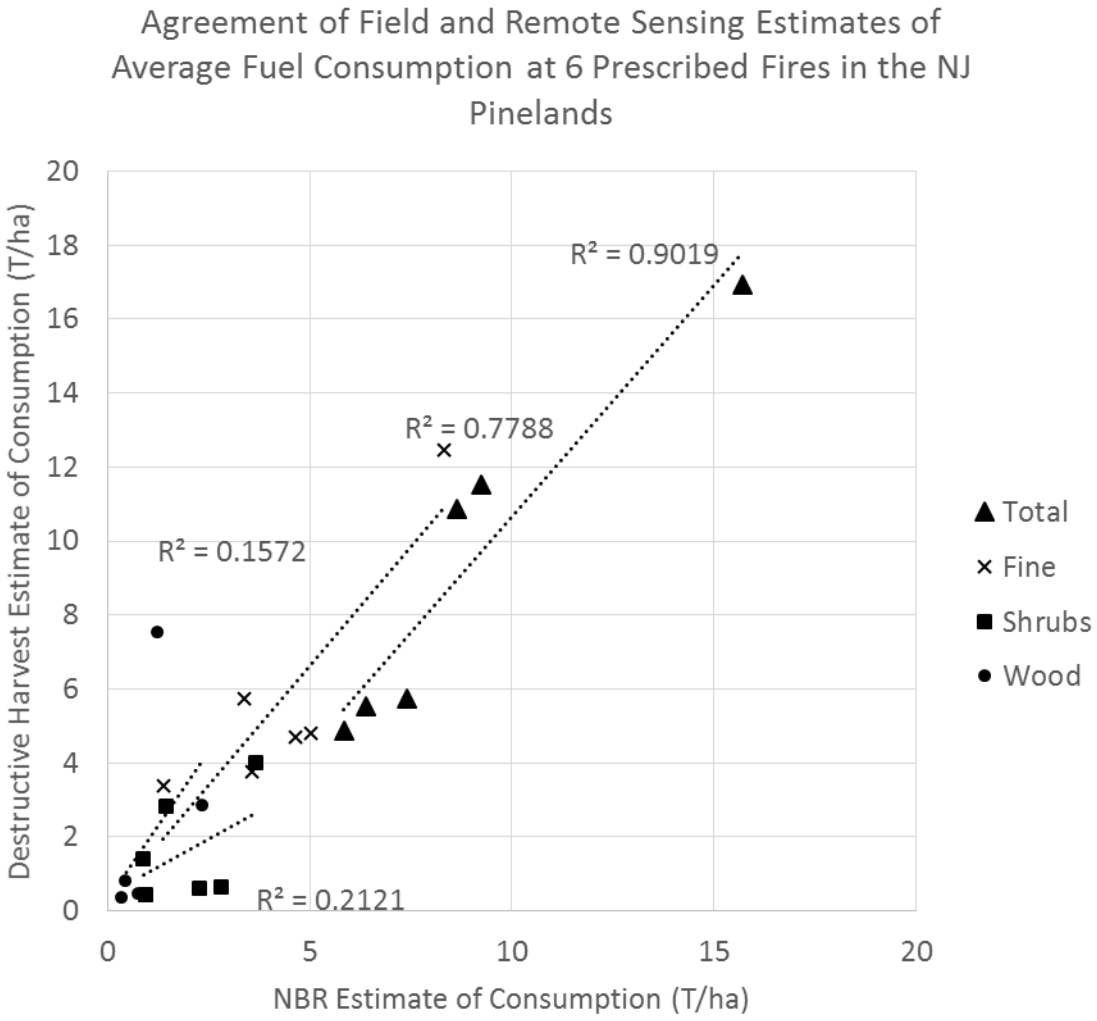

CHAPTER 5: Trends of Burn Severity by Fire Type, Size, and Timing in the New Jersey Pinelands (2006-2015)

Abstract

Over the past century, the wildland fire regime in the New Jersey Pinelands National Reserve has shifted dramatically, as a result of aggressive wildland fire management, cultural changes among the population of humans in the area, and weather. These changes are documented in state records as decreases in acreage burned and the numbers of fires, however this monitoring approach provides little indication to the current quality of fire on this landscape, or how that may differ from historic times. I used a remotely sensed burn severity index, the relative differenced normalized burn ratio (rdNBR) to examine the distributional properties of recent fire across the central area of the New Jersey Pinelands National Reserve, which constitutes New Jersey Forest Fire Service's central management zone. I derived burn severity for over 400 fires over the ten year period from 2006 – 2015 from LANDSAT TM and ETM+ archived data, and compared burn severity attributes with timing of fires. The results of this analysis demonstrate a strong seasonal influence of burn severity that ultimately limits the upper range of severity. Future analysis that integrates these results about the seasonal patterns of burn severity with fuel consumption, tree mortality, and regeneration rates, will provide an enhanced understanding of the role of fire in the community dynamics of this landscape, carbon balance over time, and how the outcomes of prescribed and wildfire on this landscape may shift with altered management policy and climate change.

Introduction

Wildland fire has shaped and reshaped the pine and oak forests throughout much of eastern North America, largely at the hand of humans, since before European settlement (Abrams 1992). For at least the first half of the last millennium, Native Americans implemented

fire extensively across this region, shaping the forest to promote forest food crops and clearing understory vegetation to improve overland travel. With the colonization of this region by Europeans, Native Americans' were forced from the area taking with them, the fire regimes they had facilitated preceding centuries. The new, more agrarian society that replaced them, was focused on producing food in more domestic ways and had begun fragmenting the landscape with permanent settlements, and conducted comparatively little controlled burning.

Analyses of tree rings, sediment cores, and historic documents indicate that regular, low intensity fire dominated the fire regime across this region shortly before European settlement. This frequency of fire would have limited the accumulation of fuels required to enable larger and more severe fires in most places. Tree ring records also show seasonal variability in this use of fire, which has silvicultural significance in producing different effects in vegetation and fuel consumption. For instance, dormant season fire kills a smaller proportion of trees overall, and can reduce understory fuel loading, while promoting a dense, raised canopy, whereas growing season fire tends to be more damaging, especially to hardwoods. Similarly, the suitability of conditions for germination and seedling establishment for certain species, like pitch pine, are dependent on specific fire effects that only comes with higher intensity fire. Following European settlement, tree ring records indicate a long period of decreased fire activity.

The ecological roles of fire in the pine and oak forests of this region include cycling nutrients, preparing seed beds, releasing seeds, and modifying forest structure in ways that creates habitat for a variety of flora and fauna. Fire also has a strong role in moderating the selective pressures within forest communities, such that role of wildland fire has been compared to that of an herbivore, which presumably defoliates and kills some vegetation, while giving the withstanding vegetation and its associates a competitive advantage (Bond and Keeley 2005). An expansion on this idea would be to compare the role of fire, in pyrogenic forests such

as pine and oak forests of eastern North America, to that of a keystone species, without which, the populations and their functions within the system will undergo dramatic changes until a new balance is reached. For instance, the strength of a fire's initial impacts is correlated with large shifts in the presence and activities of avifaunal species (Rose et al. 2016). Then, within a two decades following the cessation of fire, large shifts in forest structure can be observed (Skowronski et al. 2011, Angelo, Duncan and Weishampel 2010), as well as shifts in the presence and population densities of avifaunal species (Engstrom, Crawford and Baker 1984, Loeb and Waldrop 2008). Further, within a century, dramatic shifts in forest tree species occur (La Puma, Lathrop and Keuler 2013). This process, which has been coined "mesophication", results in compositional shifts from pine and oak dominated forest types, to forests of more mesic compositions, dominated by maples, beeches, and gums, which decrease forest flammability as their dominance increases (Nowacki and Abrams 2008).

While fragmentation, fire suppression, and mesophication have characterized much of the forested land that is or was once dominated by pine and oak in North America's Mid-Atlantic region over the past 100+ years (Nowacki and Abrams 2008), the New Jersey Pinelands National Reserve (PNR) remains the largest contiguously forested area in the coastal plain of this region and maintains the highest level of fire activity in the region (Clark, Skowronski and Gallagher 2014a). Historic fire records for the PNR provide a rich context in terms of fire occurrence in this region (La Puma et al. 2013), however, only limited quantitative description about the variety fire effects have ever been characterized for this region, with respect to fire type and seasonality. Further, available descriptions were produced between the 1930s and 1960s (Clark et al. 2014a), however, the current level of forest maturation, which has not been seen since before colonial times, brings to question the applicability of these descriptions.

Although historically, quantitative data about fire effects has been insufficiently monitored across most landscapes, analysis of remotely sensed burn severity provides the ability to study changes in forests after they occur with archived reflectance data. Numerous bandwidths of data are available from a variety of sensor platforms, however those within the NIR (700 – 1500nm) and SWIR range (1500 – 2400nm) are most effective for determining burn severity (Garcia and Caselles 1991). The differenced normalized burn ratio (dNBR), and the relative differenced normalized burn ratio (rdNBR) are the most commonly used remote sensing indices of burn severity, and are usually calculated with data collected by the Landsat program's TM, ETM+, or OLS sensors; which collectively have archived NIR and SWIR data since 1984 at a day interval or shorter (Soverel, Perrakis and Coops 2010, Soverel et al. 2011). Prior to use, however, substantial field work is required to calibrate remote sensing outputs to field observations of severity.

Researchers from western North America have begun using this technique to analyze fire effects at landscape and regional scales. For instance, Picotte et al. (2016) analyzed 4893 fires between 1984 and 2010 across the coterminous United States, and produced results that suggest burn severity and fire size had not changed substantially in most vegetation groups, although this study did not differentiate unique eastern fire-adapted ecosystem, such as coastal plain oak and pine barrens, and only included fires <404ha, which is two orders of magnitude larger than the average fire size in New Jersey (Table 1). Other studies of this type have similarly focused on western landscapes and provide little context for recent fire in eastern pyrogenic landscapes, such as the PNR (Rivera-Huerta, Safford and Miller 2016, Dennison et al. 2014, Miller and Safford 2012). However, recent work in the PNR, using the commercially available high resolution Worldview3 sensors (Warner, Skowronski and Gallagher 2017) and Landsat TM and ETM+ data (Chapter 1) has demonstrated the potential for long term landscape-scale

studies of burn severity integrated over time. Further, recent work in the PNR demonstrates that variability in relative fuel consumption and pitch-pine mortality rates following fire are correlated with the variability observed in remotely sensed burn severity. A stronger understanding of the distribution of burn severity on this landscape, and the importance of seasonality in modifying that distribution, would have important implications of various landscape-scale fire management strategies and climate change on forest carbon stocks, vegetation dynamics, and risk management, and benchmarks the current fire regime.

Despite increasing fire activity in other parts of the country, the Pinelands has followed the trends represents one of many landscapes where acreage burned shown a declining trend over much of the past 80 years. Around the turn of the 20th century, area burned by wildfires in the Pinelands averaged on the order of 40,000 hectares per year, peaking at approximately 92,000 ha in 1930 (Forman and Boerner 1981, Kümmel 1902). Since then, annual area burned in wildfires has declined steadily due to fire suppression efforts, with the exception of a complex of large fires in 1963, when approximately 75,000 ha burned in wildfires (La Puma et al. 2013, Forman and Boerner 1981, Boyd 2008). While the current prescribed burning program treats approximately 6,000 – 8,000 ha of forest and grass annually, the average combined area burned by wildfire or prescribed fire remains 1-2 orders of magnitude less than it was 100 years ago (New Jersey Department of the Treasury 2014, New Jersey Department of the Treasury 2012, New Jersey Department of the Treasury 2016). Recent work, aiming to provide insight to disturbances for the mid-Atlantic region, found that climate change may further limit fire activity in this region through altering seasonal humidity and precipitation patterns (Clark et al. 2014b). Aside from acreage burned, however, qualitative shifts in the fire regime on this landscape have remained poorly characterized, making it difficult to develop predictive tools to estimate potential shifts in ecological responses and guide appropriate management responses.

This study is focused on evaluating the current fire regime, inclusive of both wild and prescribed fire, in terms of a burn severity index for the fire-dependent pitch pine dominated landscape of the PNR. I first mapped burn severity index, in terms of the relative differenced normalized burn ratio (rdNBR) for fires that occurred during the decade of 2006 -2015. From those maps, I extracted burn severity index distributions of 447 independent fires, and analyzed seasonal trends and the overall distribution of fire on this landscape. I then discuss results in terms of fire management, and the implications these results have on past and future management scenarios.

Methods

Site Description

The New Jersey Pinelands National Reserve (PNR) occupies an area of approximately 445,000 ha, in southern and central New Jersey. This study focused on a large section of the northern PNR located in Burlington, Ocean, and Atlantic Counties, that comprises the management zone of New Jersey Forest Fire Services central division, and is the locale of the majority of the fire in the state. Forests of the PNR are dominated by oaks and pines in the uplands and cedar, pine, and maple in the lowlands (Forman 2012, Robichaud and Anderson 1994). Upland forests account for approximately 62% of the forested area of the PNR and experience a high frequency of both wild and prescribed fire, whereas wetlands experience less. Upland forests are made up of 3 distinct communities, all of which contain Pitch Pine (*Pinus rigida*): (1) oak-dominated stands, comprised of chestnut oak (*Quercus. prinus* L.), black oak (*Q. velutina* Lam.), white oak (*Q. alba* L.), scarlet oak (*Q. coccinea* Muenchh.), with scattered shortleaf pine (*P. echinata* Mill.) and Pitch Pine, (2) mixed pine-oak stands, with an overstory of pitch pine and mixed oaks, and (3) pitch pine-dominated stands, containing few overstory oaks, but with an understory of abundant scrub oaks (*Q. marlandica* Münchh and *Q. ilicifolia* Wangenh.) (Boerner

and Forman 1982, Forman and Boerner 1981, Forman 2012, Lathrop and Kaplan 2004, Robichaud 1973). By the end of the late 19th century, large fires regularly burned across scrubby young forests that had grown up with the cessation of industrial scale harvesting in the mid-1800s (Kümmel 1902). Similar fire occurrences continued through the early 20th century, however by late century large fires had become comparatively infrequent due to a variety of cultural changes and the development of the New Jersey Forest Fire Service (Forman and Boerner 1981). Data about fire effects during the 19th and 20th centuries is methodologically inconsistent and qualitative, and subsequently, provides little context for today's fire regime.

Recent Fire History

All available records of fire perimeters, types, and, when available, ignition dates, were compiled for all prescribed fires and wildfires greater than 1 ha in a central region of the New Jersey Pinelands National Reserve, specified as the management areas of New Jersey Forest Fire Service's Central Region, Joint Base Dix-McGuire-Lakehurst, and the Warren Grove Range, were gathered from local fire management agencies. Together, these areas delineate the region of the highest numbers of fires and acreage burned, annually, in the state (Bien 2016). Records of area burned and fire occurrence data for land owned by the state of NJ is summarized in annual, state budget reports. These data were combined with similar data for federally managed lands in this area, and compared with the estimates of fire only in the Pinelands region, to provide context for this study (Table 1). These measures do not account for a small amount of burning conducted by on National Park Service land, small military installations, and agricultural areas.

Remote Sensing of Burn Severity

Burn severity maps were generated for all prescribed and wildfires in the study, using the relative differenced normalized burn ratio (RdNBR). RdNBR is a remote sensing method which has been used extensively in recent years to characterize the variability of fire effects in

numerous forest environments (Miller and Thode 2007, Miller et al. 2009, Soverel et al. 2010), and has been demonstrated to have strong correlations with field observations in the PNR (Chapter 2). RdNBR is estimated from NIR and SWIR data, collected before and after fires, and describes the magnitude of change that fire has had on vegetated environments. NIR and SWIR data, collected specifically by the Landsat TM and ETM+ sensors as bands 4 and 7, are the most frequently used to derive RdNBR (Chapter 1). This approach is quite sensible because these bands have a relatively high spatial resolution, are highly uncorrelated with each other but are sensitive to the effects of fire, and are freely available (Garcia and Caselles 1991). Timing of remote sensing data collection is also an important factor that influences burn severity estimates (Key 2005). While most studies have used data collected within a timeframe of ± 2 – 8 weeks before and after fires (Key and Benson 2006), recent work in the PNR suggests that using growing season imagery from before and after fires can be useful for comparing fires that have occurred different seasons in temperate deciduous and mixed forests (Chapter 2, Chapter 3, Chapter 4), which can have broadly varying reflectances between seasons (Isaacson, Serbin and Townsend 2012). Considering the collection of fire data analyzed in this chapter represents fire in every month of the year, I selected to generate RdNBR burn severity for individual fires using growing season Landsat data, as described in Chapter 2.

Landsat TM and ETM+ band 4 and band 7 data were acquired from the USGS GLOVIS online database for all years of the study (http://usgs.glovis.gov/). Digital imagery reflectance values were converted to top of atmosphere reflectance and were radiometrically corrected (Chander, Markham and Helder 2009). Additional normalization between imagery was achieved by adjusting scaling in images to match values of dense conifer forest, specifically dense stands of Atlantic white cedar (*Chameacyparis thyoides* (L.) Britton, Sterns & Poggenb.), which maintain similar reflectances through time (Isaacson et al. 2012). Clouds and cloud shadows were

manually masked as necessary, and pixels with incomplete information at the edges of ETM+ imagery were converted to null values (See Markham et al. (2004)). Resulting gaps in images were filled by mosaicking multiple incomplete leaf on images from the same year, which produced nearly complete images (Howard and Lacasse 2004). Processed raw data was then used to derive the normalized burn ratio (NBR), and ultimately RdNBR coverages for all years, using the following equations.

$$NBR = \frac{NIR-SWIR}{NIR+SWIR}, \quad \text{(Key and Benson 1999)}$$

$$RdNBR = \frac{NBR_{pre} - NBR_{post}}{\sqrt{ABS(\frac{NBR_{pre}}{1000})}}, \quad \text{(Miller and Thode 2007)}$$

Fire perimeter data was used to extract wall-to-wall burn severity coverages for each individual fire from RdNBR maps. Burn severity coverages were summarized as mean severity, maximum severity, and the standard deviation of severity for each fire, and these statistics were plotted against day of year, when ignition dates were available. Burn severity data was also pooled in order to derive overall burn severity distributions by fire type and by month of year. We also combined data for each month of the year, and summarize the proportions of fire typically observed in each month of the year that are in High (RdNBR = [], Moderate, Low, and No Effect Severity classes in each month of the year. Perimeter and fire type information was available for a total of 81 wildfires and 367 prescribed fires, which occurred on state and federally owned public lands in this region. Exact dates of ignition were available for a total of 148 fires, including 56 wildfires and 92 prescribed fires.

Analysis of Burn Severity Patterns 2005-2015

I evaluated 1) the distribution of burn severity among different types of fire 2) season variability of burn severity statistics, 3) the relationship between fire size and those burn severity characteristics listed above, and 4) the influence of pre-burn fuel conditions on severity.

To examine the distribution of burn severity among wildfire, prescribed fire, and all fire, pixel values of all fires in all years were pooled into three groups, wildfire, prescribed fire, and all fire, and plotted the frequencies of severities for each group. To examine seasonal variability, maximum, mean, and variety of pixel values of individual fires were pooled by the week in which they occurred (for fires in which date information was available). To assess the importance of fire size, log fire size was regressed with maximum, mean, and variability of fire severity for each fire. Finally, pre-burn cover conditions, visually estimated as part of the CBI evaluation protocol, were regressed with rdNBR burn severity estimates. As the maps were produced using mid to late growing season imagery, this worked reasonably well to account for most fires in a given year, considering the vast majority of fires on this landscape occur during the spring and early summer; however, occasional late season fires occurred after imagery for that year was collected. Therefore extracted from the following year's imagery for those late season fires. Burn severity statistics were extracted as Zonal Statistics using the fire history shapefiles, described in the previous section, with ArcGIS 10.x software. This data was then saved to a database where they were matched with fire size, year, type (wildfire or prescribed fire), and date information (when available) from fire history records.

Results

Recent Fire History

Between 2006 and 2015, NJ Forest Fire Service, Joint Base Dix-McGuire Lakehurst, and the Warren Grove Gunnery Range reported a total of 84,049 acres burned in wildfires, and a total of 155552 acres burned with prescribed fire. Specific wildfire and prescribed fire frequency figures were not available, except for the number of wildfires responded to by NJFFS, which totaled 12440 over the 10 year period. However, a plot of the data comprised in Table 1 by day of year illustrates the possible distribution of wild and prescribed fire frequency over a

given year (Figure 1). While the shapefile data for 80 wildfires represent less than 1% of the number of fires on this landscape, it does in fact represent 57% of the area burned in wildfires during this time. Exact frequency of individual prescribed fires was unavailable, however the shapefile data of this study represents 36% of the area burned in prescribed fires. Combined, this data represents a 44% sample of the total area burned over the ten year period. Shapefile data with exact fire dates, represents a 44% of the area burned in wildfires and 10% of the area burned with prescribed fire. These percentages represent sampled area in relation to the total area burned across the state by prescribed fire, because there was no way distinguish the exact locations of fire occurrence from the data available at the time of the study (Table 1). However, it is well understood that the vast majority of both wild and prescribed fire in the state occur within the Pinelands, the ecosystem of interest for this study.

Remote Sensing of Burn Severity

Due to SLC-off missing data, cloud cover, or images that did not completely cover the study area, multiple images were mosaicked to create more complete images for all years except 2007, 2010, and 2011. A listing of all imagery used and the percent coverage of the final image used in each year is provided in Table 2, as well as the area of missing data from fires for each year, if applicable. Of the 447 fires, 45 fires had between 1 - 49% of their pixel data missing, with an average of 18% missing data for those fires. Across the entire dataset, this amounted to less than 2% of the data.

Analysis of Burn Severity Patterns 2005-2015

RdNBR of wildfires and prescribed fires ranged 0 – 1279 and 0 – 1040, respectively. In each group, however, a large percentage of pixels reported as burned had values of zero, and likely represent unburned interior area or are a result slight misalignment of fire perimeters and burn severity maps that resulted in the inclusion of unburnt edges. For wildfires, a total of

29,281 pixels, or 14% of the area reported as burned, had a value of zero. Similarly, for prescribed fires, a total of 46,096 pixels, or 17% of the area reported as burned, had a value of zero. I excluded zero value data as unburned forest in all subsequent analyses. Mean burn severity of wildfire and prescribed fire was 415 and 175, respectively, however, shapes of their distributions varied substantially. Prescribed fire had a unimodal distribution, skewed toward the low end of the range of possible burn severity, whereas the distribution of wildfires was bimodal, with peaks in both the low and high range (Figure 2). This is likely due to broadly differing seasonal constraints on fire, as will be discussed in the next section. Overall, wildfire exhibited a greater and somewhat more uniform range of burn severity, than did prescribed fire.

Fire size played little role in explaining burn severity within burn units. Mean burn severity had no relationship with fire size while maximum burn severity was only weakly correlated with fire size. The variance of severity was also unrelated to fire size (Figure 3). Fire size also had little influence on the percent of unburned area (e.g. burn severity of zero), as the coefficient of determination between the two was only $R^2 = 0.01$.

However, distributions of burn severity varied widely with the timing of fire. Burn severity in the winter and early spring months was strongly skewed toward the low end of the spectrum (Figure 4). By the summer months, burn severity had a much more uniform distribution and reached the highest degree of severity observed. As summer transitioned to fall, a rapid decrease in severity was observed. Maximum, mean, and the variance of burn severity peaked in weeks 26 – 30 (late June - July), 23-27 (mid-June – mid-July), 27 – 31 (July – early August), respectively (Figure 5). Timing of fires was uncorrelated with the percent of unburned area in fires ($R^2 = 0.02$).

Discussion

The results of this study suggest that of timing of fire, fire size, and fire type, timing has the strongest link to burn severity patterns. Seasonality and fire size have been assumed to play important roles in the dynamics of fire effects in the Pinelands national reserve, however, prior to this study only qualitative data and anecdotal accounts provided any evidence for these assumptions. This study, however, provides a quantitative description of burn severity over the range of fire size and timing that has been present in the Pinelands over the past five years. The data reported in this study can serve as a benchmark for future research on fire effects on this landscape, and can help fill in regional gaps in burn severity reporting that has been missed in previous studies. Overall, this study demonstrates the importance of the timing of fire, with relation to seasons, and the relative low importance of fire size. Further, this study demonstrates key differences in the distributions of prescribed fire severity and wildfire severity in this system, at least which has been present over the past 10 years.

Our study suggests that the distribution of burn severity generally follows predictable patterns over the course of the year, and that burn severity arises independently from fire size. Further, timing of fire imposes limitations to the maximum and minimum burn severity that can occur on a given day of the year. Although I observed that average and maximum severity of fires generally increases from January through August, and then decreases though December, that not all fires will have high severity and that low severity fires can be observed at any time of year. Similarly, I found that prescribed fires, which are conducted January – March in this area, tend to have a much lower burn severity than wildfires, which tend to occur at the end of prescribed fire season and continue throughout November (Figure 1). However, this difference is more likely an effect of seasonality than fire type. Mechanistically, timing may be important in dictating the severity because of changes in burning conditions such as weather and fuel conditions.

In contrast with other studies, I found that fire size was of little importance in explaining burn severity distributions. For instance Duffy et al. (2007) found that average burn severity was positively correlated with the natural logarithm of fire size in Alaskan boreal forest. Similarly, Boelman, Rocha and Shaver (2011) found that the proportion of unburned area within the fire perimeter decreases with fire size, while, I the proportion of unburnt area (e.g. burn severity of zero) and fire size to be uncorrelated. These studies did not consider seasonal variation as a factor, however in places like the Alaskan boreal forest, the window for wildfires is much shorter than in the PNR and therefor may not be an important factor there.

Through damaging and killing vegetation, consuming biomass, and heating seeds, transient fire events thin the forest structure, cycle nutrients, prepare seedbeds, and releases seeds, thereby providing important habitat conditions for flora and fauna and maintaining a varied mix of habitats, successional stages, diverse organisms, and ecosystem functionality (Forman 2012, Robichaud 1973, Robichaud and Anderson 1994). Other work with burn severity at spring time prescribed fires and late spring and early summer wildfires has found that fuel consumption and pitch pine mortality are positively correlated with burn severity. The results of this study therefore imply that the range of effects possible from prescribed burning, under the current management strategy, is limited by the time frame in which burning is conducted and therefore falls short of mimicking wildfire. Further, since prescribed fires make up approximately 2/3 of the acreage burned in a given year, the majority of the fire on the landscape is of far lesser severity than wildfires area. Growing season fires can be difficult to extinguish quickly and can cause greater air quality issues, which can make growing season prescribed burns unpopular in this region, however adopting strategic “fire use” practices that allow fires to burn in low risk areas and use natural boundaries, when opportune could allow fire managers to accomplish a broader range of silvicultural, ecological, and fuel reduction goals.

Further, this data suggests that at the right time of year, even small fires can have a high severity, suggesting that small growing season burns could be a viable management option where outcomes of high severity fire are highly valued, such as fuel management near homes, preservation of fire dependent flora, or thinning of overstocked forests. Specifically, managers should expect to find the greatest range of fire effects between weeks 23 – 31 of the calendar year.

Future research in this environment can incorporate the findings of this paper in a variety of ways fire effects and behavior. For instance, understanding linkages between burn severity and shifts in species communities can help better define the appropriate balance of fire on this landscape and employ management practices that will better meet conservation goals. Further, quantitative links between measures of fire behavior, such as spread rate, temperature, and resonance time, and burn severity would help shed light on the spatial variability of fire behavior and guide experiments intended to quantify fire behavior.

Conclusions

Timing plays an important role in dictating burn severity of fires PNR. Prescribed fire tends to be of lower burn severity than wildfire, however, prescribed burning is only conducted during the time of year when burn severity tends to be low. Although extending the timing of prescribed fire into the growing season may be culturally unacceptable, promoting "fire use" strategies among managers, when risks are low, would likely enable managers to accomplish a broader range of silvicultural, ecological, and fuel reduction goals. Future work should focus on incorporating burn severity into fire behavior, botanical, and wildlife studies in order to further identify how timing of fire can be manipulated to better meet management objectives.

References

Abrams, M. D. (1992) Fire and the development of oak forests. *BioScience,* 42**,** 346-353.

Angelo, J. J., B. W. Duncan & J. F. Weishampel (2010) Using lidar-derived vegetation profiles to predict time since fire in an oak scrub landscape in East-Central Florida. *Remote sensing,* 2**,** 514-525.

Bien, W. F. 2016. (Personal Communication).

Bien, W. F., H. W. Avery, J. R. Spotila, R. M. Smith, K. L. Clark, N. S. Skowronski, M. Sobel, and D. Ward. 2009. Ecological Studies in Support of the Warren Grove Gunnery Range Integrated Resources Management Plan: Ecosystem Fire Control Model, Final Report. 96.

Boelman, N. T., A. V. Rocha & G. R. Shaver (2011) Understanding burn severity sensing in Arctic tundra: exploring vegetation indices, suboptimal assessment timing and the impact of increasing pixel size. *International journal of remote sensing,* 32**,** 7033-7056.

Boerner, R. E. & R. Forman (1982) Hydrologic and mineral budgets of New Jersey Pine Barrens upland forests following two intensities of fire. *Canadian Journal of Forest Research,* 12**,** 503-510.

Bond, W. J. & J. E. Keeley (2005) Fire as a global 'herbivore': the ecology and evolution of flammable ecosystems. *Trends in ecology & evolution,* 20**,** 387-394.

Boyd, H. P. 2008. *ecological Pine Barrens of New Jersey*. Plexus Pub.

Chander, G., B. L. Markham & D. L. Helder (2009) Summary of current radiometric calibration coefficients for Landsat MSS, TM, ETM+, and EO-1 ALI sensors. *Remote sensing of environment,* 113**,** 893-903.

Clark, K. L., N. Skowronski & M. Gallagher. 2014a. The fire research program at the Silas Little Experimental Forest, New Lisbon, New Jersey. In *USDA Forest Service experimental forests and ranges*, 515-534. Springer.

Clark, K. L., N. Skowronski, H. Renninger & R. Scheller (2014b) Climate change and fire management in the mid-Atlantic region. *Forest Ecology and Management,* 327**,** 306-315.

Dennison, P. E., S. C. Brewer, J. D. Arnold & M. A. Moritz (2014) Large wildfire trends in the western United States, 1984–2011. *Geophysical Research Letters,* 41**,** 2928-2933.

Duffy, P. A., J. Epting, J. M. Graham, T. S. Rupp & A. D. McGuire (2007) Analysis of Alaskan burn severity patterns using remotely sensed data. *International Journal of Wildland Fire,* 16**,** 277-284.

Engstrom, R. T., R. L. Crawford & W. W. Baker (1984) Breeding bird populations in relation to changing forest structure following fire exclusion: a 15-year study. *The Wilson Bulletin***,** 437-450.

Forman, R. 2012. *Pine Barrens: ecosystem and landscape*. Elsevier.

Forman, R. T. & R. E. Boerner (1981) Fire frequency and the pine barrens of New Jersey. *Bulletin of the Torrey Botanical Club***,** 34-50.

Garcia, M. L. & V. Caselles (1991) Mapping burns and natural reforestation using Thematic Mapper data. *Geocarto International,* 6**,** 31-37.

Howard, S. M. & J. M. Lacasse (2004) An evaluation of gap-filled Landsat SLC-off imagery for wildland fire burn severity mapping. *Photogrammetric Engineering and Remote Sensing,* 70**,** 877-880.

Isaacson, B. N., S. P. Serbin & P. A. Townsend (2012) Detection of relative differences in phenology of forest species using Landsat and MODIS. *Landscape ecology,* 27**,** 529-543.

Key, C. 2005. Remote sensing sensitivity to fire severity and fire recovery. In *5th International Workshop on Remote Sensing and GIS Applications to Forest Fire Management: Fire Effects Assessment*, 29-39.

Key, C. H. & N. C. Benson (1999) The Normalized Burn Ratio (NBR): A Landsat TM radiometric measure of burn severity. *United States Geological Survey*.

Key, C. H. & N. C. Benson (2006) Landscape assessment (LA). *FIREMON: Fire effects monitoring and inventory system. Gen. Tech. Rep. RMRS-GTR-164-CD, Fort Collins, CO: US Department of Agriculture, Forest Service, Rocky Mountain Research Station*.

Kümmel, H. B. 1902. New Jersey Geological Survey: Annual Report of the State Geologist for the Year 1902. ed. N. J. G. Survey. Trenton, NJ: John B. Murphy Pub. Co.

La Puma, I. P., R. G. Lathrop & N. S. Keuler (2013) A large-scale fire suppression edge-effect on forest composition in the New Jersey Pinelands. *Landscape Ecology,* 28**,** 1815-1827.

Lathrop, R. & M. Kaplan (2004) New Jersey land use/land cover update: 2000–2001. *New Jersey Department of Environmental Protection,* 35.

Loeb, S. C. & T. A. Waldrop (2008) Bat activity in relation to fire and fire surrogate treatments in southern pine stands. *Forest Ecology and Management,* 255**,** 3185-3192.

Markham, B. L., J. C. Storey, D. L. Williams & J. R. Irons (2004) Landsat sensor performance: history and current status. *IEEE Transactions on Geoscience and Remote Sensing,* 42**,** 2691-2694.

Miller, J. D. & H. Safford (2012) Trends in wildfire severity: 1984 to 2010 in the Sierra Nevada, Modoc Plateau, and southern Cascades, California, USA. *Fire Ecology,* 8**,** 41-57.

Miller, J. D., H. D. Safford, M. Crimmins & A. E. Thode (2009) Quantitative Evidence for Increasing Forest Fire Severity in the Sierra Nevada and Southern Cascade Mountains, California and Nevada, USA. *Ecosystems,* 12**,** 16-32.

Miller, J. D. & A. E. Thode (2007) Quantifying burn severity in a heterogeneous landscape with a relative version of the delta Normalized Burn Ratio (dNBR). *Remote Sensing of Environment,* 109**,** 66-80.

New Jersey Department of the Treasury, O. o. M. a. B. 2012. State of New Jersey: The Governor's FY2013 Detailed Budget. 563.

---. 2014. State of New Jersey: The Governor's FY2015 Detailed Budget. 586.

---. 2016. State of New Jersey: The Governor's FY2017 Detailed Budget. D-114.

Nowacki, G. J. & M. D. Abrams (2008) The demise of fire and “mesophication” of forests in the eastern United States. *BioScience,* 58**,** 123-138.

Picotte, J. J., B. Peterson, G. Meier & S. M. Howard (2016) 1984–2010 trends in fire burn severity and area for the conterminous US. *International Journal of Wildland Fire,* 25**,** 413-420.

Rivera-Huerta, H., H. D. Safford & J. D. Miller (2016) PATTERNS AND TRENDS IN BURNED AREA AND FIRE SEVERITY FROM 1984 TO 2010 IN THE SIERRA DE SAN PEDRO MÁRTIR, BAJA CALIFORNIA, MEXICO. *Fire Ecology,* 12**,** 52-72.

Robichaud, B. 1973. *Vegetation of New Jersey*. New Brunswick, NJ: Rutgers University Press.

Robichaud, B. & K. Anderson. 1994. *Plant communities of New Jersey: a study in landscape diversity*. New Brunswick, NJ: Rutgers University Press.

Rose, E. T., T. R. Simons, R. Klein & A. J. McKerrow (2016) Normalized burn ratios link fire severity with patterns of avian occurrence. *Landscape Ecology***,** 1-14.

Skowronski, N. S., K. L. Clark, M. Duveneck & J. Hom (2011) Three-dimensional canopy fuel loading predicted using upward and downward sensing LiDAR systems. *Remote Sensing of Environment,* 115**,** 703-714.

Soverel, N. O., N. C. Coops, D. D. Perrakis, L. D. Daniels & S. E. Gergel (2011) The transferability of a dNBR-derived model to predict burn severity across 10 wildland fires in western Canada. *International Journal of Wildland Fire,* 20**,** 518-531.

Soverel, N. O., D. D. B. Perrakis & N. C. Coops (2010) Estimating burn severity from Landsat dNBR and RdNBR indices across western Canada. *Remote Sensing of Environment,* 114**,** 1896-1909.

Warner, T. A., N. S. Skowronski & M. R. Gallagher (2017) High spatial resolution burn severity mapping of the New Jersey Pine Barrens with WorldView-3 near-infrared and shortwave infrared imagery. *International Journal of Remote Sensing,* 38**,** 598-616.

Table 1. Summary of New Jersey statewide wild and prescribed fire occurrence data for the period 2006 - 2015. The vast majority of this fire occurred in the Pinelands National Reserve.

Year	Wildfires Reported	Wildfire Acres Reported	Prescribed Fire Acres Reported	Wildfires Sampled	Prescribed Fires Sampled	Wildfire Acres Sampled	Prescribed Fire Acres Sampled
2006	2,367[a]	3,886[af]	20,470[af]	11	26	2,832	6,546
2007	1,271[a]	21,841[af]	11,550[af]	10	26	20,483	5,256
2008	1,618[b]	20,392[bfg]	13,510[bfg]	9	50	8,909	6,940
2009	1,054[b]	3,681[bfh]	24,025[bfh]	1	36	53	6,326
2010	883[c]	7,222[cfh]	3,624[cfh]	10	8	5,891	415
2011	1,228[c]	5,563[cfh]	18,215[cfh]	11	25	808	7,148
2012	1,479[d]	5,946[dfh]	22,609[dfh]	8	61	3,804	6,168
2013	830[d]	1,502[dfh]	16,086[dfh]	4	55	354	7,247
2014	1,063[e]	10,481[efh]	19,422[efh]	11	72	2,695	9,777
2015	373[e]	3,535[efh]	7,948[efh]	5	8	1,981	1,904
Total	*12,166*	*84,049*	*157,459*	*80*	*367*	*47,810*	*57,727*

[a]New Jersey Department of Treasury 2008

[b]New Jersey Department of Treasury 2010

[c]New Jersey Department of Treasury 2012

[d]New Jersey Department of Treasury 2014

[e]New Jersey Department of Treasury 2016

[f]Stevenson 2016

[g]Bien et al. 2009

[h]Bien 2016

Table 2. Imagery used to develop annual growing season mosaics.

Year	% Missing after Mosaicking	Dates of Imagery	Path	Row	Landsat Image ID
2005	<1	14-Aug	14	32	lt50140322005226
		8-Sep	13	32	lt50130322005251
2006	<1	16-Jul	14	32	lt50140322006197
		1-Aug	14	32	lt50140322006213
2007	1	5-Sep	14	32	lt50140322007248
2008	<1	23-Aug	14	32	lt50140322008235
		8-Sep	14	32	lt50140322008251
		24-Sep	14	32	lt50140322008267
2009	6	1-Aug	14	32	le70140322009213
		10-Aug	13	32	le70130322009222
		10-Aug	13	33	le70130332009222
		17-Aug	14	32	le70140322009229
		25-Aug	14	32	lt50140322009237
2010	5	28-Aug	14	32	lt50140322010240
2011	0	14-Jul	14	32	lt50140322011195
2012	2	2-Jul	13	32	le70130322012183
		12-Jun	13	32	le70130322012263
		3-Aug	13	32	le70130322012215
2013	4	25-Jun	14	32	le70140322013176
		5-Aug	13	32	le70130322013217
		6-Sep	13	32	le70130322013249
		15-Oct	14	32	le70140322013288
2014	0	28-Jun	14	32	le70140322014179
		30-Jun	14	33	le70140332014211
		7-Jul	13	32	le70130322014188
		30-Jul	14	33	le70140332014211
		8-Aug	13	32	le70130322014220
		15-Aug	14	32	le70140322014227
2015	28	25-Jun	13	32	le70130322015175
		17-Jul	14	32	le70140322015198
		26-Jul	13	23	le70130322015207
		18-Aug	14	32	le70140322015230

Figure 1. Average frequency of prescribed fire and wildfire occurrence (> 1 hectare) over a ten year period by day of year.

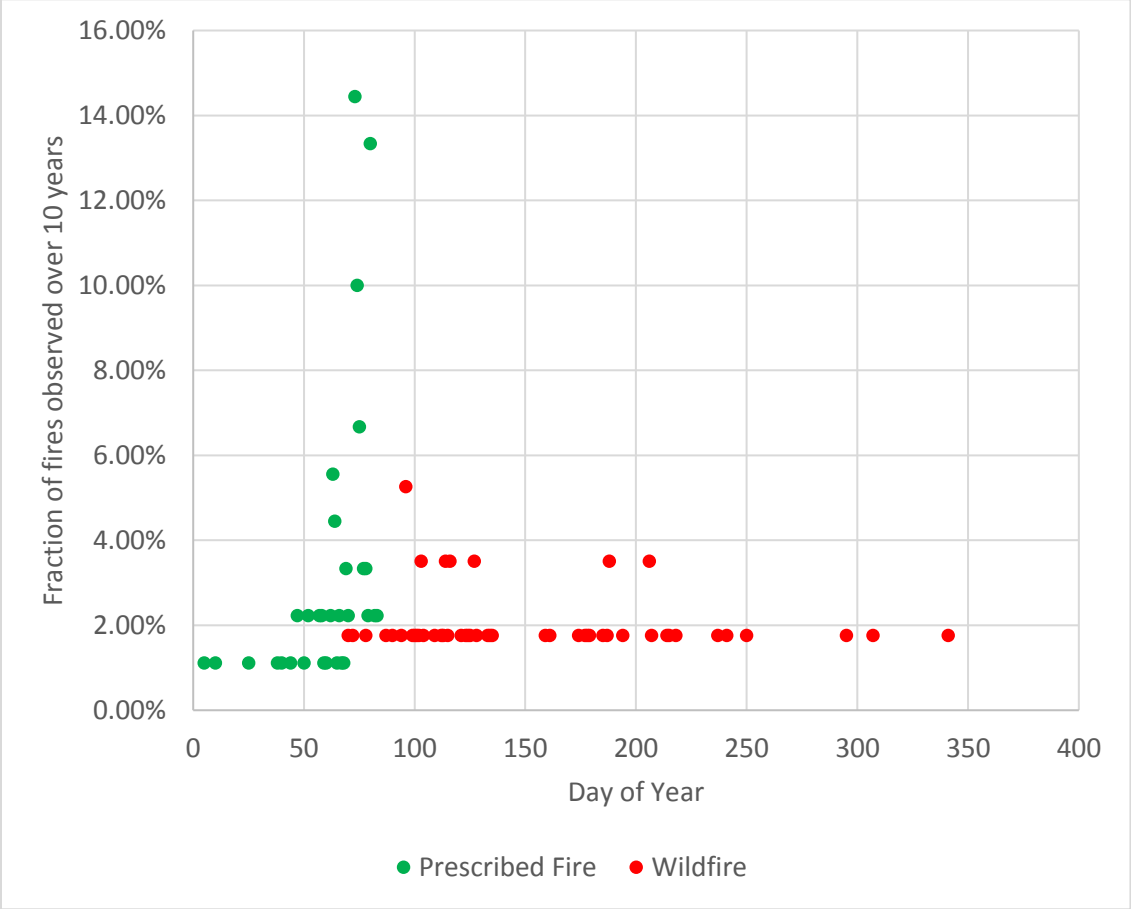

Figure 2. Histogram of pixel values observed at 367 prescribed fires and 80 wildfires that occurred in the New Jersey Forest Fire Service's central region from 2006 – 2015.

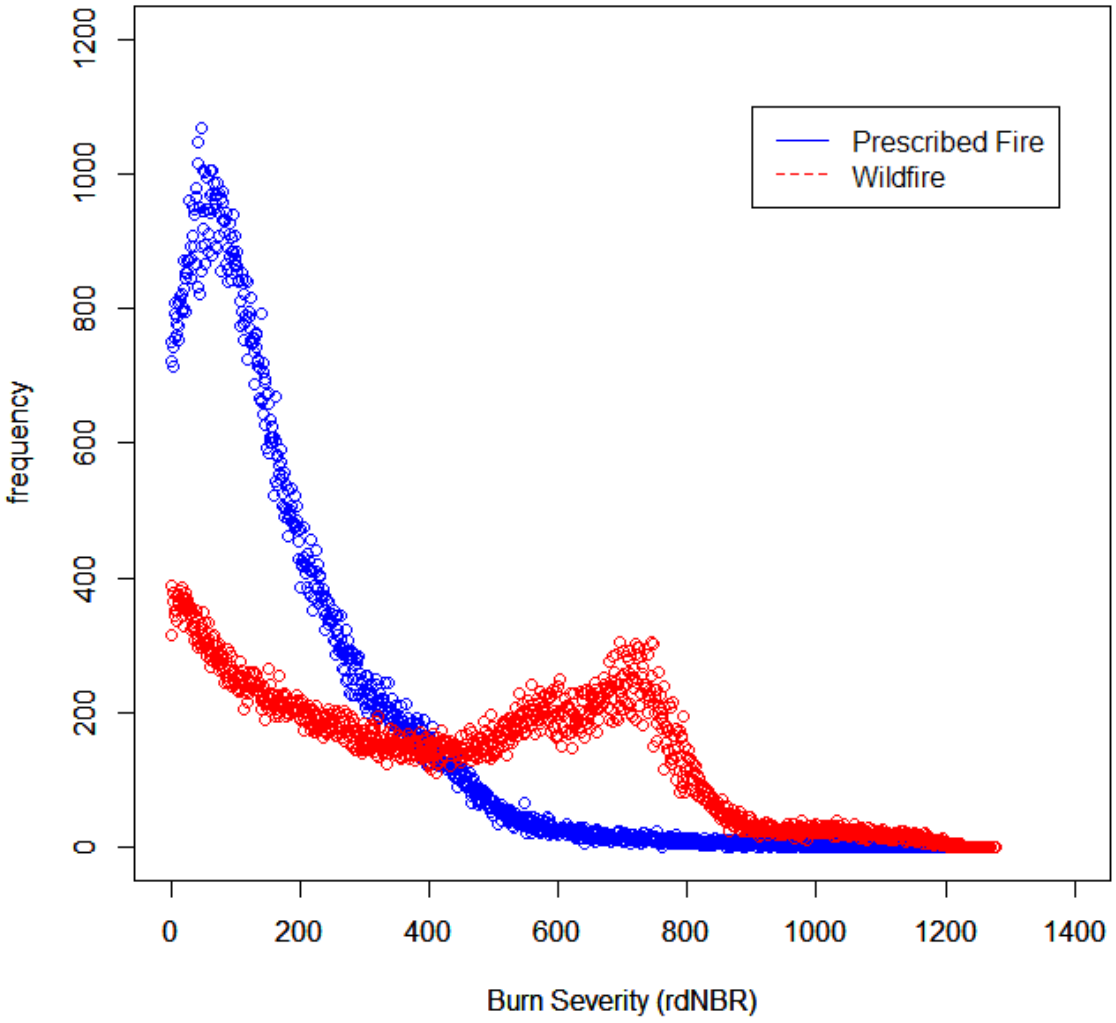

Figure 3. Mean and maximum burn severities of wild and prescribed fires (shown together) were poorly correlated with fire size.

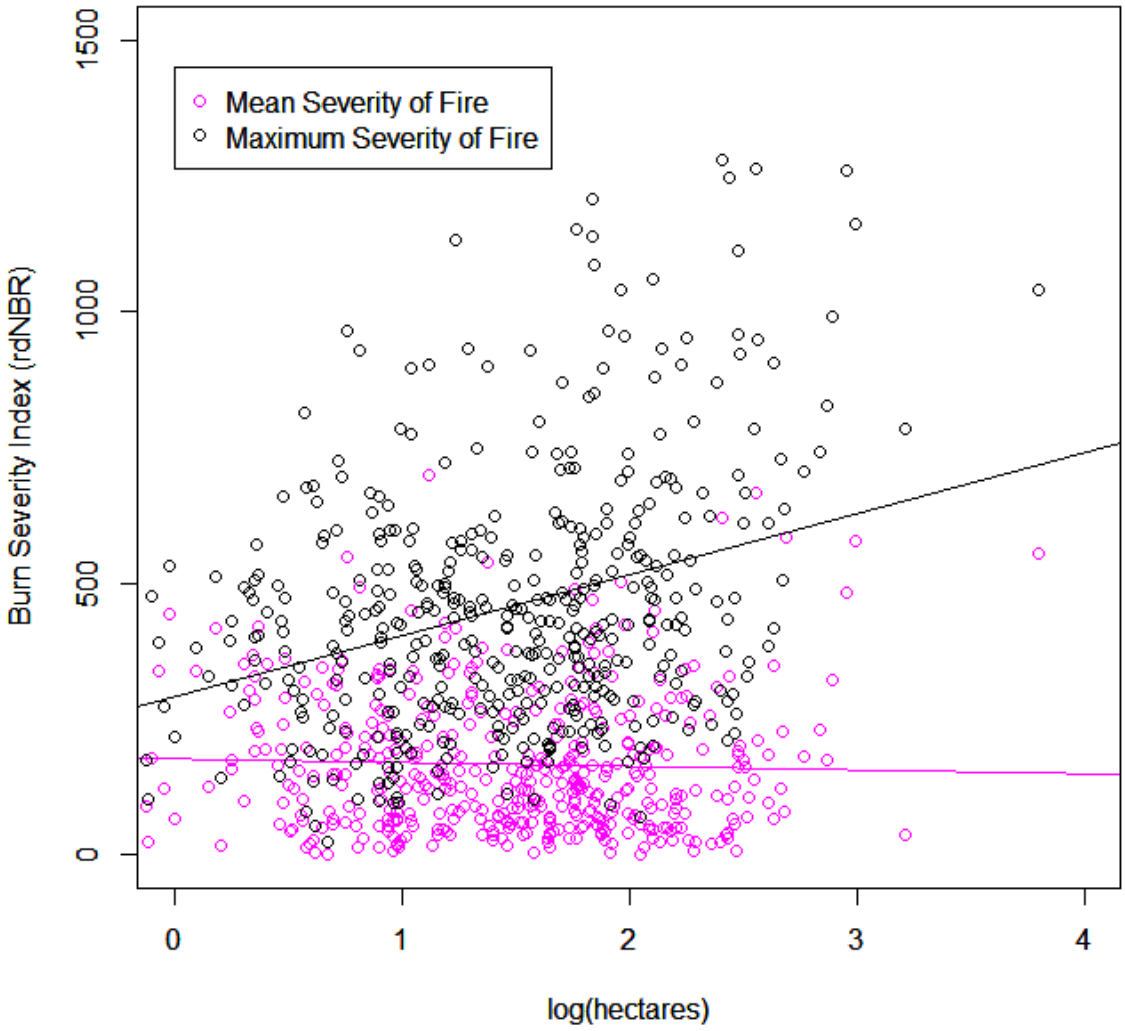

.

Figure 4. Monthly distributions of burn severity for 2006 – 2015

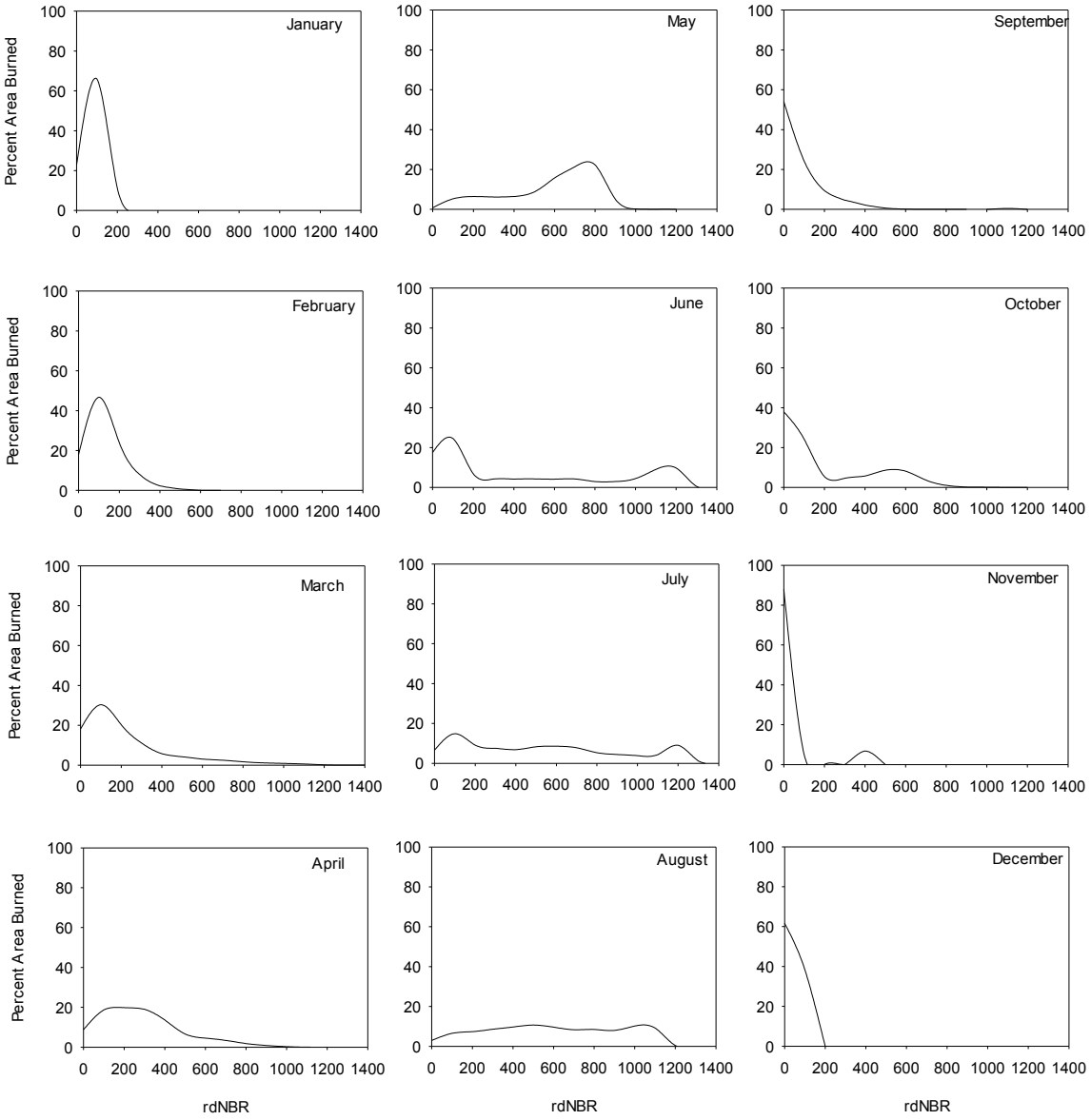

Figure 5. Weekly maximum, mean, and range of burn severity in the Pinelands National Reserve averaged over a ten year period (2006-2016).